



12-2008

Optimal Control of Epidemic Models Involving Rabies and West Nile Viruses

Timothy Joseph Clayton
University of Tennessee - Knoxville

Recommended Citation

Clayton, Timothy Joseph, "Optimal Control of Epidemic Models Involving Rabies and West Nile Viruses." PhD diss., University of Tennessee, 2008.
https://trace.tennessee.edu/utk_graddiss/486

This Dissertation is brought to you for free and open access by the Graduate School at Trace: Tennessee Research and Creative Exchange. It has been accepted for inclusion in Doctoral Dissertations by an authorized administrator of Trace: Tennessee Research and Creative Exchange. For more information, please contact trace@utk.edu.

To the Graduate Council:

I am submitting herewith a dissertation written by Timothy Joseph Clayton entitled "Optimal Control of Epidemic Models Involving Rabies and West Nile Viruses." I have examined the final electronic copy of this dissertation for form and content and recommend that it be accepted in partial fulfillment of the requirements for the degree of Doctor of Philosophy, with a major in Mathematics.

Suzanne Lenhart, Major Professor

We have read this dissertation and recommend its acceptance:

Charles Collins, Louis Gross, Vladimir Protopopescu

Accepted for the Council:

Carolyn R. Hodges

Vice Provost and Dean of the Graduate School

(Original signatures are on file with official student records.)

To the Graduate Council:

I am submitting herewith a dissertation written by Timothy Joseph Clayton entitled “Optimal Control of Epidemic Models Involving Rabies and West Nile Viruses”. I have examined the final electronic copy of this dissertation for form and content and recommend that it be accepted in partial fulfillment of the requirements for the degree of Doctor of Philosophy, with a major in Mathematics.

Suzanne Lenhart, Major Professor

We have read this dissertation
and recommend its acceptance:

Charles Collins

Louis Gross

Vladimir Protopopescu

Accepted for the Council:

Carolyn R. Hodges

Vice Provost and Dean of the
Graduate School

(Original signatures are on file with official student records.)

**Optimal Control of Epidemic Models
Involving Rabies and West Nile Viruses**

A Dissertation

Presented for the

Doctor of Philosophy

Degree

The University of Tennessee, Knoxville

Timothy Joseph Clayton

December 2008

Copyright © 2008 by Timothy Joseph Clayton.

All rights reserved.

Dedication

This dissertation is dedicated to my parents Howard and Wanda Clayton for the commitment they have shown to their family.

Acknowledgments

I would like to express my sincere gratitude to my advisor, Professor Suzanne Lenhart and the members of my committee, Professors Charles Collins, Louis Gross, and Vladimir Protopopescu, for their advice and guidance in the compilation of this project.

Abstract

This research considers the application of *Optimal Control* theory to minimize the spread of viral infections in disease models. The population models under consideration are systems of ordinary differential equations and represent epidemics arising due to either rabies or West Nile virus. Optimal control strategies are analyzed using Pontryagin's Maximum Principle and illustrated based upon computer simulations.

The first model describes a population of raccoons and its interaction with the rabies virus, thus dividing the animals into four classes: *susceptible*, *exposed*, *immune*, and *recovered* (*SEIR*). The model includes a birth pulse during the spring of the year and an equation reflecting the dynamics of a potential vaccine. The vaccine equation contains a linear control variable representing the rate at which the vaccine is distributed. The goal is to minimize the number of infected raccoons and the cost of vaccine distributed. Due to linearity in the control, there is the possibility of a singular control and the generalized Legendre-Clebsch condition will be satisfied to obtain new necessary conditions for the singular case. A scenario with a limited amount of vaccine is also investigated. The system is modified to include a density-dependent death rate for each of the *S*, *E*, *I*, *R* classes, and the results of this model are compared with those of the non-density dependent model to determine how the different death rates affect control strategies.

The second disease model considered describes the dynamics of mosquito, bird and human populations exposed to the West Nile virus. The mosquito and bird categories will be divided into *susceptible* and *infected* classes. In addition to these two groups, humans will also have the potential of entering the *exposed*, *hospitalized* and *recovered* classes. In this model, birth and death rates are assumed to be density-dependent. Two controls are

applied with one control representing pesticide efforts to decrease the number of mosquitos and a second control representing prevention and repellant methods. The basic reproduction number is considered to justify the need for control.

Approximations of the optimal solutions of the models are obtained using an iterative method. The numerical algorithm, Runge-Kutta of order four, is programmed in Matlab. Graphical results show the appropriate amount of control for various situations.

Contents

1	Introduction	1
1.1	Optimal Control	2
1.2	Numerical Approximation	4
1.3	Epidemic Models Involving Viral Diseases	7
2	An Epidemic Model of Rabies in Raccoons	12
2.1	The Infected Raccoon Population	15
2.2	Introducing Vaccine Dynamics	18
2.3	Finding an Optimal Control	19
2.4	Numerical Results	25
2.5	Limited Vaccine	38
2.6	Conclusion	40
3	An Epidemic Model of Rabies in Raccoons with Density Dependent Mor-	
	tality	43
3.1	Introduction	43
3.2	The Infected Raccoon Population	45
3.3	Introduction of Vaccine	46
3.4	Finding an Optimal Control	47
3.5	Numerical Results	52
3.6	Conclusions	58

4 An Epidemic Model of West Nile Virus	63
4.1 Introduction	63
4.2 Model Formulation	64
4.3 Basic Reproduction Number	73
4.4 Numerical Simulation	74
4.5 Conclusion	84
Bibliography	87
Appendices	92
A The First Appendix	93
Vita	108

List of Tables

2.1	State Variables and Parameters	19
2.2	Parameter Values	26
2.3	New Parameter Values	36
A.1	State Variables and Parameters	106
A.2	State Variables and Parameters	107

List of Figures

2.1	One year projection of disease free raccoon population starting on January 1	27
2.2	Populations of system 2.1 with initial values of 1, 40 and 100 infected raccoons and no control. Note the horizontal segment indicates the days of the birth pulse.	29
2.3	Optimal control results of system 2.2 projected for 1 year with $I_0 = 40$, $u = 1$ for days 1-14, 77-189. $B = 10^{-2}$	30
2.4	Disease free raccoon population results of system 2.1 starting on March 1	31
2.5	State variables of system 2.1 with disease and no control: Simulation begins on March 14.	32
2.6	Optimal control results of system 2.2 for (a) $B = 10^{-4}$, (b) $B = 10^{-2}$, (c) $B = 10^0$	33
2.7	Comparison of system 2.2 with varying cost coefficients beginning on March 14, seven days before the birth pulse.	35
3.1	One year projection of disease free raccoon population starting on January 1	52
3.2	Populations of system 3.1 with initial values of 1, 40 and 100 infected raccoons and no control	54
3.3	Infected Populations of system 3.2 with varying natural immunity	55
3.4	Optimal control results of system 3.2 projected for one year with $I_0 = 40$. $u = 1$ for days 77-185. $B = 10^{-2}$	56
3.5	Populations of system 3.2 using initial values of 1, 40 and 100 infected raccoons with control	57

3.6	Control results of system 3.2 for a 28 day interval:(a) without a birth pulse. (b) during a birth pulse. (c) beginning on day 73 (shortly before the birth pulse).	59
3.7	Control results of system 3.2 for a 28 day interval:(a) beginning March 1. (b) beginning February 20.	60
3.8	Populations results of system 3.2 with a 28 day interval:(a) beginning March 14. (b) beginning March 1. (c) beginning February 20.	61
4.1	Disease free populations of mosquito, bird and humans	75
4.2	Effects of system 4.3-4.7 with 1000 infected mosquitos	75
4.3	Effects of system 4.3-4.7 with 1000 infected mosquitos when cost coefficients are unity.	77
4.4	State and control system 4.3-4.7 with $A_3 = 10^{-4}$ and $A_3 = 10^{-4}$, $A_1 = A_2 = 1$, $B_1 = 1$, $B_2 = 10^3$	78
4.5	State system 4.3-4.7 with $A_1 = 10^{-1}$, $A_2 = 1$, $A_3 = 10^{-4}$, $B_1 = 1$, $B_2 = 10^3$	80
4.6	State system 4.3-4.7 with $A_1 = A_2 = 10^{-1}$, $A_3 = 10^{-4}$, $B_1 = 1$, $B_2 = 10^3$	81
4.7	Controls of system 4.3-4.7 for varying cost coefficients with $B_1 = 1$, $B_2 = 10^3$.	82
4.8	State system 4.3-4.7 with $A_1 = 10$, $A_3 = 10^{-3}$, $B_2 = 10^3$, $0 \leq u_1 \leq 0.8$, $0 \leq u_2 \leq 0.9$	83
4.9	Control of system 4.3-4.7 with $A_1 = 1$, $A_3 = 10^{-3}$, $B_2 = 10^3$, $0 \leq u_1 \leq 0.8$, $0 \leq u_2 \leq 0.9$	85
A.1	Controlled populations of system 2.2 during a 28 day interval (a) without a birth pulse. (b) during a birth pulse. (c) beginning on day 73 (about 1 week before the birth pulse).	94
A.2	Controlled populations of system 2.2 during a 28 day interval:(a) beginning March 1. (b) beginning February 20.	95

A.3	Results of system 2.2 with upper bound of 5 on the control for a 28 day interval:(a) beginning March 14. (b) beginning March 1. (c) beginning February 20.	96
A.4	Disease free population for 1 year	97
A.5	Populations of system 2.1 with initial values of 1, 40 and 100 infected raccoons and no control	98
A.6	Optimal control results of system 2.2 projected for 1 year with $I_o = 40$. $u = 1$ for days 75-191.	99
A.7	Disease free raccoon population starting on March 1	99
A.8	State variables of system 2.2 with disease and no control: Simulation begins on March 14.	100
A.9	Controlled results of system 2.2 from new parameters when (a) $B = 10^{-4}$, (b) $B = 10^{-2}$, (c) $B = 10^0$	101
A.10	New parameter results of system 2.2 for a 28 day interval:(a) without a birth pulse. (b) during a birth pulse. (c) beginning on day 73 (shortly before the birth pulse).	102
A.11	Results of system 2.2 from new parameters for a 28 day interval:(a) beginning March 1. (b) beginning February 20.	103
A.12	Results of system 2.2 from new birth and death rate but the old infection period α beginning March 1.	104
A.13	Results of system 2.2 from control constraint case (a) 28 day interval without a birth pulse. (b) 28 day interval beginning on March 14.	105

Chapter 1

Introduction

The dynamics of a given population's density or abundance may be represented by an ordinary differential equation. If the population is exposed to a viral infection, the original group of organisms can be divided into different classes, namely *susceptible*, *exposed*, *infected* and possibly a *recovered* class. Given a diseased population and a control function which affects its dynamics, a possible goal is to choose a control to minimize the spread of the infection and maximize the size of the non-diseased population. Optimal control theory may be used to theoretically solve a minimization problem of this type. This procedure is an analytical method applied to a given objective functional that yields the optimal path to be taken by variables of a dynamical process in continuous time. In the disease models to be considered here, the dynamical process is represented by a system of ordinary differential equations (ODEs) and the objective functional to be minimized could depend upon some combination of the infected class and some control quantity. L.S. Pontryagin and his co-workers developed this method in the 1950's based on their formulation of the maximum principle for optimal control of ordinary differential equations [25]. In optimal control, variables are classified as being either a state or control variable. The path of a state variable is determined by a first order ordinary differential equation. Control variables are Lebesgue measurable functions of time and influence the dynamical process.

1.1 Optimal Control

Before considering the optimal control problem for a system of differential equations, the single ODE case will be considered. The state variable, $x(t)$, is the solution to the state differential equation:

$$x'(t) = g(t, x(t), u(t)),$$

where g is a continuously differentiable function and u is the control function. It is assumed that an objective functional with an integrand $f(t, x(t), u(t))$ and the state equation are both influenced by the control function $u(t)$. The problem may be written as:

$$\min \int_{t_0}^{t_1} f(t, x(t), u(t)) dt$$

over the Lebesgue measurable control functions u on $[t_0, t_1]$ subject to

$$x'(t) = g(t, x(t), u(t)), \quad x(t_0) = x_0, \quad x(t_1) \text{ free.}$$

For this simple optimal control problem, with f and g continuously differentiable in x and u , Pontryagin's Maximum Principle [20] can be stated as:

Theorem 1.1.1. *If $u^*(t)$ and $x^*(t)$ are optimal for the above problem, then there exists a piecewise differentiable adjoint variable $\lambda(t)$ such that*

$$H(t, x^*(t), u(t), \lambda(t)) \geq H(t, x^*(t), u^*(t), \lambda(t))$$

for all controls u at each time t , where the Hamiltonian H is

$$H(t, x, u, \lambda) = f(t, x(t), u(t)) + \lambda(t)g(t, x(t), u(t)),$$

and

$$\lambda'(t) = -\frac{\partial H(t, x^*(t), u^*(t), \lambda(t))}{\partial x}, \quad \lambda(t_1) = 0.$$

The state and adjoint equations form the optimality system

$$\begin{aligned} x'(t) &= g(t, x(t), u(t)), \quad x(t_0) = x(0) \text{ fixed} \\ \lambda'(t) &= G(t, x(t), u(t), \lambda(t)), \quad \lambda(t_1) = 0, \end{aligned} \tag{1.1}$$

where $G(t, x(t), u(t), \lambda(t)) = -\frac{\partial H}{\partial x}$, and u^* is represented in terms of x and λ from maximizing H with respect to u . Usually the optimality equation, $\frac{\partial H}{\partial u} = 0$ at u^* , is used to solve for this representation of u^* .

If H is nonlinear with an unbounded control class, then the optimality condition is $\frac{\partial H}{\partial u} = 0$ at u^* , coming from maximizing the Hamiltonian with respect to u at u^* . However, if the Hamiltonian is linear in the control, then the control does not appear in $\frac{\partial H}{\partial u}$. If $\frac{\partial H}{\partial u} = 0$ over a time interval with positive length, then the optimal control is called singular.

A generalization of the Pontryagin maximal principle was developed in the 1970's, providing new necessary conditions for an optimal control problem [19, 5, 26, 18, 14]. This method, called the High Order Maximal Principle, generalizes the Legendre-Clebsch condition,

$$\frac{\partial^2}{\partial u^2} H \geq 0 \text{ at } u^*.$$

The degree $h + 1$ of the singular control, $u_0(t)$, on the subinterval (t_*, \bar{t}) of (t_0, t_1) is defined such that h is the smallest integer for which a solution exists for

$$\lambda'(t) = -\lambda(t) \frac{\partial g(t, x(t), u_0(t))}{\partial x}$$

as well as

$$\frac{d^k}{dt^k} \frac{\partial}{\partial u} H(\lambda(t), x(t), u_0(t)) = 0$$

for $k = 0, 1, 2, \dots$ such that for such t in the subinterval of $[t_1, t_2]$,

$$\frac{\partial}{\partial u} \frac{d^{h+1}}{dt^{h+1}} \frac{\partial H(\lambda(t), x(t), u_0(t))}{\partial u} \neq 0.$$

This condition will be satisfied in the rabies model of the next chapter.

The generalized Legendre-Clebsch condition [19]

Theorem 1.1.2. *Assume that $u_0(t)$ and $x(t)$ are defined for $x'(t) = g(t, x(t), u(t))$, $x(t_0) = x_0(0)$ on $[t_0, t_1]$. If u_0 is singular of degree $h+1$ on a subinterval $(t^*, \bar{t}) \subset [t_0, t_1]$ and h is finite, then h is odd. If u_0 is optimal, then there exists a $\lambda(t)$ satisfying the Pontryagin Maximum Principle on $[t_0, t_e]$ such that*

$$(-1)^{\frac{h+1}{2}} \frac{\partial}{\partial u} \frac{d^{h+1}}{dt^{h+1}} \frac{\partial H(\lambda(t), x(t), u_0(t))}{\partial u} \geq 0 \text{ on } (t_*, \bar{t}).$$

1.2 Numerical Approximation

Solving the optimality system, which is the state and adjoint ODEs together with the optimal control representation, requires an iterative scheme. This involves use of an algorithm such as Runge-Kutta of order four. First, we discuss the numerical method by approximating a single ordinary differential equation and its associated adjoint equation. In the Runge-Kutta method of order four, the interval $[t_0, t_1]$ is partitioned into N subdivisions of equal length, $N > 1$. Assuming that u is known at the original N grid points, then we may solve the state equation $x'(t) = g(t, x(t), u(t))$, with $x(t_0) = x_0$ fixed, according to the following difference equation:

$$w_0 = x(0) \tag{1.2}$$

$$\begin{aligned} k_1 &= hg(t_i, w_i, u_i) \\ k_2 &= hg\left(t_i + \frac{h}{2}, w_i + \frac{k_1}{2}, \frac{1}{2}[u_i + u_{i+1}]\right) \\ k_3 &= hg\left(t_i + \frac{h}{2}, w_i + \frac{k_1}{2}, \frac{1}{2}[u_i + u_{i+1}]\right) \\ k_4 &= hg(t_{i+1}, w_i + k_3, u_{i+1}) \\ w_{i+1} &= w_i + \frac{1}{6}(k_1 + 2k_2 + 2k_3 + k_4), \end{aligned}$$

for each $i = 0, 1, 2, \dots, N - 1$ where $N \gg 1$ and $h = \frac{t_1 - t_0}{N}$ and t_i is the grid point [20]. The value of w_i is the approximation of the solution of the ordinary differential equation at $t_i = t_0 + ih$, $i = 0, 1, 2, \dots, N - 1$. Since u is not necessarily constant throughout the subdivision $[t_i, t_{i+1}]$, $i = 1, 2, \dots, N - 1$, we approximate the control at $t_i + \frac{h}{2}$ by taking the average of u_i and u_{i+1} in the calculation of k_2 and k_3 .

One may use the same step technique to approximate $\lambda(t)$. However, since its value at the final time is known instead of at the initial time, we set $w_N = 0$, with the difference equation:

$$w_N = 0 \tag{1.3}$$

$$\begin{aligned} k_1 &= hG(t_{N-i}, w_{N-i}, u_{N-i}, x_{N-i}) \\ k_2 &= hG\left(t_{N-i} - \frac{h}{2}, w_{N-i} - \frac{k_1}{2}, \frac{1}{2}[u_{N-i} + u_{N-i-1}], \frac{1}{2}[x_{N-i} + x_{N-i-1}]\right) \\ k_3 &= hG\left(t_{N-i} - \frac{h}{2}, w_{N-i} - \frac{k_1}{2}, \frac{1}{2}[u_{N-i} + u_{N-i-1}], \frac{1}{2}[x_{N-i} + x_{N-i-1}]\right) \\ k_4 &= hG(t_{N-i-1}, w_{N-i} - k_3, u_{N-i-1}, x_{N-i-1}) \\ w_{N-i-1} &= w_{N-i} - \frac{1}{6}(k_1 + 2k_2 + 2k_3 + k_4), \end{aligned}$$

for $i = 0, 1, \dots, N - 1$.

Approximate solutions of the optimality system are obtained using an iterative method in combination with the above 4th-order Runge-Kutta scheme.

Starting with an initial condition for the state variable and an initial guess for the control, forward sweep with the Runge-Kutta scheme (1.2) may be used to obtain an approximate solution for the state equation. Using this estimate, the solution of the adjoint equation is approximated using backward sweep (1.3) from the final time condition. The control is updated by using an average of its previous values and its values from the control characterization. Iterations continue until successive values of all variables from current and previous iterations are sufficiently close.

Convergence is determined by requiring the values from two successive iterations to satisfy the relations

$$\frac{\| x - \text{old}x \|}{\| x \|} \leq \epsilon \quad \text{and} \quad \frac{\| u - \text{old}u \|}{\| u \|} \leq \epsilon$$

where ϵ is the accepted tolerance, x is the vector of state values from the current iteration, u is the vector of control values from the current iteration, $\text{old}x$, $\text{old}u$ are the corresponding vectors from the previous iteration, and $\| \cdot \|$ refers to the sum of the absolute value of the terms. Allowing for the possibility of the variables to be zero, the convergence relation may be expressed as

$$\epsilon \| x \| - \| x - \text{old}x \| \geq 0 \quad \text{and} \quad \epsilon \| u \| - \| u - \text{old}u \| \geq 0.$$

For the models described below, the inclusion of an infection in a population model produces additional classes, each of which has a corresponding ODE and an associated adjoint equation. The resulting model is a system of state equations with a corresponding system of adjoint equations requiring a numerical procedure to approximate the optimal solution. In this case, after a forward sweep solution of the state system and a backward sweep solution of the adjoint system, the values of successive iterates for each of the state, adjoint and control variables are compared until all differences fall below a prescribed margin

of error.

1.3 Epidemic Models Involving Viral Diseases

These methods will be applied to population models that have been invaded by an infectious agent called a *virus*. A virus is a DNA or RNA molecule encased in a protein coat that has the ability to move through filters and invade a cell that may serve as a host. Once inside the host, the virus has the ability to replicate itself, initiating the onset of a particular disease. In 1898, a disease that stunted the growth of tobacco plant leaves was classified as a virus. After the turn of the 20th century, microbiologists began growing viruses in petri dishes to more closely study their effects on cultured cells. The research of viruses in cultured cells is used to identify potential vaccines to contain the spread of infections [21]. This project will consider the *rabies* and *West Nile* viruses.

Chapter 2 introduces a population model for raccoons that interacts with the rabies virus. This model divides the raccoons into four classes: *susceptible*, *exposed*, *immune*, and *recovered* (*SEIR*), including a birth pulse during the spring time of the year and an equation reflecting the dynamics of a potential vaccine. The goal is to find optimal strategies for distributing vaccine packets to minimize the infected population and the cost of implementing the control. The effect of the birth pulses on this strategy is investigated. This scenario, with control u as the rate of vaccine distribution, may be described with the system:

$$\begin{aligned}
S' &= -\left(\beta I + b + \frac{c_0 V}{K + V}\right)S + a(S + E + R)\chi(t)_{[t_0, t_1]} & (1.4) \\
E' &= \beta I S - (\sigma + b)E \\
R' &= \sigma(1 - \rho)E - bR + \frac{c_0 V S}{K + V} \\
I' &= \sigma \rho E - \alpha I \\
V' &= -V[c(S + E + R) + c_1] + u.
\end{aligned}$$

Here S , E , I , R are given in terms of numbers of raccoons. The vaccine V is the amount of vaccine. Further explanation of the model may be found in chapter 2.

To minimize the infected population as well as the cost of the vaccine, we consider the objective functional

$$J(u) = \int_0^T [I(t) + Bu(t)]dt.$$

The set of all admissible controls is

$$U = \{u : [0, T] \rightarrow [0, M_1] | u \text{ is Lebesgue measurable}\}$$

where M_1 is a positive constant and the upperbound of u .

Note that the vaccine equation contains a linear control variable representing the rate at which the vaccine is distributed. The linearity of the control in (1.4) and in the objective functional raises the possibility of a singular control and generalized Legendre-Clebsch conditions that must be satisfied to obtain new necessary conditions for the singular case. A scenario with a limited amount of vaccine is also investigated. Results from numerical simulations show the optimal distribution of vaccine so as to minimize the objective functional.

In the next chapter, the system is modified to include a density-dependent death rate

for each of the S , E , R classes. This term is expressed as the product of the death rate, state variable, and the total non-infectious population, i.e., $bS(S + E + R)$, $bE(S + E + R)$, $bR(S + E + R)$. The model with density-dependent deaths is:

$$\begin{aligned}
S' &= -\left(\beta I + \frac{c_0 V}{K + V}\right)S + a(S + E + R)\chi(t)_{[t_0, t_1]} - bS(S + E + R) & (1.5) \\
E' &= \beta IS - \sigma E - bE(S + E + R) \\
R' &= \sigma(1 - \rho)E - bR(S + E + R) + \frac{c_0 V S}{K + V} \\
I' &= \sigma \rho E - \alpha I \\
V' &= -V[c(S + E + R) + c_1] + u,
\end{aligned}$$

with the same objective functional as described above. The results of this model are compared with those of the first to determine how the different death rates affect control strategies.

Control intervention efforts in an epidemiological model of the West Nile virus are considered in chapter 4. This model describes the dynamics of mosquito, bird and human populations exposed to the West Nile virus. The mosquito and bird categories will be divided into the *susceptible* and *infected* classes and may be described by the system:

$$\begin{aligned}
\frac{dM_s}{dt} &= \gamma_M N_M (1 - u_1(t)) - \frac{b_1 \beta_1 M_s B_i}{N_B} - \mu_M M_s - r_0 u_1(t) M_s & (1.6) \\
\frac{dM_i}{dt} &= \frac{b_1 \beta_1 M_s B_i}{N_B} - \mu_M M_i - r_0 u_1(t) M_i \\
\frac{dB_s}{dt} &= \lambda_B + \rho N_B - \frac{b_1 \beta_2 M_i B_s}{N_B} - \delta B_s - \mu_B B_s \\
\frac{dB_i}{dt} &= \frac{b_1 \beta_2 M_i B_s}{N_B} - d_B B_i - \delta B_i - \mu_B B_i
\end{aligned}$$

Here M_s , M_i , B_s , B_i are given in terms of numbers of mosquitos and birds respectively.

In addition to the *susceptible* and *infected* groups, humans will also have the potential to enter the *exposed*, *hospitalized*, and *recovered* classes. The dynamics of the human population may be described by the system:

$$\begin{aligned}
\frac{dS}{dt} &= \lambda_H + \gamma_H N_H - \frac{b_2 \beta_3 M_i S (1 - u_2(t))}{N_H} - \mu_H S \\
\frac{dE}{dt} &= \frac{b_2 \beta_3 M_i S (1 - u_2(t))}{N_H} - \alpha E - \mu_H E \\
\frac{dI}{dt} &= \alpha E - \sigma I - d_I I - r I - \mu_H I \\
\frac{dH}{dt} &= \sigma I - d_H H - \tau H - \mu_H H \\
\frac{dR}{dt} &= \tau H + r I - \mu_H R.
\end{aligned} \tag{1.7}$$

Here S , E , I , R , H are given in terms of numbers of humans. Note that for this model, the birth and death rates are assumed to be density dependent. Note the control u_1 represents the effort to apply pesticide to the mosquitos population and the control u_2 represents the prevention efforts to minimize the spread of infection to humans to mosquitos. Further explanation of the model may be found in chapter 4.

We formulate an optimal control problem with the objective (cost) functional given by

$$J(u_1, u_2) = \int_0^T \left(A_1 E(t) + A_2 I(t) + A_3 N_M(t) + B_1 u_1^2 + B_2 u_2^2 \right) dt \tag{1.8}$$

subject to the constraint (state system) given by (1.6-1.8). Thus, the total cost arising from the *exposed*, *infected*, total number of mosquitos, and controls is being minimized.

The cost of implementing the controls is assumed to be nonlinear and here we take the cost to be proportional to the square of the corresponding control functions. Part of our goal is to find optimal control functions (u_1^*, u_2^*) such that

$$J(u_1^*, u_2^*) = \min\{J(u_1, u_2) \mid (u_1, u_2) \in \Gamma\}$$

subject to the system of equations given by (1.6-1.8), where

$$\Gamma = \{(u_1, u_2) | u_i(t) \text{ is Lebesgue measurable on } [0, T], \quad 0 \leq u_i(t) \leq a_i, \quad i = 1, 2\} \quad (1.9)$$

is the control set and a_i is a positive constant and the upperbound of u_i for $i = 1, 2$. The basic reproduction number is assumed to be large enough to require a control strategy. Numerical simulations are given to illustrate various scenarios.

We note that there are limitations and possible extensions of this model and control problem. The model may be extended to include separate pesticides for the larvae and adult stages of mosquitos, suggesting the use of two controls of the insects. One could add a control for efforts to adjust the rate of hospitalization. A limitation is the difficulty in obtaining reasonable estimates for the parameters in this model to apply to a specific location. The optimal controls and their resulting populations strongly depend on the choice of parameters.

These results show the utility of the optimal control tools in designing strategies for slowing the spread of this epidemic. Given a specific set of parameters (including cost coefficients), one can decide which of the two controls to give more emphasis.

Chapter 2

An Epidemic Model of Rabies in Raccoons

Rabies is a common RNA virus that is transmitted between wildlife causing death to an infected organism after an incubation period. Only the Antarctic, Australia, and other island nations are unafflicted by the rabies virus. There are over 25,000 known cases per year worldwide. This virus is a member of the genus *Lyssavirus* of the family *Rhabdoviridae*, and order *Mononegavirales* [33]. Pasteur first developed a rabies vaccine from exposed specimens by experimenting on rabbits and dogs [17]. Since the discovery of vaccine, attention has been focused on using vaccination to contain the spread of various types of diseases in infected populations.

Today, raccoons have been identified as the most common terrestrial wildlife carrier of the rabies virus in the eastern United States. In an effort to contain the spread of the disease, various states have distributed vaccine baits in their respective wildlife habitats with varying degrees of success. In 1996, the reported cost of programs designed to contain the spread of infection exceeded \$300 million[33]. Fish meal and oil are sometimes used as bait to coat plastic packaging containing the vaccine. The vaccine packets are then frequently dropped from airplanes flying above a given region inhabited by wildlife [3].

Ordinary differential equations (ODEs) as well as partial differential equations (PDEs) have been used to model the dynamics of populations afflicted with the rabies virus. Murray

et al. [24] used ODEs to study the dynamics of *susceptible* and *infected* foxes in Europe coupled with a PDE describing the dispersal of the *rabid* class. This paper also discussed various vaccination and culling strategies. In a later paper, an *immune* class was included, influencing the behavior of the periodic outbreaks associated with oscillating tail of the epidemic wave [23]. Evans and Pritchard extended Murray's 1986 model to include a vaccinated class of foxes with the goal of controlling the density of the infected population to be below a predetermined number [12]. An ODE model developed by Coyne et al., divided raccoons into six categories: *susceptible*, *exposed*, *infected*, *rabid*, *naturally immune*, and *vaccinated*. These model results showed that the least expensive control strategy involved exclusively either culling or vaccination. A combined approach is cheaper only when the per capita cost of vaccination is less than 20% of the per capita cost of culling [9].

A stochastic spatial model developed by Smith et al. described the spread of rabies in Connecticut raccoons and suggested that rivers act as a semipermeable barrier slowing the outbreak of infection [31]. A later paper analyzed how long-distance translocation events influenced the spread of the rabies epidemic in Connecticut [32]. This assumed an adjacency network of Townships within the state divided into infected and undocumented regions. Forested areas were found to slow the spread of rabies. A similar stochastic spatial model was used by Russell et al. to analyze data from Ohio [30]. These results show that vaccine barriers are permeable and subject to breaches. Members of this team later authored another paper using an ODE model to show that the spread of rabies may be controlled by distributing vaccine behind barriers such as rivers [29].

Asano et al. [3] first applied optimal control to a system modeling an infected raccoon population. This *SIR* model included three classes in 9 spatial compartments giving a total of 27 ODEs. Results showed that a higher rate of vaccination is needed for a larger population but a lower distribution of vaccine given a high cost of vaccination. Recently, Ding et al. investigated the distribution of vaccine baits in a rabies epidemic in raccoons using a model discrete in time and space. The results showed that optimal distribution of vaccine depended on the location of the rabies infection. If the virus is detected in the middle of a patch, vaccine is applied heaviest to the center of the spread of infection. If the

infection is observed in a corner of a patch, the distribution of the vaccine is given around the edges to prevent the spread of the infection [11].

Since raccoons only give birth during specific times of the year, a more realistic model could include a ‘birth pulse’ where organisms are added to a population which grows during a specific time interval. Many models use the term ‘pulse’ to mean the population has a discontinuous jump. Here the population is continuous with an expected increase in animals for a period of time during the year. A comparison of continuous birth rate, where births may occur at any time of the year, and annual birth pulses was provided by Roberts and Kao. They investigated control of the spread of tuberculosis in possums, showing that periodic births may be approximated with a model with continuous births [28]. Tang et al. observed the birth pulses to cause a sequence of period-doubling bifurcations resulting from small amplitude periodic solutions [34]. Gao et al. modified the model of Tang to include the invasion of a disease and concludes that the controlling of disease is more efficient when prevention is seasonal [13].

A new feature of the model presented here is the investigation of birth pulses on the distribution of vaccine. One of the conclusions is that the distribution of the vaccine depends on the time that the rabies infection is detected relative to the birth pulse. The closer the detection is to the time of the seasonal births, the more sustained the level of vaccination. This project also uses optimal control strategies for a system that includes the dynamics of the vaccine. The goal is to find optimal strategies for distributing vaccine packets to minimize the infected population and the cost of implementing the control. The effect of the birth pulses on this strategy is investigated. The basic model is introduced in the next section followed by a discussion of the dynamics of the vaccine. Section 3 describes the existence of solutions for the corresponding adjoint system and an optimal control. Numerical results are reported in section 4 for various scenarios with section 5 considering the possibility of having a limited amount of vaccine available for distribution. We conclude with a summary and interpretation of the numerical simulations.

2.1 The Infected Raccoon Population

Various kinds of seasonal forcing have been shown to influence biological systems including infectious diseases [2, 1]. The periodic effect of annual birth pulses is a kind of forcing that occurs at the same time each year. It is assumed that raccoons give birth during the spring time of the year, March 20 - June 21. For a 365 day year starting from January 1, March 20 is day 79 and June 21 is day 172. The entire birth pulse is 93 days. There are four classes of raccoons that may be described by the system:

Our system of ODEs describe the dynamics between four classes: susceptibles, S , exposed, E , immune, R , and infecteds, I . The variable functions $S(t)$, $E(t)$, $R(t)$, and $I(t)$ are given in units of number of raccoons at time t . Any raccoon that can transmit the rabies virus will be in the *infected* class, designated as I . Raccoons that do not have the rabies virus but have the potential to contract the disease will be called *susceptible* and are identified as being in the susceptible class. When a susceptible becomes exposed to the rabies virus, an incubation period occurs during which time the raccoon does not immediately have the ability to transmit the disease but is only a latent carrier of the disease. The average time of this incubation period is $1/\sigma$. This class will be called *exposed* and represented as E . The interaction between the susceptible and exposed classes is assumed to follow mass action, so βIS where βIS is the rate that a member of the susceptible class becomes infected. Our system is given by

$$\begin{aligned}
 S' &= -(\beta I + b)S + a(S + E + R)\chi_\omega(t) \\
 E' &= \beta IS - (\sigma + b)E \\
 R' &= \sigma(1 - \rho)E - bR \\
 I' &= \sigma\rho E - \alpha I
 \end{aligned}
 \tag{2.1}$$

where the birth pulse occurs on the set $\omega = \bigcup_{k=0}^{\infty} [t_k, t_{k+1}]$, $t_k = 79 + 365k$ and $t_{k+1} =$

$172 + 365k$. (Since this paper is concerned with time intervals of one year or less, k will be taken as 0 for the remainder of the discussion.)

It is assumed that a small percentage of exposed raccoons will develop a natural immunity to the rabies virus. This percentage is $1 - \rho$, where ρ is the percentage that die from the disease. This phenomenon introduces a new class called the *immunes* and given the label R .

The per-capita birth rate per day is a during the birth pulse. During the spring, the S, E, R classes are able to give birth, and the birth rate is represented symbolically as

$$a[S(t) + E(t) + R(t)]\chi(t)_{[t_0, t_1]},$$

where $\chi(t)_{[t_0, t_1]}$ is a characteristic function of the time interval $[t_0, t_1]$ corresponding to March 20 and June 21, respectively. All births enter the susceptible class. Raccoons die of non-rabies causes at a per-capita rate per day of b . The total population at any time is $N = S + E + R + I$ with a dynamical equation of

$$N' = (a\chi_{[t_0, t_1]} - b)(S + E + R) - \alpha I.$$

Since the right hand sides of the state equations are measurable in t and continuous in the state and control variables, there exists a solution to the system (2.1) by Theorem 9.2 of [22].

We assume $E(0) = R(0) = 0$ and $S(0)$ and $I(0)$ are positive, and show the positivity of the state variables. There exists some $\hat{t} > 0$ such that $S(t), I(t)$ are both positive on the interval $(0, \hat{t})$. Consider

$$E' + (\sigma + b)E = \beta IS, E(0) = 0.$$

Since S, I are both positive on the interval $(0, \hat{t})$, we have the explicit solution

$$E(t) = e^{-(\sigma+b)t} \int_0^t e^{(\sigma+b)s} \beta IS ds.$$

Therefore $E(t) > 0$ for $t > 0$ such that

$$\int_0^t e^{(\sigma+b)s} \beta I S ds > 0,$$

and in particular $E(\hat{t}) > 0$.

Likewise for the immune class, the initial value problem

$$R' = \sigma(1 - \rho)E - bR, \quad R(0) = 0$$

yields the solution

$$R(t) = e^{-bt} \int_0^t e^{bs} \sigma(1 - \rho)s E(s) ds.$$

Therefore $R(t) > 0$ for $t > 0$ such that $\int_0^t e^{(\sigma+b)s} \beta I S ds > 0$, and $R(\hat{t}) > 0$.

Note the explicit solution for the infected class is

$$I(t) = e^{-\alpha t} \left[I(0) + \int_0^t e^{\alpha s} E(s) ds \right].$$

Using the above, we only need to consider the cases that the first state variable to decrease to zero is either S or I , i.e. $S = 0$ or $I = 0$ with \hat{t} being the first time that S or I hits 0. If $I(\hat{t}) = 0$, then $I'(\hat{t}) \leq 0$. But

$$I'(\hat{t}) = \sigma \rho E(\hat{t}) - \alpha I(\hat{t}) > 0,$$

which is a contradiction. Thus $I(t) > 0$ on the interval $(0, \hat{t}]$. If $S(\hat{t}) = 0$, then $S'(\hat{t}) \leq 0$. But

$$S'(\hat{t}) = -(\beta I(\hat{t}) + b)S(\hat{t}) + a[S(\hat{t}) + E(\hat{t}) + R(\hat{t})] \chi_\Omega > 0,$$

which is a contradiction, so $S(t) > 0$ on the interval $(0, \hat{t})$. We conclude that the state variables are positive for $t > 0$.

Note that since all the state variables are non-negative for all $t \geq 0$, then $N' \leq aN$

implies the boundedness of $N(t)$ for any finite time interval. Thus all the state variables are also bounded.

2.2 Introducing Vaccine Dynamics

The system of ordinary differential equations (2.1) is extended to include the dynamics of the amount of vaccine available to wildlife

$$\begin{aligned}
 S' &= -\left(\beta I + b + \frac{c_0 V}{K + V}\right)S + a(S + E + R)\chi(t)_{[t_0, t_1]} & (2.2) \\
 E' &= \beta I S - (\sigma + b)E \\
 R' &= \sigma(1 - \rho)E - bR + \frac{c_0 V S}{K + V} \\
 I' &= \sigma \rho E - \alpha I \\
 V' &= -V[c(S + E + R) + c_1] + u,
 \end{aligned}$$

where V is the amount of the vaccine at time t .

If vaccine baits are introduced into the environment, it is assumed that they are eaten by the susceptible raccoons with a conversion rate to the immune class as $\frac{c_0 V}{K + V}$. This term gives a saturation effect due to the foraging of raccoons on the baits. The constant K is a type of “half-saturation” constant, the value of V such that $\frac{V}{K + V}$ becomes $\frac{1}{2}$. The vaccine baits are depleted by being eaten by raccoons, other wildlife or through natural decay. The rate at which the baits are eaten by S , E and R , is c . Otherwise, the baits are eliminated at a rate of c_1 due to other causes, including natural decay and consumption by other animals. The control u is the rate of vaccine distribution. The state variables and parameters are described in Table 2.1.

Note that one can prove, as in section 2, that the states remain non-negative and bounded. We shall denote there is an upper bound on the states, M .

Table 2.1: State Variables and Parameters

Notation	Description	Units
$S(t)$	the number of susceptible at time t	raccoon
$E(t)$	the number of exposed at time t	raccoon
$R(t)$	the number of immune at time t	raccoon
$I(t)$	the number of infected at time t	raccoon
$V(t)$	amount of vaccine at time t	vaccine
c_0	rate raccoons become immune	day ⁻¹
c	rate vaccine is eaten by raccoons	day ⁻¹ raccoon ⁻¹
c_1	rate vaccine decays or eaten by other animals	day ⁻¹
K	saturation constant	raccoons
α	disease-related death rate	day ⁻¹
β	transmission rate	day ⁻¹ raccoon ⁻¹
a	birth rate	day ⁻¹
b	non-viral death rate	day ⁻¹
σ	rate raccoons move from E to I	day ⁻¹
ρ	natural immunity	none

2.3 Finding an Optimal Control

To minimize the infected population as well as the cost of the vaccine, the objective functional is

$$J(u) = \int_0^T [AI(t) + Bu(t)]dt.$$

The set of all admissible controls is

$$U = \{u : [0, T] \rightarrow [0, M_1] | u \text{ is Lebesgue measurable}\}$$

where M_1 is a positive constant and the upper bound of u . The coefficient A converts the number of infected raccoons into a cost. If we divide the objective functional by A , we will obtain the same optimal control. So the rate $\frac{B}{A}$ is a crucial parameter, and without loss we take $A = 1$. The cost coefficient B is a weight factor balancing the two terms. When B is large, then the cost of implementing the control is high. We seek to find u^* in U such that

$$J(u^*) = \min_{u \in U} J(u).$$

Theorem 2.3.1. *There exists an optimal control $u^* \in U$ which minimizes the objective functional $J(u)$.*

Proof:

Let $\{u_n(\cdot)\}_{n \geq 1}$ be a minimizing sequence and $P_n(\cdot) = (S_n, E_n, I_n, R_n, V_n)$ be the state trajectory corresponding to $u_n(\cdot)$. Since $P_n(\cdot)$ and $P_n'(\cdot)$ are both bounded in L^∞ , then $\{P_n(\cdot)\}$ is a uniformly bounded and equicontinuous sequence. Therefore, by the Arzela-Ascoli Theorem, there exists $P^*(\cdot)$ and $u^*(\cdot)$ such that

$$P_n(\cdot) \rightarrow P^*(\cdot) \text{ uniformly on } [0, T].$$

We have

$$\lim_{n \rightarrow \infty} J(u_n) = \lim_{n \rightarrow \infty} \int_0^T I_n(t) + Bu_n(t) ds = \inf_{u \in U} J(u),$$

since $I_n \rightarrow I^*$ uniformly and $u_n(t) \rightharpoonup u^*$ weakly in $L^2[0, T]$ on a subsequence due to the bounds on the controls. Passing to the limit in the state ODE system, we obtain that P^* is the state vector corresponding to control u^* . Thus we obtain

$$J(u^*) = \min_{u \in U} J(u).$$

Therefore, u^* is an optimal control. \square

To use Pontryagin's Maximum Principle [25], we form the Hamiltonian

$$\begin{aligned} H = & Bu + I + \lambda_1 \left[- \left(\beta IS + b + \frac{c_0 V}{K + V} \right) S + a(S + E + R) \chi(t)_{[t_0, t_1]} \right] \\ & + \lambda_2 [\beta IS - (\sigma + b)E] + \lambda_3 \left[\sigma(1 - \rho)E - bR + \frac{c_0 VS}{K + V} \right] \\ & + \lambda_4 [\sigma \rho E - \alpha I] + \lambda_5 \left[-V(c(S + E + R) + c_1) + u \right]. \end{aligned} \quad (2.3)$$

Grouped in terms of u

$$\begin{aligned}
H = & (B + \lambda_5)u + I + \lambda_1 \left[- \left(\beta IS + b + \frac{c_0 V}{K + V} \right) S + a(S + E + R)\chi(t)_{[t_0, t_1]} \right] \\
& + \lambda_2 [\beta IS - (\sigma + b)E] + \lambda_3 \left[\sigma(1 - \rho)E - bR + \frac{c_0 VS}{K + V} \right] \\
& + \lambda_4 [\sigma \rho E - \alpha I] + \lambda_5 \left[-V(c(S + E + R) + c_1) \right].
\end{aligned} \tag{2.4}$$

Theorem 2.3.2. *Given an optimal control u and corresponding state solutions S, E, I, R and V , there exists adjoint functions $\lambda_1(t), \lambda_2(t), \lambda_3(t), \lambda_4(t), \lambda_5(t)$ satisfying the adjoint system:*

$$\begin{aligned}
\lambda'_1 &= \lambda_1 \left(\beta I + b + \frac{c_0 V}{K + V} - a\chi(t)_{[t_0, t_1]} \right) - \lambda_2 \beta I - \lambda_3 \frac{c_0 V}{K + V} + \lambda_5 cV \\
\lambda'_2 &= -\lambda_1 a\chi(t)_{[t_0, t_1]} + \lambda_2(\sigma + b) - \lambda_3 \sigma(1 - \rho) - \lambda_4 \sigma \rho + \lambda_5 cV \\
\lambda'_3 &= -\lambda_1 a\chi(t)_{[t_0, t_1]} + \lambda_3 b + \lambda_5 cV \\
\lambda'_4 &= -1 + \lambda_1 \beta S - \lambda_2 \beta S + \lambda_4 \alpha \\
\lambda'_5 &= \frac{(\lambda_1 - \lambda_3)c_0 SK}{(K + V)^2} + \lambda_5 [c(S + E + R) + c_1]
\end{aligned} \tag{2.5}$$

with $\lambda_i(T) = 0$, for each i , and

$$u = \begin{cases} M_1 & \text{if } \lambda_5 + B < 0 \\ 0 & \text{if } \lambda_5 + B > 0 \\ u_s & \text{if } \lambda_5 + B = 0 \end{cases} \tag{2.6}$$

where the singular control is given by

$$\begin{aligned}
u_s = & -\frac{(K+V)}{2}[\beta I - a\chi(t)_{[t_0, t_1]}] + \frac{c_0(K-V)}{2} + a\frac{(K+V)}{2S}(E+R)\chi(t)_{[t_0, t_1]} \quad (2.7) \\
& + V\left[c(S+E+R) + c_1\right] + \frac{(K+V)(\lambda_1 - \lambda_2)\beta I}{2(\lambda_1 - \lambda_3)} + \frac{Bc(K+V)^3}{2c_0K(\lambda_1 - \lambda_3)}(b + a\chi(t)_{[t_0, t_1]}) \\
& + \frac{Bc(K+V)^3}{2c_0SK(\lambda_1 - \lambda_3)}\left[\sigma\rho E + (b + a\chi(t)_{[t_0, t_1]})(E+R)\right],
\end{aligned}$$

provided $0 \leq u_s \leq 1$.

Furthermore the generalized Legendre Clebsch condition is satisfied for this singular control giving necessary conditions when the optimal control is singular.

Proof: Suppose u is an optimal control and S, E, I, R, V are corresponding state variables. Using the result of Pontryagin's Maximum Principle [25], there exists adjoint variables $\lambda_1(t), \lambda_2(t), \lambda_3(t), \lambda_4(t), \lambda_5(t)$ satisfying

$$\begin{aligned}
\lambda_1' &= -\frac{\partial H}{\partial S} = \lambda_1\left[\beta I + b + \frac{c_0V}{K+V} - a\chi(t)_{[t_0, t_1]}\right] - \lambda_2\beta I - \lambda_3\frac{c_0V}{K+V} + \lambda_5cV \quad (2.8) \\
\lambda_2' &= -\frac{\partial H}{\partial E} = -\lambda_1a\chi(t)_{[t_0, t_1]} + \lambda_2(\sigma + b) - \lambda_3\sigma(1 - \rho) - \lambda_4\sigma\rho + \lambda_5cV \\
\lambda_3' &= -\frac{\partial H}{\partial R} = -\lambda_1a\chi(t)_{[t_0, t_1]} + \lambda_3b + \lambda_5cV \\
\lambda_4' &= -\frac{\partial H}{\partial I} = -1 + \lambda_1\beta S - \lambda_2\beta S + \lambda_4\alpha \\
\lambda_5' &= -\frac{\partial H}{\partial V} = \frac{(\lambda_1 - \lambda_3)c_0SK}{(K+V)^2} + \lambda_5\left[c(S+E+R) + c_1\right]
\end{aligned}$$

The behavior of the control may be obtained by differentiating the Hamiltonian with respect to u :

At time t , $H_u = B + \lambda_5$. For this minimization problem,

$$u = 0 \text{ when } H_u > 0 \text{ and}$$

$$u = M_1 \text{ when } H_u < 0.$$

Next we consider the singular case. If $H_u = 0$ on some non-empty open interval (a_1, b_1) , then $\lambda_5 = -B$ on (a_1, b_1) and $\lambda_5' = 0$. Substitution into the respective adjoint equation and rearranging gives

$$\frac{(\lambda_1 - \lambda_3)c_0SK}{(K + V)^2} = B \left[c(S + E + R) + c_1 \right]. \quad (2.9)$$

Since c_1 is a positive constant and the state variables are positive, equation (2.9) implies

$$\frac{(\lambda_1 - \lambda_3)c_0SK}{(K + V)^2} > 0$$

or

$$(\lambda_1 - \lambda_3) > 0, \text{ for all } t \text{ in } (a_1, b_1).$$

Differentiating λ_5' with respect to t yields

$$\lambda_5'' = \frac{(\lambda_1 - \lambda_3)c_0K}{(K + V)^2} \left(S' - \frac{2SV'}{K + V} \right) + \frac{c_0SK(\lambda_1' - \lambda_3')}{(K + V)^2} + \lambda_5c(S' + E' + R'). \quad (2.10)$$

Substituting for V' gives

$$\lambda_5'' = \frac{(\lambda_1 - \lambda_3)c_0K}{(K + V)^2} \left(S' + \frac{2SV[c(S + E + R) + c_1] - 2Su}{K + V} \right) + \frac{c_0SK(\lambda_1' - \lambda_3')}{(K + V)^2} + \lambda_5c(S' + E' + R').$$

Since $\lambda_5'' = 0$ on (a_1, b_1) , solving the above equation for u ,

$$u = \frac{(K + V)S'}{2S} + V[c(S + E + R) + c_1] + \frac{(K + V)(\lambda_1' - \lambda_3')}{2(\lambda_1 - \lambda_3)} + \frac{(K + V)^3}{2c_0SK(\lambda_1 - \lambda_3)} \lambda_5c(S' + E' + R').$$

Note that since $S(t)$ is positive, division by S is allowed.

Now consider

$$S' + E' + R' = -\sigma\rho E + \left[a\chi(t)_{[t_0, t_1]} - b \right] (S + E + R)$$

and

$$\begin{aligned}
\lambda'_1 - \lambda'_3 &= \lambda_1 \left(\beta I + b + \frac{c_0 V}{K + V} \right) - \lambda_2 \beta I - \lambda_3 \left(\frac{c_0 V}{K + V} + b \right) \\
&= (\lambda_1 - \lambda_3) \left(\frac{c_0 V}{K + V} + b \right) + (\lambda_1 - \lambda_2) \beta I.
\end{aligned} \tag{2.11}$$

Substitution into the expression for u with $\lambda_5 = -B$,

$$\begin{aligned}
u &= \frac{(K + V)}{2S} \left[- \left(\beta I + b + \frac{c_0 V}{K + V} \right) S + a(S + E + R) \chi(t)_{[t_0, t_1]} \right] + V \left[c(S + E + R) + c_1 \right] \\
&+ \frac{(K + V)}{2(\lambda_1 - \lambda_3)} \left[(\lambda_1 - \lambda_3) \left(\frac{c_0 V}{K + V} + b \right) + (\lambda_1 - \lambda_2) \beta I \right] \\
&- \frac{Bc(K + V)^3}{2c_0SK(\lambda_1 - \lambda_3)} \left[-\sigma\rho E + (a\chi(t)_{[t_0, t_1]} - b)(S + E + R) \right].
\end{aligned} \tag{2.12}$$

Distributing where appropriate,

$$\begin{aligned}
u &= - \frac{(K + V)}{2} (\beta I + b) - \frac{c_0 V}{2} + a \frac{(K + V)}{2S} (S + E + R) \chi(t)_{[t_0, t_1]} + V [c(S + E + R) + c_1] \\
&+ \frac{c_0 V}{2} + \frac{(K + V)b}{2} + \frac{(K + V)(\lambda_1 - \lambda_2) \beta I}{2(\lambda_1 - \lambda_3)} \\
&+ \frac{Bc(K + V)^3}{2c_0SK(\lambda_1 - \lambda_3)} [\sigma\rho E - (a\chi(t)_{[t_0, t_1]} - b)(S + E + R)].
\end{aligned} \tag{2.13}$$

Grouping like terms,

$$\begin{aligned}
u &= - \frac{(K + V)}{2} \beta I + a \frac{(K + V)}{2S} (S + E + R) \chi(t)_{[t_0, t_1]} + V [c(S + E + R) + c_1] \\
&+ \frac{(K + V)(\lambda_1 - \lambda_2) \beta I}{2(\lambda_1 - \lambda_3)} + \frac{Bc(K + V)^3}{2c_0SK(\lambda_1 - \lambda_3)} [\sigma\rho E - (a\chi(t)_{[t_0, t_1]} - b)(S + E + R)].
\end{aligned} \tag{2.14}$$

Continuing to group terms, the singular control is:

$$\begin{aligned}
u = & -\frac{(K+V)}{2}[\beta I - a\chi(t)_{[t_0, t_1]}] + a\frac{(K+V)}{2S}(E+R)\chi(t)_{[t_0, t_1]} \\
& + V[c(S+E+R) + c_1] + \frac{(K+V)(\lambda_1 - \lambda_2)\beta I}{2(\lambda_1 - \lambda_3)} - \frac{Bc(K+V)^3}{2c_0K(\lambda_1 - \lambda_3)}(a\chi(t)_{[t_0, t_1]} - b) \\
& + \frac{Bc(K+V)^3}{2c_0SK(\lambda_1 - \lambda_3)}[\sigma\rho E - (a\chi(t)_{[t_0, t_1]} - b)(E+R)].
\end{aligned} \tag{2.15}$$

Since λ_5' does not contain any u terms and λ_5'' does contain u , this singular control has order 1.

The generalized Legendre Clebsch condition [19] in a minimization problem with a singular control of order 1, is

$$(-1)\frac{\partial}{\partial u}\frac{d^2}{dt^2}\frac{\partial H}{\partial u} \geq 0,$$

and is a necessary condition for the singular control to be optimal. Our model has a singular control of order 1 and satisfies

$$(-1)\frac{\partial}{\partial u}\frac{d^2}{dt^2}\frac{\partial H}{\partial u} = -1\frac{\partial}{\partial u}\left[\frac{d^2}{dt^2}(B + \lambda_5)\right] = (-1)\frac{-2S(\lambda_1 - \lambda_3)c_0K}{(K+V)^3} > 0. \quad \square$$

Note that the numerical simulations will agree with the condition

$$(\lambda_1 - \lambda_3) > 0, \text{ for all } t.$$

The optimality system is the state system and the adjoint system coupled with the optimal control characterization. Next we illustrate our results by numerically solving the optimality system.

2.4 Numerical Results

Before we present our numerical results, we discuss our choice for parameters. The parameters were chosen based upon current literature and communication with Les Real and Scott Duke-Sylvester. Data indicated that the reproductive rate for mature female raccoons is between 1 and 8 kits/mature female/year [8]. Assuming a 50-50 sex rate, we

Table 2.2: Parameter Values

Parameter	Value	Units
c_0	0.8	day ⁻¹
c	0.01	day ⁻¹ raccoon ⁻¹
c_1	0.01	day ⁻¹
K	1.0	raccoons
α	0.182	day ⁻¹
β	0.01	day ⁻¹ raccoon ⁻¹
a	0.006	day ⁻¹
b	0.0015	day ⁻¹
σ	0.02	day ⁻¹
ρ	0.02	none

assume that half the population are mature females giving an approximate rate between 0.5 and 4 kits/raccoon/year. Since this model contains a birth pulse, dividing the extreme values by 93 days gives a range for the birth rate between 0.005 and 0.04 kits/raccoon/day.

First, we let the birth rate $a = \frac{0.006}{day}$. The death rate b was chosen to maintain a disease free population near the initial size at the end of one year. This disease free case can be solved explicitly by considering

$$S' = (a\chi_{\Omega} - b)S$$

with solution

$$S(t) = S(0)\exp\left[\int_0^t (a\chi_{\Omega}(\tau) - b)d\tau\right]$$

or

$$S(t) = S(0)\exp\left[-bt + \int_0^t a\chi_{\Omega}(\tau)d\tau\right].$$

Note that $S(t) = S(0)e^{-bt}e^{a[t_1-t_0]}$ when $t_1 \leq t \leq 365$. A sustainable population is achieved when $a[t_1 - t_0] - bt = 0$. For $t = 365$ and $t_1 - t_0 = 93$, we obtain $b = \frac{93a}{365}$. If the birth rate $a = 0.006$, then the death rate $b \approx 0.0015$. If $b > 0.0015$ then the total raccoon population N will die out. If $b < 0.0015$ then the total population N grows without bound. Figure 2.1 displays a graph of the population dynamics of raccoons for a duration of 1 year without

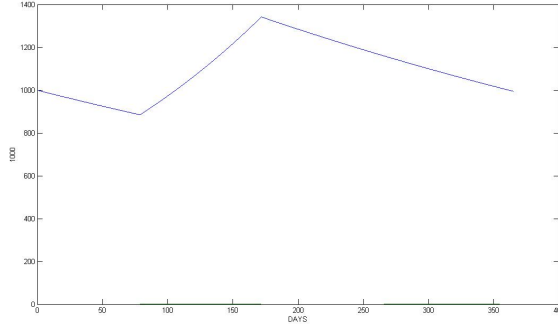


Figure 2.1: One year projection of disease free raccoon population starting on January 1 interaction with the rabies virus starting from an initial population of 1000, i.e. $S_0 = 1000$.

The period of time that infected raccoons are able to transmit the disease ranges from 3 to 14 days [9, 17]. For the following results, we assume the infectious period has a mean of 5.5 days. Therefore the rate α at which an infected raccoon leaves the infected class, $1/5.5$, is approximately 0.182. The rate of infection βI is taken to be $0.01I$ [29].

The incubation period, the time from infection until a raccoon is infectious (able to transmit the disease) or recovers, ranges from 18 to 107 days [9]. We assume a 49 day mean incubation period yielding a rate σ of approximately 0.02. Estimates for the fraction of animals that develop natural immunity ρ during the infection period have varied from 0 to 35.6% [29, 9]. We assume that 2% of the population develops natural immunity, i.e. $\rho = 0.02$.

Using [17, 9] and the form of our vaccination term in the susceptible equation we take $c_0 = 0.8$.

Johnston and Tinline [17] also state that 70% of the population will eat the vaccine if one bait per animal is provided in the range of their home. Therefore, a raccoon population of 1000 requires a distribution of approximately 714-1000 baits. The authors continue by estimating that half of all baits distributed are consumed within one week and about 80% are consumed within two weeks. If 714 baits are distributed, then 357 baits will be depleted after 7 days with a total of 571 baits consumed after 14 days. Assuming a linear relationship, we obtain a rate of 31 baits consumed per day. For a population of 1000 raccoons, the rate that the baits are eaten is at most 0.04 per day. Since the numbers include other animals

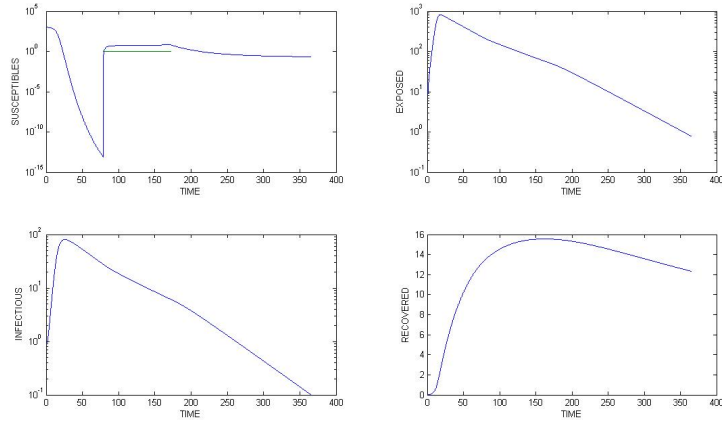
and the possibility that a raccoon may eat more than one bait, the rate used in the model for raccoons should be less than 0.04. The value of 0.01 was taken for c . We also assume that baits decay at the same rate as those eaten by the raccoons, i.e. $c_1 = 0.01$.

The graphical results involving the optimal control below were obtained using an iterative method with a 4th-order Runge-Kutta scheme programmed in MATLABTM to solve the optimality system. Starting with the initial conditions S_0, E_0, I_0, R_0, V_0 and an initial guess for the control, forward sweeps with the Runge-Kutta scheme were used to obtain approximate solutions for the state equations. Using those state values, the solutions of the adjoint equations were approximated using backward sweeps from the final time condition, $\lambda_1(T) = \lambda_2(T) = \dots = \lambda_5(T) = 0$. The control is updated by using an average of its previous values and its values from the control characterization. Iterations continue until convergence occurs, i.e., successive values of all variables from current and previous iterations are sufficiently close.

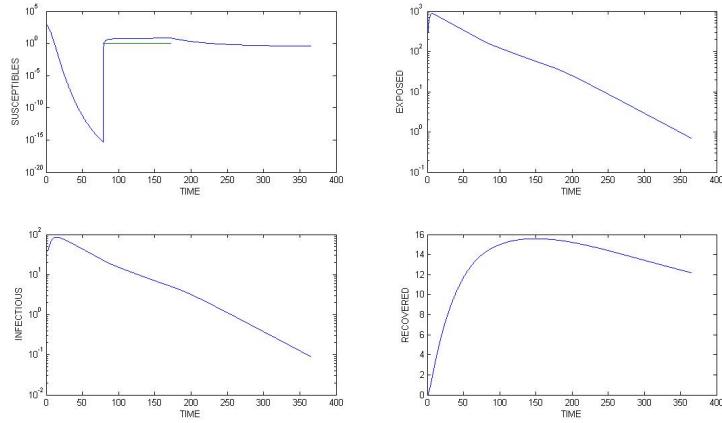
For the simulations of length 28 days, the grid was taken to be $N = 20,000$ and the tolerance was set at $\epsilon = 0.01$. If convergence was not achieved, the current values for the state and adjoint variables were used as initial and final conditions respectively and we repeated the process until reaching the desired convergence. For our results illustrated here, this process worked well.

The results that follow include representations of the states as well as the control variables. To help justify the *bang – bang* feature of the control, $|\lambda_5 + B|$ was used to verify the output of the control variable. Since the numerical results show $\lambda_1 - \lambda_3 > 0$, the singular case, which has $\lambda_1 - \lambda_3$ in the denominator, is not ruled out. But in our numerical results, the singular case does not occur.

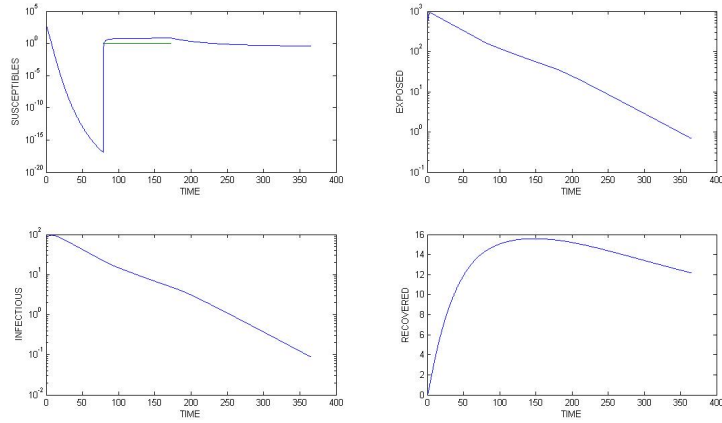
Figure 2.2 displays graphs of the populations with the same initial value for S , 1000, but with initial infected raccoons of 1, 40 and 100 with no control and for a duration of 1 year. Notice that raccoons in the susceptible class first move quickly into the exposed class and then into the infected class. Only a modest amount of raccoons move into the recovered class due to very low natural immunity. Notice the result of the birth pulse on S starting on day 79. Note the horizontal segment in this figure indicates the days of the



(a) 1 infectious raccoon



(b) 40 infectious raccoons



(c) 100 infectious raccoons

Figure 2.2: Populations of system 2.1 with initial values of 1, 40 and 100 infected raccoons and no control. Note the horizontal segment indicates the days of the birth pulse.

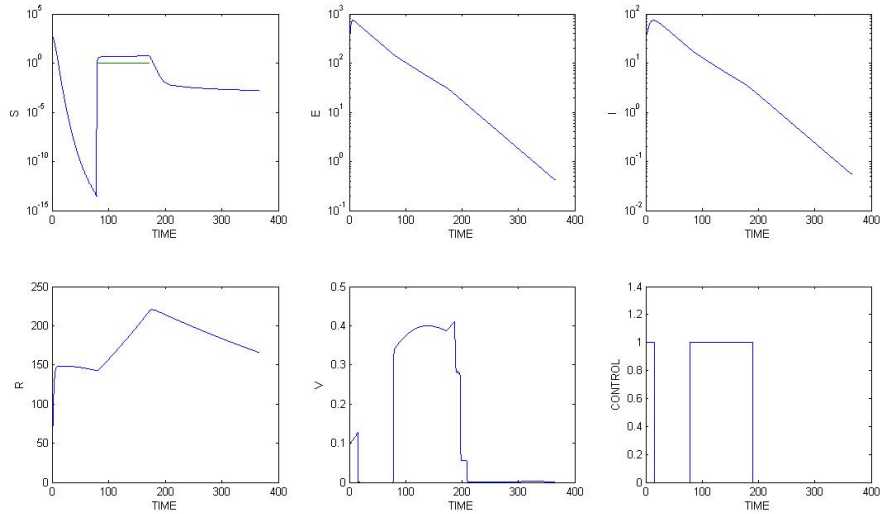


Figure 2.3: Optimal control results of system 2.2 projected for 1 year with $I_0 = 40$, $u = 1$ for days 1-14, 77-189. $B = 10^{-2}$

birth pulse.

Figure 2.3 shows the optimal results when vaccine is available during the course of 1 year beginning on January 1. The geographic area under consideration is assumed to be 100km^2 with initial populations of 1000 susceptibles and 40 infecteds, i.e., $S_0 = 1000, I_0 = 40$. It is also assumed that no exposed or immunes are initially present. The cost coefficient $B = 10^{-2}$ leads to the vaccine being distributed during the first 14 days of the year. The optimal strategy suggests resuming the distribution March 18 - July 19 (days 78-189). Note that after treatment, the immune class R assumes the pattern of the disease free scenario (figure 2.1).

Attempting to forecast the population dynamics for an entire year leads to several inherent problems. First, we do not have immigration and emigration in our system. During a year, some raccoons would come and go, so the model makes more sense for a shorter time period. Also, a month after the initial infecteds appear, the susceptible population decreases to very small numbers, and one would expect a time of quick response to stop the disease spread. Therefore, a duration of 28 days will be used in the numerical simulations that follow. Figure 2.4 displays a graph of the population dynamics of raccoons for a duration

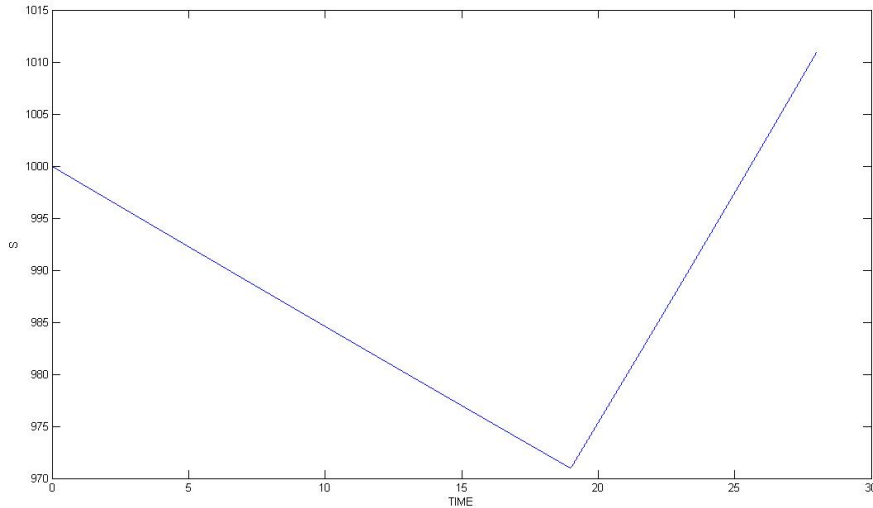


Figure 2.4: Disease free raccoon population results of system 2.1 starting on March 1

of 28 days without interaction with the rabies virus. The time period starts on March 1 (the 60th day of the year) with the birth pulse beginning on March 20 (the 79th day of the year). Like the previous examples, the initial susceptible population is 1000.

With the same initial number of susceptibles, we now introduce 40 infected raccoons on the 73th day of the year. The time period begins on March 14 for a duration of 28 days with the birth pulse starting on March 20. Since without any control the susceptibles quickly decrease in number, a logarithmic scale is used for the susceptibles in order to observe the effect of the pulse. Figure 2.5 shows the susceptibles quickly moving into the exposed class and the number of infecteds doubling approximately 12 days into the interval. Note the relatively small number in the immune class due to natural immunity.

When vaccine and the associated cost are included in the optimal control problem, the immune class increases due to the vaccination strategy. For example, under the same starting day and the same initial conditions $S_0 = 1000, I_0 = 40, R_0 = 0 = E_0$ and a cost coefficient $B = 10^{-4}$, the number of immunes increases from a maximum of 8 to almost 200. For this particular cost, the optimal control u is at 1 during days 1–27. Note that the peak of the exposed class decreases from approximately 850 to less than 60. The final numbers for the infected class decreases from 80 to less than 6. Note that the numerical results did

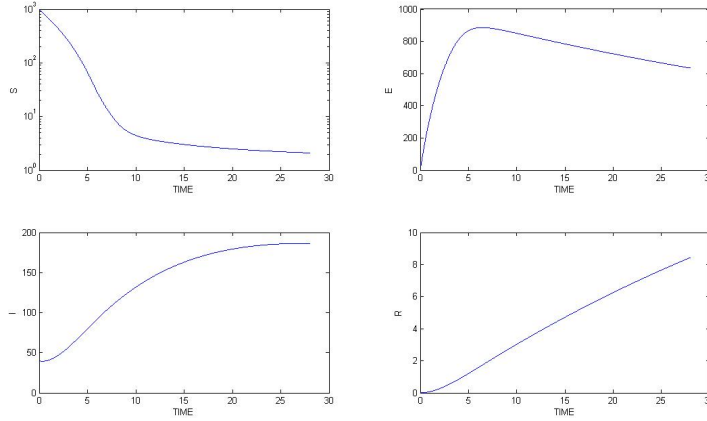
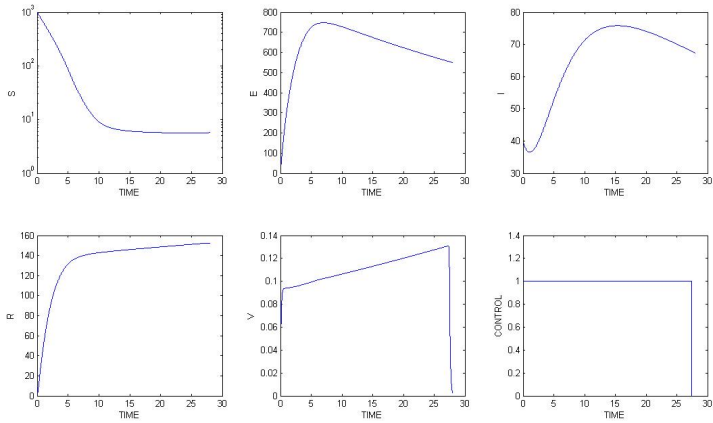


Figure 2.5: State variables of system 2.1 with disease and no control: Simulation begins on March 14.

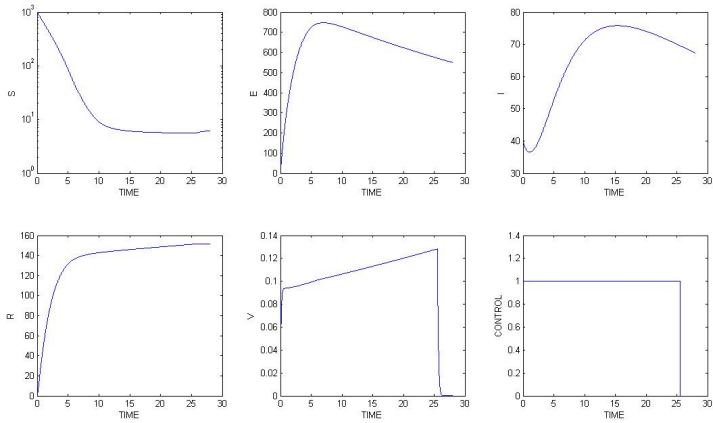
not indicate the singular case for this example. The graphical results representing this case are displayed in figure 2.6a.

With the same starting day, for a cost coefficient $B=10^{-2}$ and initial conditions $S_0 = 1000, I_0 = 40, R_0 = 0 = E_0$, the optimal control u is at 1 during days 1 – 22. While the results are similar for the state variables, the control decreases with the higher cost coefficient, being at 1 from 27 days to 22 days, due to the higher cost. Corresponding results are shown in figure 2.6b. For the larger cost coefficient of $B = 1$ and the same initial conditions, the control u is at 1 for days 1 – 9. We observe the expected result that a larger cost of distributing the vaccine corresponds to fewer days of distribution of the control. The associated graphical results are displayed in figure 2.6c.

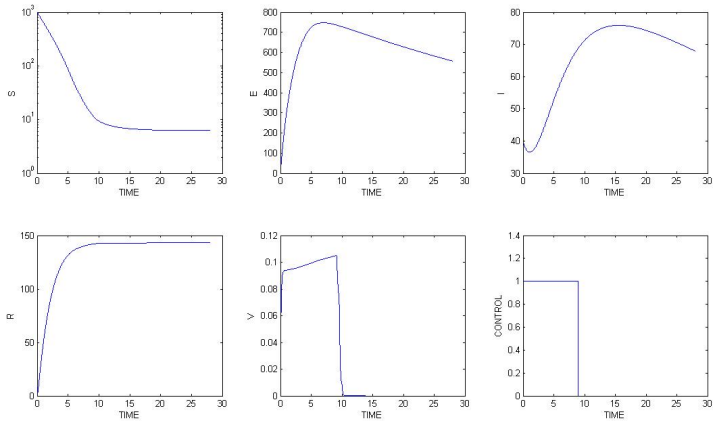
Additional simulations of a susceptible population interacting with 1, 40 and 100 infected raccoons with a cost coefficient of $B = 10^{-2}$ were completed using a start date approximately one week before the beginning of the birth pulse which corresponds approximately with March 13. These results showed that increasing I_0 decreases the number of immunes at the end of the 28 day interval however the number of days of distributing the vaccine remain approximately the same for all three cases. If the cost is increased to 10, i.e. $B = 10$, the control has similar results to those with $B = 1$, however the vaccine is distributed for only the first five days. For $B = 50$, the vaccine is further restricted



(a) $B = 10^{-4}$



(b) $B = 10^{-2}$



(c) $B = 10^0$

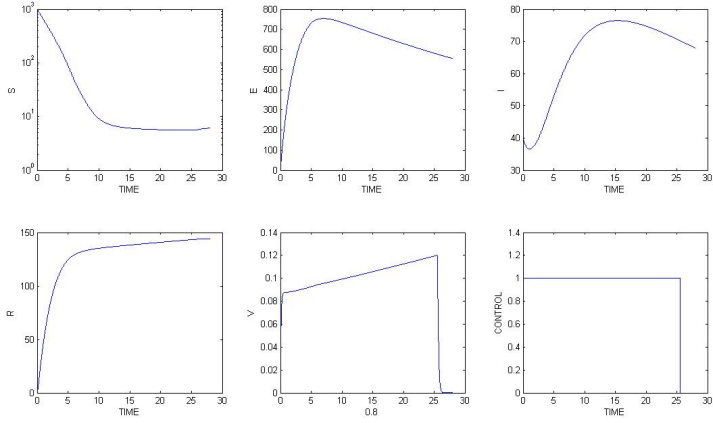
Figure 2.6: Optimal control results of system 2.2 for (a) $B = 10^{-4}$, (b) $B = 10^{-2}$, (c) $B = 10^0$

to the first two days with a noticeable reduction in the number of immunes. The findings illustrating all three cases are shown in figure 2.7.

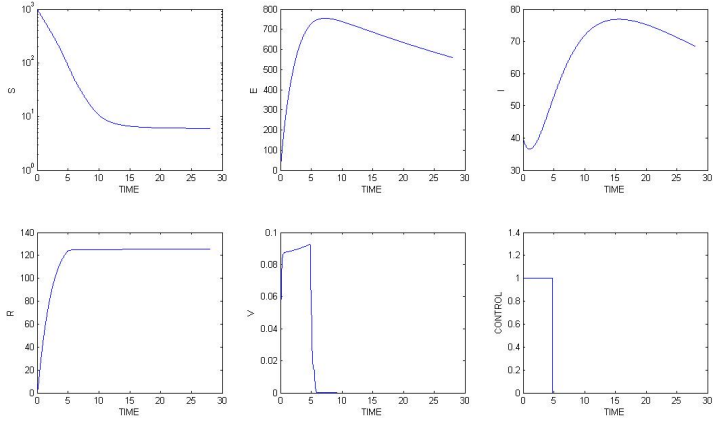
Figure A.1 show the results if the 28 day trial takes place during a time of the year without encountering a birth pulse (*a*), when the interval lies entirely within a birth pulse (*b*), and when the time interval initially begins on March 14 without a birth pulse but encounters the pulse after approximately 1 week into the interval (*c*). The control is used for nearly the entire 28 days for cases (*b*) and (*c*) when births are encountered. In the absence of births for any time during the entire 28 day interval, the amount of vaccine needed for distribution is approximately half as many as when the same duration lies within or overlaps the birth pulse. Note that (*c*) is the result from figure 2.6b.

Figure A.2a shows the results if the 28 day interval begins on March 1 approximately 3 weeks before the birth pulse. In this case vaccine is distributed for 12 days after the infection is detected and then resumes March 21-24, at the beginning of the birth pulse. If the outbreak is detected a month before the birth pulse, then the optimal amount of vaccine is distributed for the first 12 days only (figure A.2.b). In either case, results suggest starting treatment immediately for approximately two weeks. Baits are made available a second time coinciding with the addition of new susceptible raccoons into population due to the birth pulse. This case would be important to form a policy for doing a second round of vaccination when the birth pulse starts. Note that the susceptible graph displays a horizontal line representing the birth pulse beginning around March 21 corresponding to day 21.

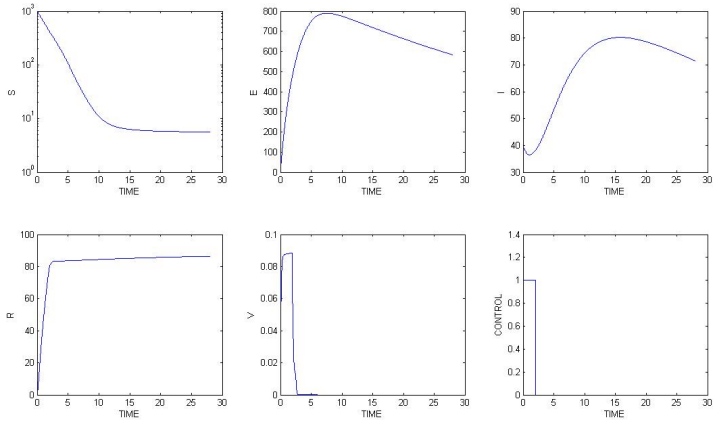
Next we change the upper bound of the controls. Figure A.3 shows the results when the upper bound for the control is increased, i.e. $0 \leq u \leq 5$. If the 28 day interval begins on March 14, the optimal distribution occurs during the first 24 days (figure A.2a). Beginning on March 1, the distribution occurs the first 10 after the infection is detected and then resumes briefly for March 21-23, a total of 13 days (figure A.3b). If the interval occurs a full month before the birth pulse, the vaccine is distributed on February 20 - March 2 and then on day 4 (figure A.3c). Each of these cases has fewer days of vaccine distribution due to a larger upper bound for u . Since the variable u represents a rate, an increased upper bound



(a) 40 infectious raccoons, $B=1$



(b) 40 infectious raccoons, $B=10$



(c) 40 infectious raccoons, $B=50$

Figure 2.7: Comparison of system 2.2 with varying cost coefficients beginning on March 14, seven days before the birth pulse.

of five for this example represents distributing five times the number of baits per unit time than was distributed for the prior simulations.

Since some parameters have a range of possible values [9], additional simulations were made using various values for the birth and death rates. For example, Coyne, et. al. gives a reproductive rate of 1.34 kits/raccoon/year. Dividing this number among a 93 day birth pulse gives approximately 0.014/raccoon/year. Recall that for the disease free case, the susceptible differential equation is

$$S' = (a\chi_\omega - b)S$$

with solution $S(t) = S(0)e^{-bt}e^{a[t_1-t_0]}$ when $t_1 \leq t \leq 365$. For $t = 365$ and $t_1 - t_0 = 93$, we obtain $b = \frac{93a}{365}$. If the birth rate $a = 0.014$, then the death rate $b \approx 0.004$. If $b > 0.004$ then the total raccoon population N will die out. If $b < 0.004$ then the total population N grows without bound. If the infectious period lasts for 14 days, this will yield an approximate value of 0.07 for α . Other parameters remained unchanged. The new set of parameter values are shown in Table 2.3.

The disease free population is shown in figure A.4 showing an equilibrium for the raccoons after one year. Note that the maximum number of raccoons for the year is significantly larger than with the old parameters.

Figure A.5 shows no control with the new parameter values. The recovered class shows the only noticeable change in the population dynamics compared to the old parameters in figure 2.2 reflecting a decrease in the number of raccoons near the end of the year.

If vaccine is available over a year, the optimal strategy distributes the control for days 75-191 when $B = 10^{-2}$. Figure A.6 displays the results for the new parameters and may be compared to figure 2.3 using the first set of parameters. The most significant difference is seen in the omission of the control until day 75.

Table 2.3: New Parameter Values

Parameter	Value	Units
α	0.07	day ⁻¹
a	0.014	day ⁻¹
b	0.004	day ⁻¹

As before, we now focus on 28 days for our time interval. With the new parameters, figure A.7 shows the disease free population for 28 days beginning on March 1. These results may be compared with those of figure 2.4 using the old parameters.

Forty infected raccoons introduced into the susceptible population on March 14 (the 73th day of the year) for 28 days yields a greater number of infecteds across time. The results without control are displayed in figure A.8. Note that more infected individuals occur with the new parameters versus the number of infected in figure 2.5 using the first set of parameters.

With the new parameters, more infected individuals occur compared to the results of figure 2.6a with a cost coefficient of $B = 10^{-4}$. The optimal control u is at 1 during days 1 – 27. With $B = 10^{-2}$ the optimal control u is at 1 during days 1 – 25, which is 3 days more than results with the old parameters. Again, more infecteds occur. For a cost coefficient $B = 10^0$ and the same initial conditions, the control u is at 1 for days 1 – 12, three more days than the results with the old parameters. The results are displayed in figure A.9 a,b,c, respectively.

Figure A.10a show the results if the 28 day interval takes place during a time of the year without encountering a birth pulse. The new parameters give 2 fewer days of control compared to the results in figure A.1a. When the interval lies within a birth pulse (b), the number of days distributing the control is the same as the results in figure A.1b. Part (c) gives the same number of days for the control distribution as in figure A.1c.

Now we change the date that the virus is detected to March 1 with figure A.11a showing the corresponding results. In this case vaccine is distributed 1-10, for 12 days after the infection is detected and then resumes March 19-25, at the beginning of the birth pulse, one day more than the old parameters. If the outbreak is detected on February 20 avoiding overlap with the birth pulse, then the optimal amount of vaccine is distributed for the first 10 days only, figure A.11b, (two days fewer than the old parameters). One style of control works for several ranges of parameters. These results should be compared with figure A.2 where fewer infected are shown for both cases.

Using the new values $a = 0.014/\text{day}$ for the birth rate and $b = 0.004/\text{day}$ for the death

rate with the old value for the time a raccoon spends infected $\alpha = 0.7$ yields results (figure A.12) more similar to the old parameter values (figure A.2a) than the new set of values (figure 2.11a). However the control is applied an additional four days including days 1-13 and 20-26.

2.5 Limited Vaccine

We now suppose a limited amount of vaccine is available for distribution. This limitation may be included in the above model by introducing a new state variable $z(t)$ such that

$$z(t) = \int_0^t u ds,$$

with

$$z(T) = \int_0^T u ds = C,$$

where $C = \text{constant}$. The new state equation becomes

$$z' = u, \text{ with boundary conditions } z(0) = 0, z(T) = C.$$

The Hamiltonian becomes

$$\begin{aligned} H = & \lambda_5 u + I + \lambda_1 \left[- \left(\beta I + b + \frac{c_0 V}{K + V} \right) S + a(S + E + R) \chi(t)_{[t_0, t_1]} \right] \\ & + \lambda_2 [\beta I - \sigma + b] + \lambda_3 \left[\sigma(1 - \rho)E - bR + \frac{c_0 V S}{K + V} \right] \\ & + \lambda_4 [\sigma \rho E - \alpha I] + \lambda_5 [-V(c(S + E + R) + c_1)] \\ & + \lambda_6 u, \end{aligned} \tag{2.16}$$

since the objective functional is

$$\min_u \int_0^T I(t) dt,$$

where the set of all admissible controls is

$$U = \{u : [0, T] \rightarrow [0, 1] | u \text{ is Lebesgue measurable}\}.$$

The adjoint equations in (2.5) above are included in the new adjoint system with the addition of

$$\lambda'_6 = -\frac{\partial H}{\partial z} = 0,$$

with no boundary conditions, since z has two boundary conditions.

The optimal control may be characterized as

$$u = \begin{cases} 1 & \text{if } \lambda_5 + \lambda_6 < 0 \\ 0 & \text{if } \lambda_5 + \lambda_6 > 0 \\ u_s & \text{if } \lambda_5 + \lambda_6 = 0 \end{cases} \quad (2.17)$$

where the singular control is given by

$$\begin{aligned} u_s = & -\frac{(K+V)}{2}[\beta I - a\chi(t)_{[t_0, t_1]}] + \frac{c_0(K-V)}{2} + a\frac{(K+V)}{2S}(E+R)\chi(t)_{[t_0, t_1]} \quad (2.18) \\ & + V[c(S+E+R) + c_1] + \frac{(K+V)(\lambda_1 - \lambda_2)\beta I}{2(\lambda_1 - \lambda_3)} + \frac{Bc(K+V)^3}{2c_0K(\lambda_1 - \lambda_3)}(b + a\chi(t)_{[t_0, t_1]}) \\ & + \frac{Bc(K+V)^3}{2c_0SK(\lambda_1 - \lambda_3)}[\sigma\rho E + (b + a\chi(t)_{[t_0, t_1]})(E+R)] \end{aligned}$$

as argued above.

After a desired target value for $z(T)$ was chosen, the code was executed repeatedly for a range of values of λ'_6 until the $z(T)$ was sufficiently close to the target value. The target was taken to be $z(T) = 10$ for the simulations below.

Figure A.13 shows the results with no birth pulse (a) and the result with the 28 day interval beginning on day 73 which is 6 days before the start of the birth pulse (b). The results show that the optimal control may be maintained during the first 10 days when no

birth pulse occurs in case (a), but requires a brief cessation in the middle of case (b).

2.6 Conclusion

The models developed and analyzed here included several new aspects to incorporate more realistic assumptions about rabies spread in racoons, with emphasis on developing optimal control schemes to determine the “best” methods to constrain the spread of the disease once it is detected. The new components incorporated include an exposed class, an explicit birth pulse which occurs seasonally, and dynamics of the vaccine packets associated with uptake by racoons as well as loss due to other factors. The key results derived illustrate the dependence on the optimal timing of distribution of vaccine packets on the timing of disease detection relative to the birth pulse. While the exact optimal timing results vary with parameter assumptions, there are a number of general results which appear to be rather robust based upon the illustrations presented here and numerous other cases also investigated.

One general result concerns a type of “rule of thumb” arising from investigation of the effect of the birth pulse on the timing of vaccine delivery which may be useful in developing policies for vaccine distribution following an outbreak detection. If the infection is detected near the start of the birth pulse, the optimal control distributes the vaccine immediately for a certain period of time (see figure A.1c). If the infection is detected a few weeks before the birth pulse, the optimal distribution of vaccine begins immediately, stops briefly and then resumes for a certain period of time (see figure A.2a). If the distribution starts at about March 1 or about 3 weeks before the start of the birth pulse, then under most situations (e.g. for most parameter sets investigated) a second round of vaccine distribution is optimal after the start of the birth pulse.

If the birth pulse occurs soon after the disease detection and the start of the vaccination distribution, the optimal treatment is necessary for a longer period of time (see figure A.1c). Thus if the disease were detected and distribution started at about March 14, more days of vaccine distribution are optimal than if the detection occurred on an earlier date. The closer the detection of the rabies outbreak is to the start of the birth pulse, the longer the

period of optimal distribution of vaccine is projected to be.

For other parameters fixed, the optimal number of days to distribute the vaccine decreases with higher cost. The general qualitative results noted above arise as well when costs are accounted for in a different manner, by assuming there is a fixed total amount of effort allowed on vaccine distribution (see figure 2.16a). The qualitative behavior of optimal solutions appears to be robust relative to differing assumptions about vaccine distribution costs.

Our examples focused on a 28 day total duration for the control period. In this situation, the number of infecteds is never completely eliminated, but if the optimal policy for vaccine distribution is followed, more raccoons join the immune class and that number exceeds the population of the infected class. The period for which the optimal solution is calculated can readily be extended using the same methodology presented here, but in this case additional assumptions must be made about immigration and emigration rates, which were ignored here due to the short duration of the time period considered. Sufficient input of new susceptibles due to immigration can effectively act as another "birth pulse" however and thus if net immigration is positive over some extended time period, the effect would be similar to a longer birth pulse. If net immigration included infected or exposed individuals, then we expect that the period of optimal vaccine distribution would be lengthened, though we have not investigated this situation.

A major use of general models such as those presented here is to evaluate under simplifying assumptions what the "best" policies would be to limit disease spread. As such they also allow elaboration of how much "worse" the impact of the disease would be (measured for example in terms of total number of deaths resulting from disease over the chosen time horizon) if the policy chosen were off by a small or large amount from the optimal one (measured for example in terms of the period for which the vaccine is distributed). This is useful for policy decisions in which there are uncertainties about the details of demographics or transmission assumptions in that they can provide a basis for determining how much effort might be effectively devoted to either obtaining more accurate data (e.g. through surveillance methods) rather than expending effort on further vaccination. Expansion of

the methods developed here to account for the trade-offs in expenditure for surveillance versus vaccination could well be a very important contributor to establishing policy decisions regarding wildlife infectious disease management.

Chapter 3

An Epidemic Model of Rabies in Raccoons with Density Dependent Mortality

3.1 Introduction

Natural death rates are frequently considered to be density dependent. For most common diseases in humans in developed countries, the assumption of a constant death rate is reasonable. For diseases among animal populations, this assumption may be unrealistic. Models that include a density dependent death rate are believed to be more realistic since infected animals die at higher rate than their noninfected counterparts and because of limited resources available to competing populations [16]. Similar considerations may hold in diseases in developing countries.

Greenhalgh investigated the structure and stability of equilibria using an ODE epidemic model for animal populations with a death rate, $f(N)$, dependent on the size of the population [16]. This compartmental epidemic model was shown to have a threshold condition for various equilibrium values. Depending on parameters and the structure of $f(N)$, the model may have one, two or three equilibria. His simulations show that the less harmful diseases may persist but diseases that cause more deaths are not as likely to continue. Roberts

discussed models with density-dependent birth, death, contact, and vertical transmission rates in wild-animal populations. The susceptible and infected classes form one model and produced at most four steady-state solutions one of which is globally asymptotically stable depending on the choice of parameters. The possibility of the endemic solution becoming unstable occurs when an exposed class is included in the dynamics [27]. In another density-dependent paper [4], control strategies are considered; sterilization and culling are shown to be more effective than vaccination when $R_0 > 3$ or when deaths are density dependent. If $R_0 < 3$ in the presence of density-dependent recruitment, culling or vaccination is more effective.

Again, our control strategy is the distribution of vaccine baits. We want to investigate how the optimal control results from the previous chapter change with a density dependent death rate. In our previous model the death rate is not density dependent. This chapter discusses a version of the previous model, with density dependence in the natural death terms.

First, let's consider the dynamical equation for the disease free population with a density dependent death rate:

$$S' = aS\chi(t)_{[t_0, t_1]} - bS^2$$

where S, a, b are defined as in the previous chapter and bS^2 reflects the density dependent death rate. The S class is able to give birth during the spring time of the year and the birth rate is represented symbolically as

$$aS(t)\chi(t)_{[t_0, t_1]},$$

where $\chi(t)_{[t_0, t_1]}$ is the characteristic function of the time interval $[t_0, t_1]$ corresponding to March 20 and June 21, respectively.

Next we will discuss the effects of exposure to the rabies virus on the model when vaccine is and is not available.

3.2 The Infected Raccoon Population

We again use an annual birth pulse, the periodic effect of which is a kind of forcing that occurs at the same time each year. It is assumed that raccoons give birth during the spring time of the year, March 20 - June 21. For a 365 day year starting from January 1, March 20 is day 79 and June 21 is day 172. The entire birth pulse is 93 days. Using the same notation as the previous chapter, there are four classes of raccoons that may be described by the system:

$$\begin{aligned}
 S' &= -\beta IS + a(S + E + R)\chi(t)_{[t_0, t_1]} - bS(S + E + R) \\
 E' &= \beta IS - \sigma E - bE(S + E + R) \\
 R' &= \sigma(1 - \rho)E - bR(S + E + R) \\
 I' &= \sigma\rho E - \alpha I,
 \end{aligned} \tag{3.1}$$

where the birth pulse occurs on the set

$$\omega = \bigcup_{k=0}^{\infty} [t_k, t_{k+1}], \text{ with } t_k = 79 + 365k \text{ and } t_{k+1} = 172 + 365k$$

and where $-bS(S + E + R)$, $-bE(S + E + R)$, and $-bR(S + E + R)$ are the natural death rates. The other terms are the same as in the previous chapter and we again assume that $\Omega = [t_0, t_1]$.

If the right hand sides of the state equation are measurable in t with bounded state variables, there exist a solution to the system (3.1) ([22], by Theorem 9.2.1).

We assume $E(0) = R(0) = 0$ and that $S(0)$ and $I(0)$ are positive. Positivity of the state variables may be shown to be positive using arguments similar to those of the previous chapter.

Note that since all the state variables are non-negative for all $t \geq 0$, then $N' \leq aN$

implies the boundedness of $N(t)$ for any finite time interval. Thus all the state variables are also bounded.

3.3 Introduction of Vaccine

When vaccine is introduced the system becomes:

$$\begin{aligned}
S' &= -\left(\beta I + \frac{c_0 V}{K + V}\right)S + a(S + E + R)\chi(t)_{[t_0, t_1]} - bS(S + E + R) & (3.2) \\
E' &= \beta IS - \sigma E - bE(S + E + R) \\
R' &= \sigma(1 - \rho)E - bR(S + E + R) + \frac{c_0 VS}{K + V} \\
I' &= \sigma\rho E - \alpha I \\
V' &= -V[c(S + E + R) + c_1] + u,
\end{aligned}$$

with initial conditions $S(0) = S_0 > 0$, $E(0) = E_0 = R(0) = 0$, $I(0) = I_0 > 0$.

As before, the infected population and the cost of the vaccine is to be minimized with the corresponding objective functional

$$\min_u \int_0^T [I(t) + Bu(t)]dt,$$

where the set of all admissible controls is

$$U = \{u : [0, T] \rightarrow [0, 1] | u \text{ is Lebesgue measurable}\}$$

and B is a weight factor balancing the two terms. When B is large, then the cost of implementing the control is high.

Arguments similar to chapter 1 may be used to show the existence, the boundedness, and positivity of the the state variables.

Now we turn to deriving the optimality system, again using Pontryagin's Maximum

Principle [25].

3.4 Finding an Optimal Control

As before the solutions of the state system exists and are bounded and non-negative. Also one can show there exists an optimal control. Now we derive the necessary conditions that an optimal control must satisfy.

The Hamiltonian grouped in terms of u is

$$\begin{aligned}
H = & (B + \lambda_5)u + I + \lambda_1 \left[- \left(\beta I + \frac{c_0 V}{K + V} \right) S + a(S + E + R)\chi(t)_{[t_0, t_1]} - bS(S + E + R) \right] \\
& + \lambda_2 [\beta I S - \sigma E - bE(S + E + R)] + \lambda_3 \left[\sigma(1 - \rho)E - bR(S + E + R) + \frac{c_0 V S}{K + V} \right] \\
& + \lambda_4 [\sigma \rho E - \alpha I] + \lambda_5 [-V(c(S + E + R) + c_1)].
\end{aligned} \tag{3.3}$$

Theorem 3.4.1. *Given an optimal control u and corresponding state solutions S, E, I, R and V , there exists adjoint functions $\lambda_1(t), \lambda_2(t), \lambda_3(t), \lambda_4(t), \lambda_5(t)$ satisfying the adjoint system:*

$$\begin{aligned}
\lambda_1' = & \lambda_1 \left[\beta I + \frac{c_0 V}{K + V} - a\chi(t)_{[t_0, t_1]} + b(2S + E + R) \right] \\
& + \lambda_2 (bE - \beta I) + \lambda_3 (bR - \frac{c_0 V}{K + V}) + \lambda_5 cV \\
\lambda_2' = & \lambda_1 [bS - a\chi(t)_{[t_0, t_1]}] + \lambda_2 [\sigma + b(S + 2E + R)] + \lambda_3 (bR - \sigma(1 - \rho)) - \lambda_4 \sigma \rho + \lambda_5 cV \\
\lambda_3' = & \lambda_1 [bS - a\chi(t)_{[t_0, t_1]}] + \lambda_2 bE + \lambda_3 b(S + E + 2R) + \lambda_5 cV \\
\lambda_4' = & -1 + \lambda_1 \beta S - \lambda_2 \beta S + \lambda_4 \alpha \\
\lambda_5' = & \frac{(\lambda_1 - \lambda_3)c_0 S K}{(K + V)^2} + \lambda_5 \left[c(S + E + R) + c_1 \right]
\end{aligned} \tag{3.4}$$

with $\lambda_i(T) = 0$, for each i , and

$$u = \begin{cases} M_1 & \text{if } \lambda_5 + B < 0 \\ 0 & \text{if } \lambda_5 + B > 0 \\ u_s & \text{if } \lambda_5 + B = 0 \end{cases} \quad (3.5)$$

where the singular control is given by

$$\begin{aligned} u = & -\frac{(K+V)}{2}[\beta I - a\chi(t)_{[t_0, t_1]}] + a\frac{(K+V)}{2S}(E+R)\chi(t)_{[t_0, t_1]} \\ & + V[c(S+E+R) + c_1] + \frac{(K+V)(\lambda_1 - \lambda_2)\beta I}{2(\lambda_1 - \lambda_3)} - \frac{Bc(K+V)^3}{2c_0K(\lambda_1 - \lambda_3)}(a\chi(t)_{[t_0, t_1]} - b(S+E+R)) \\ & + \frac{Bc(K+V)^3}{2c_0SK(\lambda_1 - \lambda_3)}[\sigma\rho E - (a\chi(t)_{[t_0, t_1]} - b(S+E+R))(E+R)] \end{aligned} \quad (3.6)$$

provided $0 \leq u_s \leq 1$.

Proof: Suppose u is an optimal control and S, E, I, R, V are corresponding state solutions. Using the result of Pontryagin's Maximum Principle[25], there exists adjoint variables $\lambda_1(t), \lambda_2(t), \lambda_3(t), \lambda_4(t), \lambda_5(t)$ satisfying

$$\begin{aligned} \lambda_1' &= -\frac{\partial H}{\partial S} \\ &= \lambda_1 \left[\beta I + \frac{c_0 V}{K+V} - a\chi(t)_{[t_0, t_1]} + b(2S+E+R) \right] + \lambda_2(bE - \beta I) + \lambda_3(bR - \frac{c_0 V}{K+V}) + \lambda_5 cV \\ \lambda_2' &= -\frac{\partial H}{\partial E} = \lambda_1(bS - a\chi(t)_{[t_0, t_1]}) + \lambda_2[\sigma + b(S+2E+R)] - \lambda_3(\sigma(1-\rho) - bR) - \lambda_4\sigma\rho + \lambda_5 cV \\ \lambda_3' &= -\frac{\partial H}{\partial R} = \lambda_1(bS - a\chi(t)_{[t_0, t_1]}) + \lambda_2 bE + \lambda_3 b(S+E+2R) + \lambda_5 cV \\ \lambda_4' &= -\frac{\partial H}{\partial I} = -1 + \lambda_1\beta S - \lambda_2\beta S + \lambda_4\alpha \\ \lambda_5' &= -\frac{\partial H}{\partial V} = \frac{(\lambda_1 - \lambda_3)c_0SK}{(K+V)^2} + \lambda_5 \left[c(S+E+R) + c_1 \right]. \end{aligned} \quad (3.7)$$

The behavior of the control may be obtained by differentiating the Hamiltonian with respect to u : at time t , $H_u = B + \lambda_5$. For this minimization problem,

$$u = 0 \text{ when } H_u > 0 \text{ and}$$

$u = 1$ when $H_u < 0$.

Next we consider the singular case. If $H_u = 0$ on some non-empty open interval (a_1, b_1) of time, then $\lambda_5 = -B$ on (a_1, b_1) and $\lambda'_5 = 0$. Substitution into the respective adjoint equation and rearranging gives

$$\frac{(\lambda_1 - \lambda_3)c_0SK}{(K + V)^2} = B \left[c(S + E + R) + c_1 \right]. \quad (3.8)$$

Since c_1 is a positive constant and the state variables are positive for $t > 0$, equation (4.6) implies

$$\frac{(\lambda_1 - \lambda_3)c_0SK}{(K + V)^2} > 0$$

or

$$(\lambda_1 - \lambda_3) > 0, \text{ for all } t \in (a_1, b_1).$$

Differentiating λ'_5 with respect to t yields

$$\lambda''_5 = \frac{(\lambda_1 - \lambda_3)c_0K}{(K + V)^2} \left(S' - \frac{2SV'}{K + V} \right) + \frac{c_0SK(\lambda'_1 - \lambda'_3)}{(K + V)^2} + \lambda_5c(S' + E' + R') + \lambda'_5[c(S + E + R) + c_1]. \quad (3.9)$$

Substituting for V' and using $\lambda'_5 = 0$ gives

$$\begin{aligned} \lambda''_5 = & \frac{(\lambda_1 - \lambda_3)c_0K}{(K + V)^2} \left(S' + \frac{2SV[c(S + E + R) + c_1] - 2Su}{K + V} \right) \\ & + \frac{c_0SK(\lambda'_1 - \lambda'_3)}{(K + V)^2} + \lambda_5c(S' + E' + R'). \end{aligned} \quad (3.10)$$

Since $\lambda''_5 = 0$ on (a_1, b_1) , solving the above equation for the u term,

$$\begin{aligned} \frac{2Sc_0K(\lambda_1 - \lambda_3)}{(K + V)^3} u = & \frac{(\lambda_1 - \lambda_3)c_0K}{(K + V)^2} S' + \frac{2c_0SVK(\lambda_1 - \lambda_3)[c(S + E + R) + c_1]}{(K + V)^3} \\ & + \frac{c_0SK(\lambda'_1 - \lambda'_3)}{(K + V)^2} + \lambda_5c(S' + E' + R'). \end{aligned} \quad (3.11)$$

and solving for u ,

$$u = \frac{(K+V)S'}{2S} + V[c(S+E+R)+c_1] + \frac{(K+V)(\lambda'_1 - \lambda'_3)}{2(\lambda_1 - \lambda_3)} + \frac{(K+V)^3}{2c_0SK(\lambda_1 - \lambda_3)} \lambda_5 c(S'+E'+R').$$

Note that since $S(t)$ is positive, division by S is allowed.

Now consider

$$S' + E' + R' = -\sigma\rho E + [a\chi(t)_{[t_0, t_1]} - b(S + E + R)](S + E + R)$$

and

$$\begin{aligned} \lambda'_1 - \lambda'_3 &= \lambda_1 \left(\beta I + b(S + E + R) + \frac{c_0 V}{K + V} \right) - \lambda_2 \beta I - \lambda_3 \left(\frac{c_0 V}{K + V} + b(S + E + R) \right) \\ &= (\lambda_1 - \lambda_3) \left(\frac{c_0 V}{K + V} + b(S + E + R) \right) + (\lambda_1 - \lambda_2) \beta I. \end{aligned} \tag{3.12}$$

Substitution into the expression for u with $\lambda_5 = -B$,

$$\begin{aligned} u &= \frac{(K+V)}{2S} \left[- \left(\beta I + b(S + E + R) + \frac{c_0 V}{K + V} \right) S + a(S + E + R) \chi(t)_{[t_0, t_1]} \right] \\ &\quad + V \left[c(S + E + R) + c_1 \right] + \frac{(K+V)}{2(\lambda_1 - \lambda_3)} \left[(\lambda_1 - \lambda_3) \left(\frac{c_0 V}{K + V} + b(S + E + R) \right) + (\lambda_1 - \lambda_2) \beta I \right] \\ &\quad - \frac{Bc(K+V)^3}{2c_0SK(\lambda_1 - \lambda_3)} \left[-\sigma\rho E + (a\chi(t)_{[t_0, t_1]} - b(S + E + R))(S + E + R) \right]. \end{aligned} \tag{3.13}$$

Distributing where appropriate,

$$\begin{aligned}
u = & -\frac{(K+V)}{2}(\beta I + b(S+E+R)) - \frac{c_0 V}{2} + a\frac{(K+V)}{2S}(S+E+R)\chi(t)_{[t_0, t_1]} \quad (3.14) \\
& + V[c(S+E+R) + c_1] + \frac{c_0 V}{2} + \frac{(K+V)b(S+E+R)}{2} + \frac{(K+V)(\lambda_1 - \lambda_2)\beta I}{2(\lambda_1 - \lambda_3)} \\
& + \frac{Bc(K+V)^3}{2c_0SK(\lambda_1 - \lambda_3)}[\sigma\rho E - (a\chi(t)_{[t_0, t_1]} - b(S+E+R))(S+E+R)]
\end{aligned}$$

Grouping like terms,

$$\begin{aligned}
u = & -\frac{(K+V)}{2}\beta I + a\frac{(K+V)}{2S}(S+E+R)\chi(t)_{[t_0, t_1]} + V[c(S+E+R) + c_1] \quad (3.15) \\
& + \frac{(K+V)(\lambda_1 - \lambda_2)\beta I}{2(\lambda_1 - \lambda_3)} + \frac{Bc(K+V)^3}{2c_0SK(\lambda_1 - \lambda_3)}[\sigma\rho E - (a\chi(t)_{[t_0, t_1]} - b(S+E+R))(S+E+R)]
\end{aligned}$$

Continuing to group terms, the singular control is:

$$\begin{aligned}
u = & -\frac{(K+V)}{2}[\beta I - a\chi(t)_{[t_0, t_1]}] + a\frac{(K+V)}{2S}(E+R)\chi(t)_{[t_0, t_1]} \quad (3.16) \\
& + V[c(S+E+R) + c_1] + \frac{(K+V)(\lambda_1 - \lambda_2)\beta I}{2(\lambda_1 - \lambda_3)} - \frac{Bc(K+V)^3}{2c_0K(\lambda_1 - \lambda_3)}(a\chi(t)_{[t_0, t_1]} - b(S+E+R)) \\
& + \frac{Bc(K+V)^3}{2c_0SK(\lambda_1 - \lambda_3)}[\sigma\rho E - (a\chi(t)_{[t_0, t_1]} - b(S+E+R))(E+R)]
\end{aligned}$$

The Legendre Clebsch condition [19] in a problem with a singular control of order 1, is

$$(-1)\frac{\partial}{\partial u}\frac{d^2}{dt^2}\frac{\partial H}{\partial u} \geq 0.$$

Since the control u occurs in the equation λ_5'' but not in λ_5' our model satisfies the same condition

$$(-1)\frac{-2S(\lambda_1 - \lambda_3)c_0K}{(K+V)^3} > 0,$$

which means the second order necessary condition is satisfied and the singular control could occur. \square

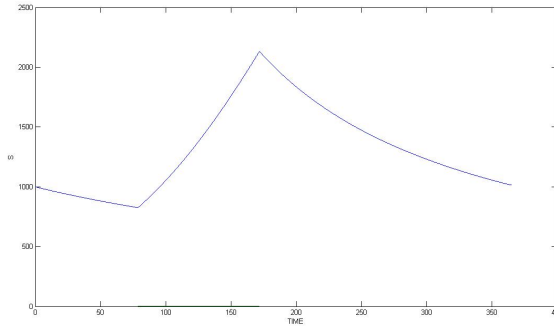


Figure 3.1: One year projection of disease free raccoon population starting on January 1

The optimality system is the state system and the adjoint system coupled with the optimal control characterization. Next we illustrate our results by numerically solving the optimality system. We note that the numerical results below will agree with the condition

$$(\lambda_1 - \lambda_3) > 0, \text{ for all } t \in (a_1, b_1).$$

3.5 Numerical Results

The second set of parameter values from chapter 2 are used again in this chapter. In particular:

$a = 0.014/\text{day}$ birth rate (constant per-capita)

$b = 0.004 \times 10^{-3}$ /day death rate (constant per-capita)

$1/\alpha = 1/0.071$ average time raccoon spends infectious

$1/\sigma = 1/0.02$ average time from infection until raccoon dies or recovers

See Table 2.2 for the other parameter values.

Figure 3.1 displays a graph of the population dynamics of raccoons for a duration of 1 year without interaction with the rabies virus starting from an initial population of 1000, $S_0 = 1000$. The impact of the birth pulse can be seen beginning on day 79 and continuing for approximately 3 months. Note that at the end of one year the population is near the initial condition of $S_0 = 1000$.

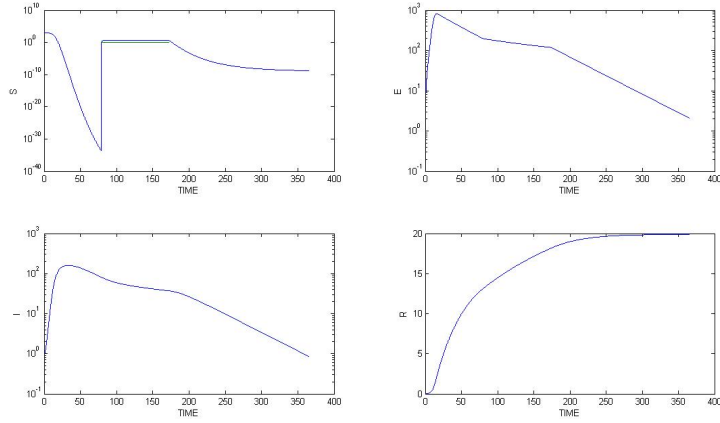
The density dependent death rate b was based on work by Scott Duke-Sylvester. Recall that the death rate b is 0.004 in the non-density dependent case. Thus in a population of 1000 raccoons with density dependent deaths, the death rate becomes 0.004×10^{-3} per raccoon. Other parameters remain unchanged. Using the same iterative method as in the second chapter on the optimality system, we compare various cases to our results from the previous chapter. Again, in our numerical results, the singular case does not occur.

Figure 3.2 displays graphs of the populations with the same initial value for S but with initial infected raccoons of 1, 40 and 100 for a duration of 1 year. A logarithmic scale is used to more clearly show the dynamics of the susceptible population including the effect of the birth pulse. Note the modest number of the recovered class due to natural immunity.

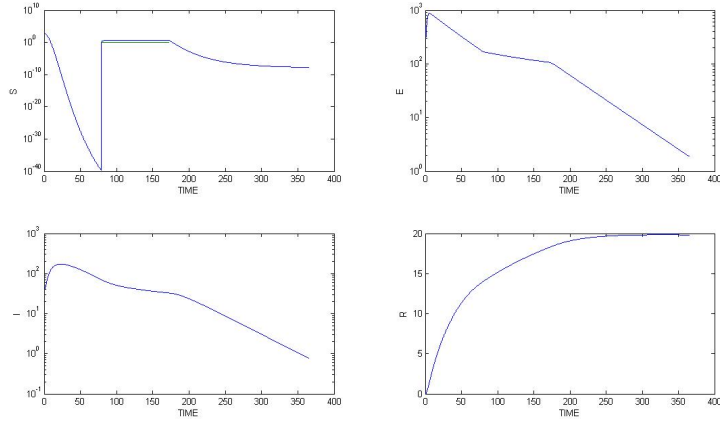
This model assumes that a percentage of raccoons will acquire immunity naturally by a factor of $1 - \rho$. Coyne indicates that the threshold density number above which the disease will persist in a population is directly proportional to the percentage of raccoons acquiring immunity after being infected [9]. Also, as the number of raccoons that develop natural immunity increases, the less the population deviates from the carrying capacity. Dynamics of the infected population are shown in figure 3.3 with different values for the rate of natural immunity $1 - \rho$. Without natural immunity, $\rho = 1$, a recurrence of rabid raccoons occurs every 4 to 5 years as shown in figure 3.3a. If 1% or 2% of the of the population acquires natural immunity, a more frequent occurrence of the infected peaks is shown in 3.3b and 3.3c respectively. For the simulations that follow, $\rho = 0.02$.

Figure 3.4 displays an optimal strategy for one year when the rabies virus is detected on January 1 and vaccine is available with a cost coefficient of $B = 10^{-2}$. The geographic area under consideration is again large enough for a susceptible population of 1000 with 40 infecteds, ie., $S_0 = 10000, I_0 = 40$. It is also assumed that no exposed or immunes are initially present. These results may be compared with the non-density dependent case of figure A.6 which has the same initial conditions and value of B . Note for figure 3.4 the distribution begins 2 days later and ends 6 days earlier as compared to figure A.6. For the second round of vaccination, the control begins on the same day but ends four days earlier.

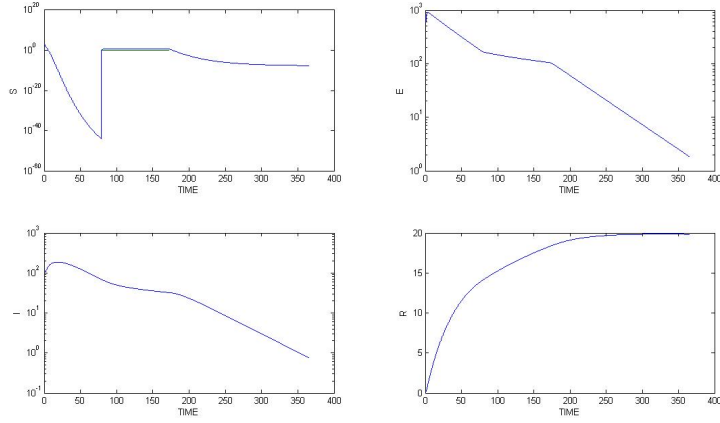
We now focus on the short term behavior for a 28 day time period beginning on March



(a) 1 infectious raccoon

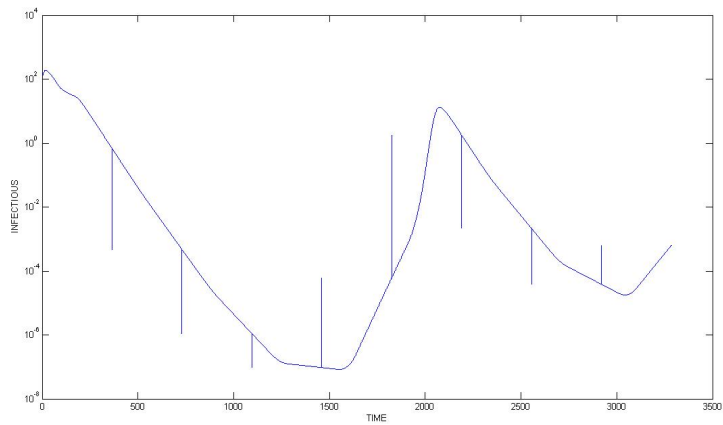


(b) 40 infectious raccoons

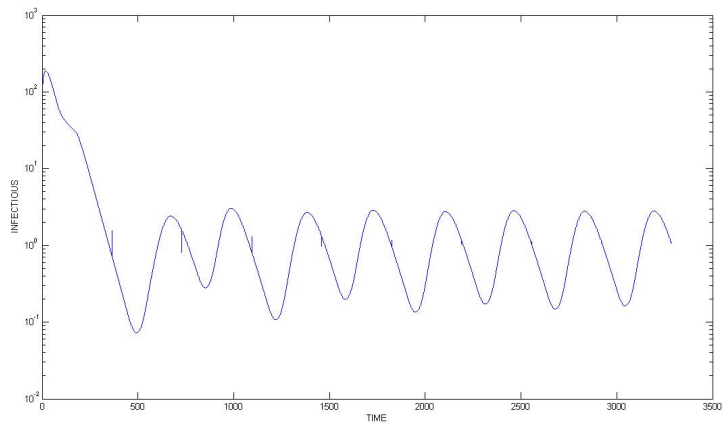


(c) 100 infectious raccoons

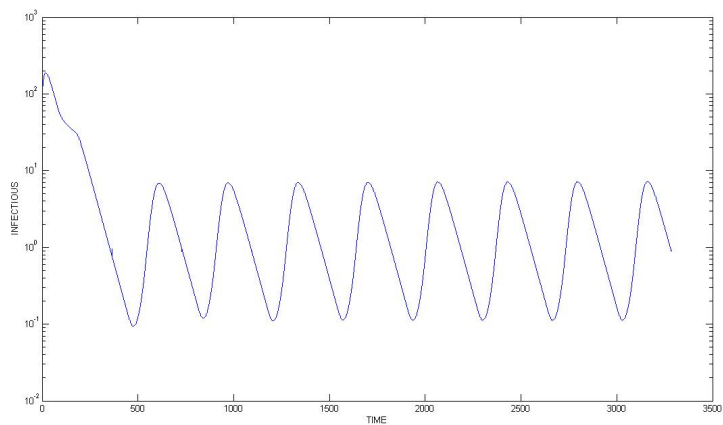
Figure 3.2: Populations of system 3.1 with initial values of 1, 40 and 100 infected raccoons and no control



(a) $\rho = 1.0$



(b) $\rho = 0.99$



(c) $\rho = 0.98$

Figure 3.3: Infected Populations of system 3.2 with varying natural immunity

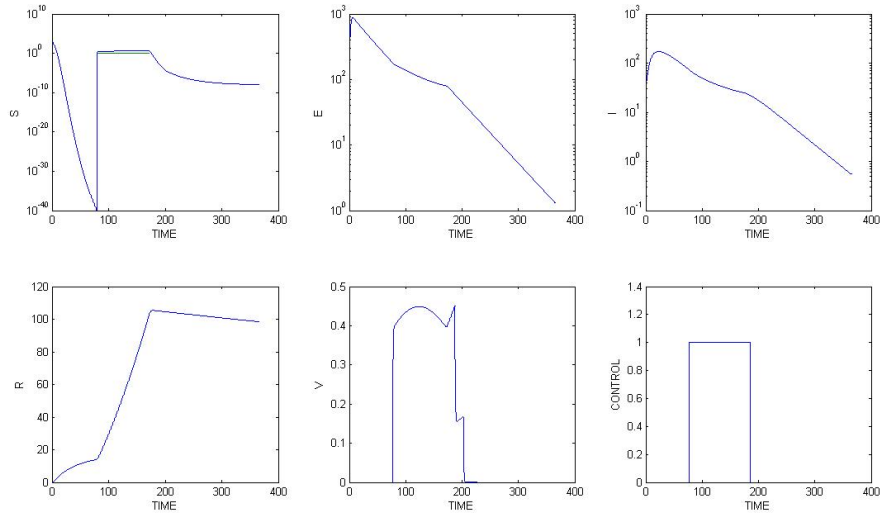
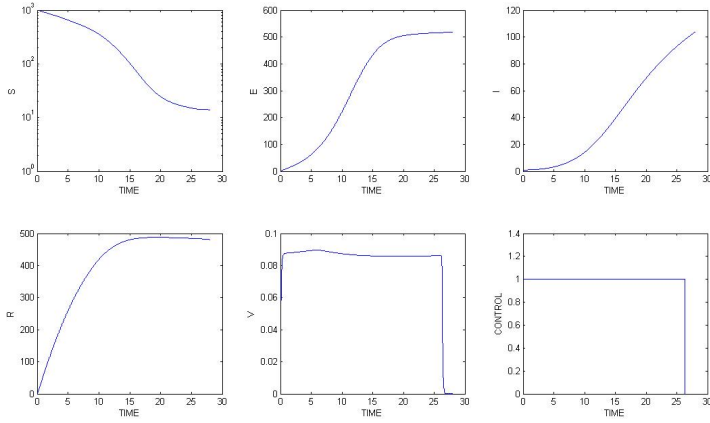


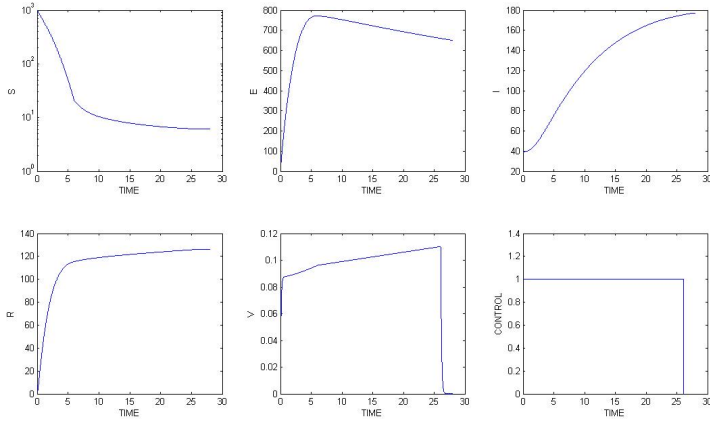
Figure 3.4: Optimal control results of system 3.2 projected for one year with $I_0 = 40$. $u = 1$ for days 77-185. $B = 10^{-2}$.

14, the 73rd day of the year. The birth pulse begins one week later on March 20. With the same number of susceptibles, $S_0 = 1000$, no exposed or immunes, and using the cost coefficient $B = 10^{-2}$, we now introduce one, forty, and one-hundred infected raccoons into the population with results displayed in figure 3.5. In all three cases, the control is implemented during a 25 day interval. As the number of initial infecteds increase, day 28 shows a larger number of infecteds and a smaller number of recovered. Since the susceptibles quickly decrease in number, a logarithmic scale is used for the susceptibles in order to observe the effect of the pulse. The susceptible graph again displays the birth pulse with a horizontal line.

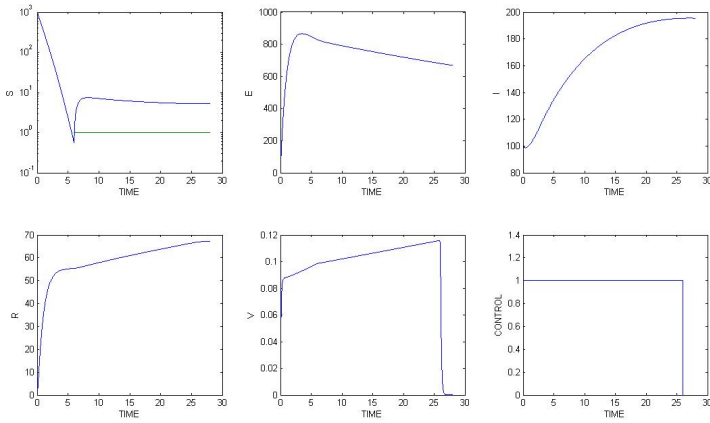
Continuing with $I_0 = 40$ and $B = 10^{-2}$, figure 3.6 show the results if the 28 day interval takes place during a time of the year without encountering a birth pulse (a), when the interval lies within a birth pulse (b), and when the time interval initially begins without a birth pulse but encounters the pulse 6 days into the interval (c). Note that (c) is the result from figure 3.5b. Part(a) shows the results beginning on February 20 and ending on March 20, the first day of the birth pulse suggesting that relatively few days are need for distributing vaccine when seasonal births are not anticipated in the near future. When



(a) 1 infectious raccoon



(b) 40 infectious raccoons



(c) 100 infectious raccoons

Figure 3.5: Populations of system 3.2 using initial values of 1, 40 and 100 infected raccoons with control

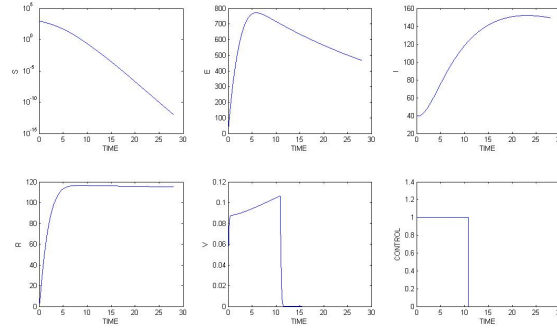
the 28 day interval lies within a birth pulse or begins a week before births occur (March 14), a greater number of days are needed for vaccine distribution. These results are similar to the corresponding non-density dependent results for both sets of parameters discussed in chapter 2 (figures A.1 and A.10). Thus the similar optimal control results for different population models shows the versatility of a common strategy.

If the 28 day interval occurs 2 weeks before the birth pulse begins then vaccine is distributed for the first 11 days, and after a brief cessation is resumed for days 21-26. Note that the second round starts one day after the birth pulse begins. If infected raccoons are detected 3 weeks before the pulse, only the first 10 days is used for distributing the vaccine, similar to the case above where no pulse occurs at all. These results are shown in figure 3.7. Figure A.11 shows the comparable non-density dependent results, which contain a few more days of applying vaccine than the density-dependent case.

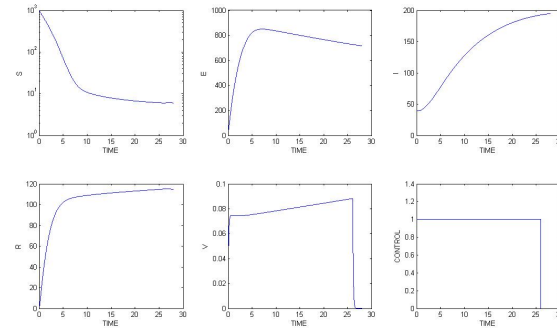
Increasing the upper bound for u decreases the optimal number of days for vaccine distribution. Figure 3.8 displays results for 28 day interval beginning on March 14 (3.8a), March 1 (3.8b), and February 20 (3.8c). Note in particular, part *b* shows the vaccine distribution for days 1-9 and 19-26. This time the vaccination begins the day before the start of the birth pulse on March 20. Also, for figure 3.8c the 28 day interval ends on March 20 at the start of the birth pulse and therefore does not need another round of vaccine. Each of these cases has fewer days of vaccine distribution due to a larger upper bound for u . The density dependent case shows that slightly fewer days of control are needed as compared to figure A.10 (a) and (c).

3.6 Conclusions

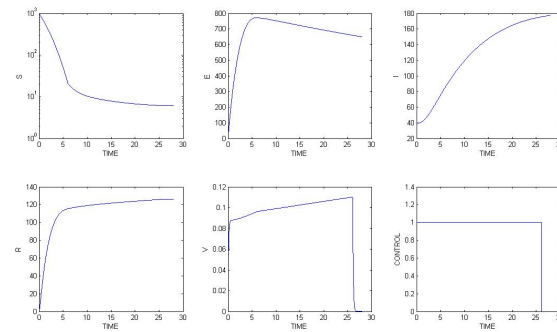
Taking account of different mortality assumptions, through inclusion of density-dependence in this model component, did not qualitatively change the nature of the optimal control solution for vaccine distribution. This robustness of the optimal solution for alternative model forms was only investigated for a few parameter sets however, so there may be situations in which alternative assumptions about mortality have larger qualitative impacts. Our results do provide some hope however that even if the exact demographic details of



(a) $u = 1$ for days 1-9. $B = 10^{-2}$

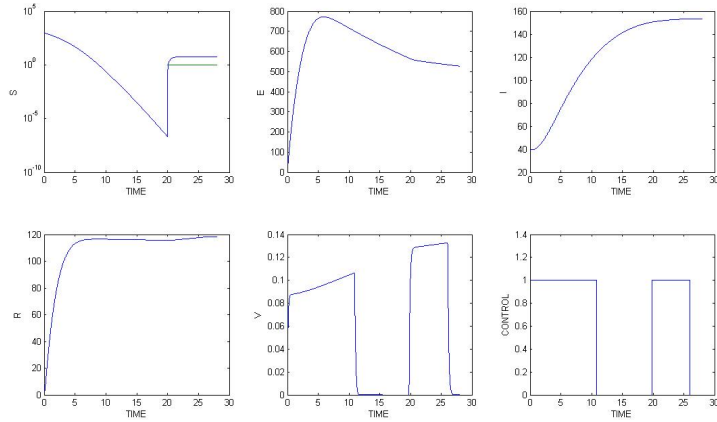


(b) $u = 1$ for days 1-25. $B = 10^{-2}$

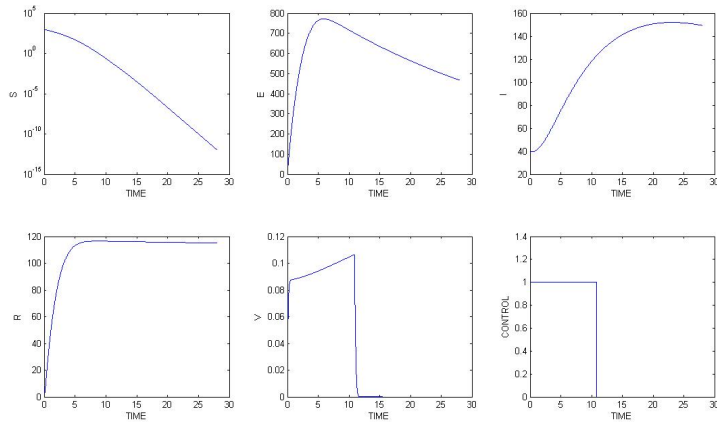


(c) $u = 1$ for days 1-25. $B = 10^{-2}$

Figure 3.6: Control results of system 3.2 for a 28 day interval:(a) without a birth pulse. (b) during a birth pulse. (c) beginning on day 73 (shortly before the birth pulse).

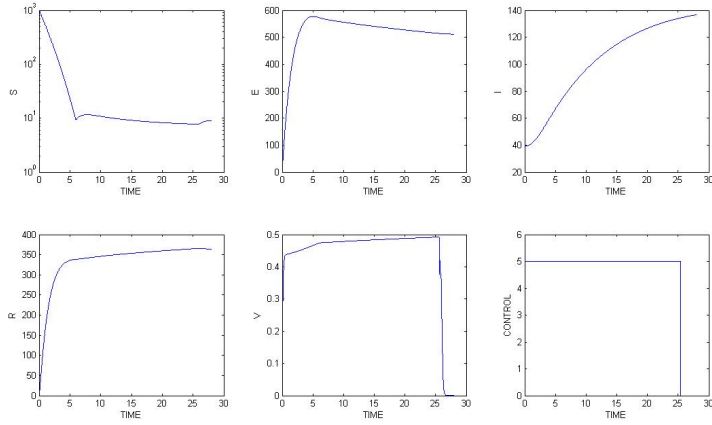


(a) $u = 1$ for days 1-11, 21-26. $B = 10^{-2}$

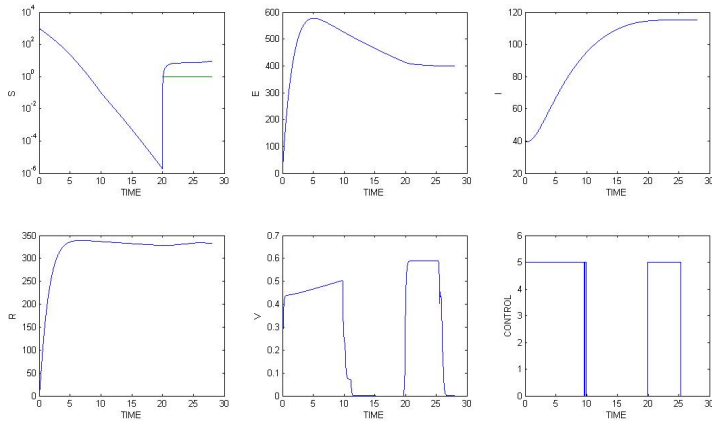


(b) $u = 1$ for days 1-11. $B = 10^{-2}$

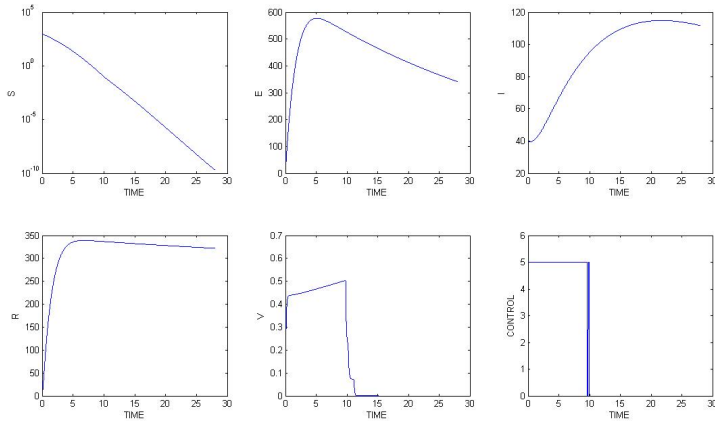
Figure 3.7: Control results of system 3.2 for a 28 day interval:(a) beginning March 1. (b) beginning February 20.



(a) $u = 5$ for days 1-25. $B = 10^{-2}$



(b) $u = 5$ for days 1-10, 21-25. $B = 10^{-2}$



(c) $u = 5$ for days 1-10. $B = 10^{-2}$

Figure 3.8: Populations results of system 3.2 with a 28 day interval:(a) beginning March 14. (b) beginning March 1. (c) beginning February 20.

population dynamics are not well-specified, the general patterns of optimal control would still apply.

One of the few differences between the models of chapter 2 and 3 include a non-decreasing trend in the recovered class near the end of the year in figure 3.2 as compared to figure 2.2. Figure 3.4 is similar to figure 2.3 except for the density dependent recovered class which shows a more gradual increase in the population. The density dependent case also has fewer days of the control and then only at the beginning of the birth pulse. Similar dynamics can also be seen when a 28 day interval is considered as demonstrated in figures 3.7 and A.2. In general, all cases considering the 28 day interval indicate to begin treatment immediately for a period of time and then resuming implementation of the control if a birth pulse is anticipated. It should be noted that we only investigated the type of density dependence deaths of the form $S(S + E + R)$, $E(S + E + R)$, $R(S + E + R)$ and other types of density dependence may be used for further research.

The assumption of natural immunity affects the population dynamics including the reoccurrence of infected individuals. When natural immunity does not exist, a second wave of infection occurs after approximately $5\frac{1}{2}$ years (see figure 3.3a). When 1 percent of the population acquires natural immunity, the infection reappears 5 times during the same time interval (figure 3.3b). If 2 percent of the population acquires natural immunity the same oscillating pattern occurs as seen in figure 3.3b but with a larger amplitude (figure 3.3c).

Chapter 4

An Epidemic Model of West Nile Virus

4.1 Introduction

West Nile virus (WNV) is a single-stranded RNA virus of the genus *Flavivirus* and the family *Flaviviridae*. The virus is spread by female mosquitos that feed on infected birds such as Blue jays and crows [10]. The mosquitos in turn make contact with humans causing the potential for sickness and deaths. There is no transmission of infection directly between birds. West Nile virus is different from some other mosquito-borne diseases in that it is a cross-infection between birds and mosquitoes and the birds can travel with no natural (or spatial) boundaries. The potential for an epidemic is compounded due to the fact that birds are not constrained to a particular location. Attempts at containing the spread of infection sometimes takes the form of killing the mosquitos or applying insect repellent to humans. Since the detection of the virus in the West Nile district of Uganda in 1937 (Smithburnit et al., 1940), the disease has spread outward making its arrival to North America in 1999 [7].

WNV is a type of vector-borne infectious disease that is carried by mosquitos from one host to another [15]. Recent studies have considered bird or human hosts. Wonham investigates the transmission of WNV between mosquitos and birds for a single season using a

SIR system of ordinary differential equations. That paper applied analytical and graphical methods that determines the proper control strategies for each group and calculates the disease reproduction number R_0 . Simulations show that mosquito control reduces the chances of an outbreak while the chances are increased when using a bird control strategy [36]. Cruz-Pacheco et. al. presents an *SIR* model that compares mosquitos and various species of birds yielding different R_0 values [10]. Parameters are given for various birds species including Blue jay, Common grackle, House finch, American crow, House sparrow, Ring-billed gull, Black-billed magpie, and Fish crow. The ODE system used by Bowman, et al., [7] includes humans in a single season mosquito-bird cycle. Mosquito reduction and personal protection strategies are used to prevent the spread of infection. The resulting R_0 values are also calculated to determine the stability of equilibria. Gourley presents an age structured model distinguishing between adult and juvenile populations in both susceptible and infected hosts. Adult mosquitos are considered to be the vector. A system of reaction-diffusion equations are also derived that shows the spatial spread of the infection [15].

This project is the first ODE model that uses optimal control to minimize the spread of WNV. The two controls represent the level at which pesticide is applied to the mosquito population and the prevention efforts to minimize human-mosquito contacts. The next section will discuss the model, including the dynamics of the mosquito, bird and human populations as well as appropriate optimality conditions. Section 3 gives a brief description of the basic reproduction number R_0 . Proposed strategies based on numerical computations are presented in section 4. Section 5 summarizes the results and offers areas for further investigation.

4.2 Model Formulation

We present a model that extends the work of Bowman et. al. [7] to include control variables designed to limit the number of mosquitos and infected humans and to include density dependent mortality and recruitment rates. The notation and parameters for this model can be found in Table 4.1. Let N_M, N_B and N_H represent the total number of mosquitoes, birds

and humans in a given community, respectively. The infected female mosquito is divided into susceptible M_s and infected M_i groups. The quantity $b_1 = b_1(N_M, N_B, N_H)$ describes the per capita biting rate of mosquitoes on birds per unit time, and $b_2 = b_2(N_M, N_B, N_H)$ is the per capita biting rate of mosquitoes on humans per unit time,

$$\begin{aligned} b_1 &= \frac{bN_B}{N_B + N_H} \\ b_2 &= \frac{bN_H}{N_B + N_H}. \end{aligned} \tag{4.1}$$

The term, $N_B + N_H$, is the number of hosts (birds and human) for mosquitos.

The model includes immigration of birds and humans. The birth rates and the immigration rates are

$$\gamma_M N_M, \lambda_B + \rho N_B, \text{ and } \lambda_H + \gamma_H N_H$$

for the mosquitos, birds and humans respectively, where λ_B and λ_H are immigration rates and $\gamma_M N_M$, ρN_B , and $\gamma_H N_H$ are the birth rates. The death rates of the mosquitos and the humans are density dependent and are given by:

$$\begin{aligned} \mu_M &= \mu_1 + \mu_2 N_M, \quad \gamma_M > \mu_1 \\ \mu_H &= \mu_3 + \mu_4 N_H. \end{aligned} \tag{4.2}$$

The units for immigration, death and birth parameters can be found in table A.1 in appendix A.

The mosquito control is primarily utilized to diminish the mosquito population in a designated area by killing adults and reducing larva production. The reproduction rate of larva is reduced by applying some type of insecticide, $u_1(t)$, with the effect of lowering the growth rate of mosquitos by a factor of $1 - u_1(t)$. Additionally, the model also assumes that the mortality rate of mosquitoes increases at a rate proportional to $u_1(t)$, where the rate constant is $r_0 > 0$.

The dynamics are given by

$$\frac{dM_s}{dt} = \gamma_M N_M (1 - u_1(t)) - \frac{bN_B}{N_B + N_H} \frac{\beta_1 M_s B_i}{N_B} - (\mu_1 + \mu_2 N_M) M_s - r_0 u_1(t) M_s. \quad (4.3)$$

$$\frac{dM_i}{dt} = \frac{bN_B}{N_B + N_H} \frac{\beta_1 M_s B_i}{N_B} - (\mu_1 + \mu_2 N_M) M_i - r_0 u_1(t) M_i. \quad (4.4)$$

where r_0 is a rate constant for the death rate of mosquitos due to the control $u_1(t)$, the level that insecticide is applied to the mosquito population. The coefficient β_1 is the probability of transmission from infected bird to susceptible mosquito.

The bird population is assumed to be infected through contact with mosquitoes which get the disease from infected birds. We assume that in the bird population, the natural death rate μ_B is higher than the disease induced death rate d_B . Birds are assumed to immigrate at a constant rate of λ_B . They also exit the community through emigration at a rate of δ .

The bird dynamics are governed by these two ODEs:

$$\begin{aligned} \frac{dB_s}{dt} &= \lambda_B + \rho N_B - \frac{bN_B}{N_B + N_H} \frac{\beta_2 M_i B_s}{N_B} - \delta B_s - \mu_B B_s \\ \frac{dB_i}{dt} &= \frac{bN_B}{N_B + N_H} \frac{\beta_2 M_i B_s}{N_B} - d_B B_i - \delta B_i - \mu_B B_i. \end{aligned} \quad (4.5)$$

Note that the coefficient β_2 is the probability of transmission from infected mosquito to susceptible bird.

The human population is divided into five categories susceptible, exposed, infectious, hospitalized and recovered designated by S, E, I, H, R respectively. The rate of infection is reduced by a factor of $(1 - u_2(t))$, where $u_2(t)$ measures successful prevention efforts such as insect repellents, treating indoor areas, and using treated bed nets to cover bed areas at

night time. The susceptible and exposed DEs are given by

$$\begin{aligned}\frac{dS}{dt} &= \lambda_H + \gamma_H N_H - \frac{bN_H}{N_B + N_H} \frac{\beta_3 M_i S(1 - u_2(t))}{N_H} - (\mu_3 + \mu_4 N_H)S \\ \frac{dE}{dt} &= \frac{bN_H}{N_B + N_H} \frac{\beta_3 M_i S(1 - u_2(t))}{N_H} - \alpha E - (\mu_3 + \mu_4 N_H)E.\end{aligned}\tag{4.6}$$

with density dependent death and birth rates. The coefficient β_3 is the probability of transmission from infected mosquito to susceptible human.

Once a human being is exposed to the disease, either the person dies of natural causes (at a rate of μ_H) or becomes infectious (at a rate α) per unit time. After developing infection, the patient experiences anyone of these: death due to the disease (at a rate of d_I) or due to natural causes, recovery from infectious stage (at a rate of $r \ll 1$) or recovery after hospitalization (at a rate of τ). It is assumed that the death rate of infected humans, d_I , is greater than the death rate of hospitalized humans, d_H . Also, the natural death for humans in any of the four compartments is μ_H as given in (4.2). Infected humans are hospitalized at a rate σ . This leads to our last three state equations:

$$\begin{aligned}\frac{dI}{dt} &= \alpha E - \sigma I - d_I I - rI - (\mu_3 + \mu_4 N_H)I \\ \frac{dH}{dt} &= \sigma I - d_H H - \tau H - (\mu_3 + \mu_4 N_H)H \\ \frac{dR}{dt} &= \tau H + rI - (\mu_3 + \mu_4 N_H)R.\end{aligned}\tag{4.7}$$

A description of the state variables and parameters is given in Table A.1 in appendix A.

Adding the equations for the compartments in mosquitos (4.3) - (4.4), birds (4.5) and humans (4.6)-(4.7) we obtain

$$\begin{aligned}\frac{dN_M}{dt} &= N_M[\gamma_M(1 - u_1) - (\mu_1 + \mu_2 N_M) - r_0 u_1] \\ \frac{dN_B}{dt} &= \lambda_B + \rho N_B - (\delta + \mu_B)N_B \\ \frac{dN_H}{dt} &= \lambda_H + \gamma_H N_H - d_I I - (\mu_3 + \mu_4 N_H)N_H - d_H H.\end{aligned}\tag{4.8}$$

Note that for bounded Lebesgue measurable controls and non-negative initial conditions,

non-negative bounded solutions to this system exist [22].

We formulate an optimal control problem with the objective functional given by

$$J(u_1, u_2) = \int_0^T \left(A_1 E(t) + A_2 I(t) + A_3 N_M(t) + B_1 u_1^2 + B_2 u_2^2 \right) dt \quad (4.9)$$

subject to the state system given by (4.3)-(4.7). In this formulation, A_1 , A_2 and A_3 are respectively, the weight constants of the exposed, infected human group and the total mosquito populations. Weight constants for the mosquito and the prevention controls are given by B_1 and B_2 . It is assumed that the cost of each process are proportional to the square of the corresponding control function. Our goal is to find optimal control functions (u_1^*, u_2^*) such that

$$J(u_1^*, u_2^*) = \min\{J(u_1, u_2) \mid (u_1, u_2) \in \Gamma\}$$

subject to the system of equations given by (4.3)-(4.7), with given initial conditions, $M_s(0) = 10^4, M_i(0) = 10^3, B_s(0) = 10^3, S(0) = 10^3$, and with zero initial conditions for the rest. The set of controls is

$$\Gamma = \{(u_1, u_2) \mid u_i(t) \text{ is Lebesgue measurable on } [0, T], \quad 0 \leq u_i(t) \leq a_i, \quad i = 1, 2\}. \quad (4.10)$$

Note that our control set is clearly closed and convex. Next we prove the existence of the optimal control and then characterize it.

Following Pontryagin's Minimum Principle [25], the Hamiltonian is:

$$\begin{aligned}
\mathbf{H} = & A_1 E(t) + A_2 I(t) + A_3 N_M(t) + B_1 u_1^2 + B_2 u_2^2 \tag{4.11} \\
& + \lambda_1 \left[\gamma_M N_M (1 - u_1(t)) - \frac{b\beta_1 M_s B_i}{N_B + N_H} - (\mu_1 + \mu_2 N_M) M_s - r_0 u_1(t) M_s \right] \\
& + \lambda_2 \left[\frac{b\beta_1 M_s B_i}{N_B + N_H} - (\mu_1 + \mu_2 N_M) M_i - r_0 u_1(t) M_i \right] \\
& + \lambda_3 \left[\lambda_B + \rho N_B - \frac{b\beta_2 M_i B_s}{N_B + N_H} - \delta B_s - \mu_B B_s \right] \\
& + \lambda_4 \left[\frac{b\beta_2 M_i B_s}{N_B + N_H} - d_B B_i - \delta B_i - \mu_B B_i \right] \\
& + \lambda_5 \left[\lambda_H + \gamma_H N_H - \frac{b\beta_3 M_i S (1 - u_2(t))}{N_H + N_B} - (\mu_3 + \mu_4 N_H) S \right] \\
& + \lambda_6 \left[\frac{b\beta_3 M_i S (1 - u_2(t))}{N_H + N_B} - \alpha E - (\mu_3 + \mu_4 N_H) E \right] \\
& + \lambda_7 \left[\alpha E - \sigma I - d_I I - r I - (\mu_3 + \mu_4 N_H) I \right] \\
& + \lambda_8 \left[\sigma I - d_H H - \tau H - (\mu_3 + \mu_4 N_H) H \right] \\
& + \lambda_9 \left[\tau H + r I - (\mu_3 + \mu_4 N_H) R \right].
\end{aligned}$$

Theorem 4.2.1. *Given an optimal control (u_1^*, u_2^*) , and solutions of the corresponding state system (4.3) - (4.7), there exists adjoint variables, λ_i , $i = 1, \dots, 9$, satisfying*

$$\begin{aligned}
\lambda_1' = -\frac{\partial \mathbf{H}}{\partial M_s} = & -A_3 - \lambda_1 \left[\gamma_M (1 - u_1(t)) - \frac{b\beta_1 B_i}{N_B + N_H} - \mu_2 M_s - (\mu_1 + \mu_2 N_M) - r_0 u_1(t) \right] \\
& - \lambda_2 \left[\frac{b\beta_1 B_i}{N_B + N_H} - \mu_2 M_i \right] \\
= & -A_3 + (\lambda_1 - \lambda_2) \frac{b\beta_1 B_i}{N_B + N_H} - \lambda_1 \left[\gamma_M (1 - u_1(t)) - (\mu_1 + \mu_2 N_M) - r_0 u_1(t) \right] \\
& + \lambda_2 \mu_2 M_i + \lambda_1 \mu_2 M_s
\end{aligned} \tag{4.12}$$

$$\begin{aligned}
\lambda'_2 = -\frac{\partial \mathbf{H}}{\partial M_i} = & -A_3 - \lambda_1 \left[\gamma_M(1 - u_1(t)) - \mu_2 M_s \right] + \lambda_2 \left[\mu_1 + \mu_2 N_M + \mu_2 M_i + r_0 u_1 \right] \\
& + \lambda_3 \left[\frac{b\beta_2 B_s}{N_B + N_H} \right] - \lambda_4 \left[\frac{b\beta_2 B_s}{N_B + N_H} \right] + \lambda_5 \left[\frac{b\beta_3 S(1 - u_2)}{N_B + N_H} \right] - \lambda_6 \left[\frac{b\beta_3 S(1 - u_2)}{N_B + N_H} \right]
\end{aligned} \tag{4.13}$$

$$\begin{aligned}
\lambda'_3 = -\frac{\partial \mathbf{H}}{\partial B_s} = & -\lambda_1 \left[\frac{b\beta_1 B_i M_s}{(N_B + N_H)^2} \right] + \lambda_2 \left[\frac{b\beta_1 B_i M_s}{(N_B + N_H)^2} \right] \\
& - \lambda_3 \left[\rho - b\beta_2 M_i \left(-\frac{B_s}{(N_B + N_H)^2} + \frac{1}{N_B + N_H} \right) - \delta - \mu_B \right] \\
& - \lambda_4 \left[b\beta_2 M_i \left(\frac{1}{N_B + N_H} - \frac{B_s}{(N_B + N_H)^2} \right) \right] - \lambda_5 \left[\frac{b\beta_3 M_i S(1 - u_2)}{(N_B + N_H)^2} \right] \\
& + \lambda_6 \left[\frac{b\beta_3 M_i S(1 - u_2(t))}{(N_B + N_H)^2} \right]
\end{aligned} \tag{4.14}$$

$$\begin{aligned}
\lambda'_4 = -\frac{\partial \mathbf{H}}{\partial B_i} = & -\lambda_1 \left[-b\beta_1 M_s \left(\frac{-B_i}{(N_B + N_H)^2} + \frac{1}{N_B + N_H} \right) \right] \\
& - \lambda_2 \left[b\beta_1 M_s \left(\frac{-B_i}{(N_B + N_H)^2} + \frac{1}{N_B + N_H} \right) \right] - \lambda_3 \left[\rho + \frac{b\beta_2 M_i B_s}{(N_B + N_H)^2} \right] \\
& + \lambda_4 \left[\frac{b\beta_2 M_i B_s}{(N_B + N_H)^2} + (d_B + \delta + \mu_B) \right] - \lambda_5 \left[\frac{b\beta_3 M_i S(1 - u_2)}{(N_B + N_H)^2} \right] \\
& + \lambda_6 \left[\frac{b\beta_3 M_i S(1 - u_2(t))}{(N_B + N_H)^2} \right]
\end{aligned} \tag{4.15}$$

$$\begin{aligned}
\lambda'_5 = -\frac{\partial \mathbf{H}}{\partial S} = & -\lambda_1 \left[\frac{b\beta_1 B_i M_s}{(N_B + N_H)^2} \right] - \lambda_2 \left[-\frac{b\beta_1 B_i M_s}{(N_B + N_H)^2} \right] - \lambda_3 \left[\frac{b\beta_2 M_i B_s}{(N_B + N_H)^2} \right] \\
& - \lambda_4 \left[-\frac{b\beta_2 M_i B_s}{(N_B + N_H)^2} \right] \\
& - \lambda_5 \left[\gamma_H - b\beta_3 M_i (1 - u_2) \left(\frac{1}{N_B + N_H} - \frac{S}{(N_B + N_H)^2} \right) - \mu_4 S - (\mu_3 + \mu_4 N_H) \right] \\
& - \lambda_6 \left[b\beta_3 M_i (1 - u_2) \left(\frac{1}{N_B + N_H} - \frac{S}{(N_B + N_H)^2} \right) - \mu_4 E \right] \\
& + \lambda_7 \mu_4 I + \lambda_8 \mu_4 H + \lambda_9 \mu_4 R
\end{aligned} \tag{4.16}$$

$$\begin{aligned}
\lambda'_6 = -\frac{\partial \mathbf{H}}{\partial E} = & -A_1 - \lambda_1 \left[\frac{b\beta_1 B_i M_s}{(N_B + N_H)^2} \right] - \lambda_2 \left[-\frac{b\beta_1 B_i M_s}{(N_B + N_H)^2} \right] - \lambda_3 \left[\frac{b\beta_2 M_i B_s}{(N_B + N_H)^2} \right] \\
& - \lambda_4 \left[-\frac{b\beta_2 M_i B_s}{(N_B + N_H)^2} \right] \\
& - \lambda_5 \left[\gamma_H + \frac{b\beta_2 M_i B_s (1 - u_2)}{(N_B + N_H)^2} - \mu_4 S \right] \\
& + \lambda_6 \left[\frac{b\beta_3 M_i S (1 - u_2)}{(N_B + N_H)^2} + \alpha + \mu_4 E + \mu_3 + \mu_4 N_H \right] \\
& - \lambda_7 \left[\alpha - \mu_4 I \right] + \lambda_8 \mu_4 H + \lambda_9 \mu_4 R
\end{aligned} \tag{4.17}$$

$$\begin{aligned}
\lambda'_7 = -\frac{\partial \mathbf{H}}{\partial I} = & -A_2 - \lambda_1 \left[\frac{b\beta_1 B_i M_s}{(N_B + N_H)^2} \right] - \lambda_2 \left[-\frac{b\beta_1 B_i M_s}{(N_B + N_H)^2} \right] - \lambda_3 \left[\frac{b\beta_2 M_i B_s}{(N_B + N_H)^2} \right] \\
& - \lambda_4 \left[-\frac{b\beta_2 M_i B_s}{(N_B + N_H)^2} \right] \\
& - \lambda_5 \left[\gamma_H + \frac{b\beta_3 M_i S(1-u_2)}{(N_B + N_H)^2} - \mu_4 S \right] \\
& + \lambda_6 \left[\frac{b\beta_3 M_i S(1-u_2)}{(N_B + N_H)^2} + \mu_4 E \right] + \lambda_7 \left[\sigma + (d_I + r) + (\mu_4 I + \mu_3 + \mu_4 N_H) \right] \\
& - \lambda_8 \left[\sigma - \mu_4 H \right] - \lambda_9 \left(r - \mu_4 R \right)
\end{aligned} \tag{4.18}$$

$$\begin{aligned}
\lambda'_8 = -\frac{\partial \mathbf{H}}{\partial H} = & -\lambda_1 \left[\frac{b\beta_1 B_i M_s}{(N_B + N_H)^2} \right] - \lambda_2 \left[-\frac{b\beta_1 B_i M_s}{(N_B + N_H)^2} \right] - \lambda_3 \left[\frac{b\beta_2 M_i B_s}{(N_B + N_H)^2} \right] \\
& - \lambda_4 \left[-\frac{b\beta_2 M_i B_s}{(N_B + N_H)^2} \right] - \lambda_5 \left[\gamma_H + \frac{b\beta_3 M_i S(1-u_2)}{(N_B + N_H)^2} - \mu_4 S \right] \\
& + \lambda_6 \left[\frac{b\beta_3 M_i S(1-u_2)}{(N_B + N_H)^2} + \mu_4 E \right] \\
& + \lambda_7 \mu_4 I \\
& + \lambda_8 \left[(d_H + \tau) + \mu_4 H + \mu_3 + \mu_4 N_H \right] - \lambda_9 (-\mu_4 R + \tau)
\end{aligned} \tag{4.19}$$

$$\begin{aligned}
\lambda'_9 = -\frac{\partial \mathbf{H}}{\partial R} = & -\lambda_1 \left[\frac{b\beta_1 B_i M_s}{(N_B + N_H)^2} \right] + \lambda_2 \left[\frac{b\beta_1 B_i M_s}{(N_B + N_H)^2} \right] - \lambda_3 \left[\frac{b\beta_2 M_i B_s}{(N_B + N_H)^2} \right] \\
& + \lambda_4 \left[\frac{b\beta_2 M_i B_s}{(N_B + N_H)^2} \right] - \lambda_5 \left[\gamma_H + \frac{b\beta_3 M_i S(1-u_2)}{(N_B + N_H)^2} - \mu_4 S \right] \\
& + \lambda_6 \left[\frac{b\beta_3 M_i S(1-u_2)}{(N_B + N_H)^2} + \mu_4 E \right] \\
& + \lambda_7 \mu_4 I + \lambda_8 \mu_4 H + \lambda_9 (\mu_4 R + \mu_3 + \mu_4 N_H).
\end{aligned} \tag{4.20}$$

The terminal conditions are:

$$\lambda_i(T) = 0 \text{ for } i = 1, \dots, 9. \quad (4.21)$$

Furthermore, the optimal functions u_1^* and u_2^* are represented by

$$\begin{aligned} u_1^* &= \max\{0, \min\{1, \frac{1}{2B_1}[\lambda_1(\gamma_M N_M + r_0 M_s) + \lambda_2 r_0 M_i]\}\} \\ u_2^* &= \max\{0, \min\{1, \frac{1}{2B_2} b \beta_3 M_i S \frac{1}{2(NB(i) + NH(i))} (\lambda_6 - \lambda_5)\}\}. \end{aligned} \quad (4.22)$$

Proof: The state variables in these characterizations are solutions of system (4.3) - (4.7) and the λ_i 's are solutions of the adjoint system (4.12)-(4.20) all corresponding to the optimal control functions (u_1^*, u_2^*) .

The behavior of the controls may be obtained by differentiating the Hamiltonian with respect to u ; on the interior of the control set, u_1^* , u_2^* satisfy

$$\begin{aligned} \frac{\partial H}{\partial u_1} &= 2B_1 u_1 - \lambda_1 \gamma_M N_M - r_0 M_s - \lambda_2 r_0 M_i = 0 \\ \frac{\partial H}{\partial u_2} &= 2B_2 u_2 + \lambda_5 \frac{b \beta_3 M_i S}{N_H + N_B} + \lambda_6 \frac{b \beta_3 M_i S}{N_H + N_B} = 0. \end{aligned}$$

Solving for u_1^* , u_2^* and using the bounds gives (4.22).

The state adjoint system (4.12)-(4.20) results from Pontryagin's Principle [25]. \square

4.3 Basic Reproduction Number

For an epidemic model, a threshold number exists that determine whether or not a disease will persist. The threshold number is known the basic reproduction number, and is designated R_0 . Mathematically, it is defined to be the spectral radius of the next generation matrix [35]. If $R_0 > 1$, then the disease free equilibrium is asymptotically stable. Biologically, when $R_0 > 1$, each infected organism infects more than one susceptible causing the disease to spread. If $R_0 < 1$, then each infected organism infects less than one susceptible individual and the virus does not spread [35]. For this problem without the density dependence in the birth and death rates, the basic reproduction number is:

$$R_0 = \frac{b\sqrt{\beta_1\beta_2\frac{\lambda_M}{\mu_M}\frac{\lambda_B}{\mu_B+\delta}}}{\sqrt{\mu_M k_2(\frac{\lambda_B}{\mu_B+\delta})}} \quad (4.23)$$

which is calculated in Blayneh et. al. [6] using the techniques from [35].

4.4 Numerical Simulation

Before we show our numerical results, we discuss our choice of parameters. In the literature [7], [10], [15], [36], the natural death rate for humans ranges from $3.91 * 10^{-5}$ to 0.005. Since the death rate is assumed to be density dependent, $\mu_H = \mu_3 + \mu_4 N_H$, values of $\mu_3 = 9 * 10^{-4}$ and $\mu_4 = 2 * 10^{-6}$ gave a death rate in the above range. The death rate due to the disease is between $5 * 10^{-7}$ and 0.015. Since it is assumed that the death rate of infected humans, d_I , is greater than the death rate of hospitalized humans, d_H , the value of $d_I = d_H + 10^{-5}$ is chosen where $d_H = 5 * 10^{-7}$. For mosquitos the natural death rate is between 0.016-0.07. Since $\mu_M = \mu_1 + \mu_2 N_M$, $\gamma_M > \mu_1$, the values of $\mu_1 = 1 * 10^{-3}$ and $\mu_2 = 5 * 10^{-6}$ gave the above range. The natural death rate for birds is between 0.0001-0.1429. Thus we take $\mu_B = 1 * 10^{-4}$. and death rate in the presence of WNV is less than 0.2. For these results, $d_B = 0.015$. Parameter values are shown in table A.2 in appendix A.

For the examples below, we used the parameters in table A.2, which give $R_0 > 1$ from the model without density dependence in the birth and death rates [6].

Figure 4.1 shows the population levels for mosquito, bird and human populations during a 50 day period of time without the West Nile virus beginning with 10,000 mosquitos, 1000 birds and 1000 humans.

Next, we introduce 1000 mosquitos infected with the West Nile virus with the corresponding effects on the susceptible class in figure 4.2a. Note the rapid decrease in the number of organisms for each group and the corresponding increase in each of the newly formed infected classes shown in figure 4.2b. Similar results occurred when including a 100 infected birds in addition to 1000 infected mosquitos.

Several control scenarios are now presented using initial conditions of 1000 infected

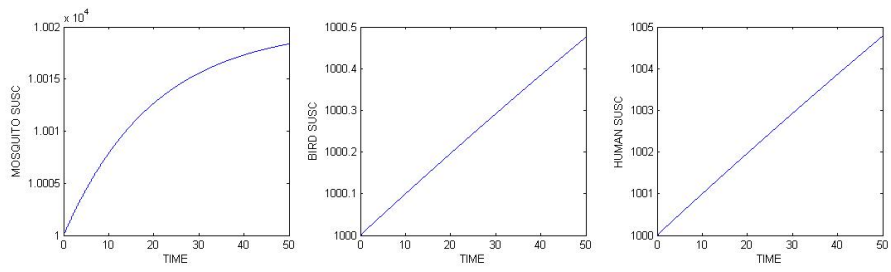
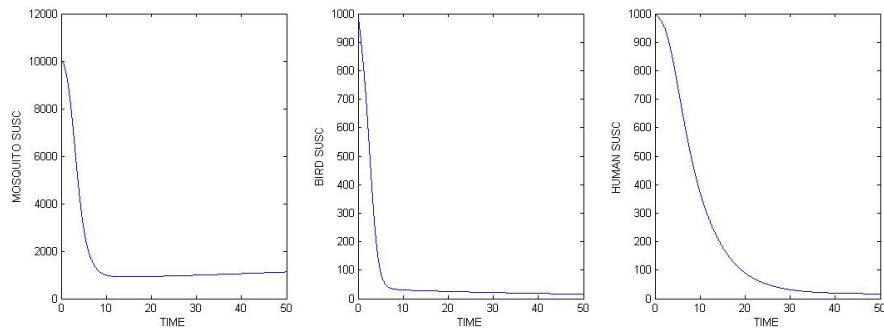
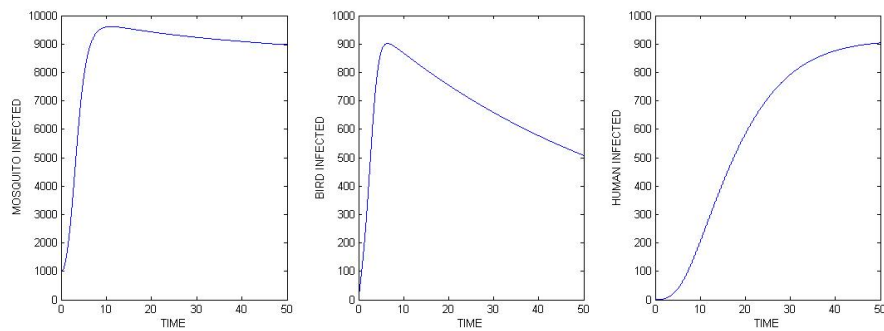


Figure 4.1: Disease free populations of mosquito, bird and humans



(a) Susceptible population



(b) Infected population

Figure 4.2: Effects of system 4.3-4.7 with 1000 infected mosquitos

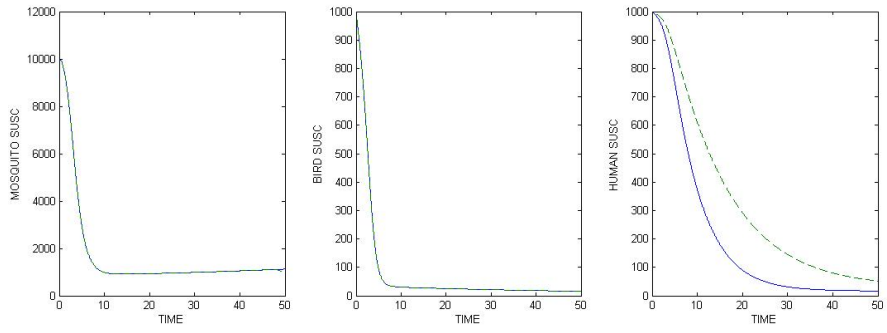
mosquitos and 0 infected birds interacting with 10000 susceptible mosquitos, 1000 susceptible birds and 1000 susceptible humans. We now consider controls u_1 and u_2 and assume that the relative importance of each term of the objective functional is the same, ie.:

$$A_1 = A_2 = A_3 = B_1 = B_2 = 1.$$

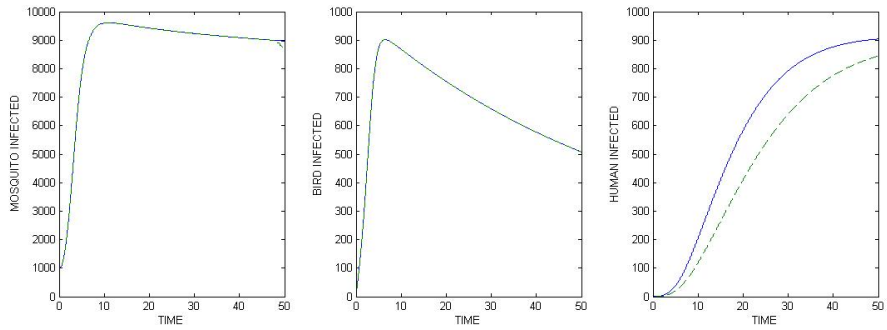
We consider the corresponding results for the susceptible and infected populations and note that little change occurs in the mosquito and bird dynamics. However the human susceptible shows a significant increase whereas a decrease is shown in the human infecteds. We also note that a decrease in the human hospitalized and recovered classes occurred with mixed results for the exposed group. These results are due to the optimal distribution of the control where it is assumed that $0 \leq u_1 \leq 0.8$ and $0 \leq u_2 \leq 0.5$. For this case, the optimal solution requires a maximum level of distribution of control u_2 suggesting intense efforts at preventing human and mosquito contact. On the other hand effort at controlling the spread of infected mosquitos is needed only near the end of the 50 day period as is reflected in the graph of u_1 . Here and throughout the remaining chapter, solid lines indicate the case with no control and the dashed lines represent the situation when the controls are made available. Results for the state and control variables are shown in figure 4.3.

If minimizing the total number of mosquitos becomes less important, the coefficient of N_M becomes smaller. Letting $A_3 = 10^{-4}$ and $A_i = 1$ for $i = 1, 2$ and the cost of preventing human/mosquito contact $B_2 = 10^3$. Using these parameters yields a noticeable increase in the number of infected mosquitos and a slight reduction in the total human population. Corresponding state and control results are given in figure 4.4. For this case, note that preventing human/mosquito contact is applied first followed by effort at eliminating infected mosquitos.

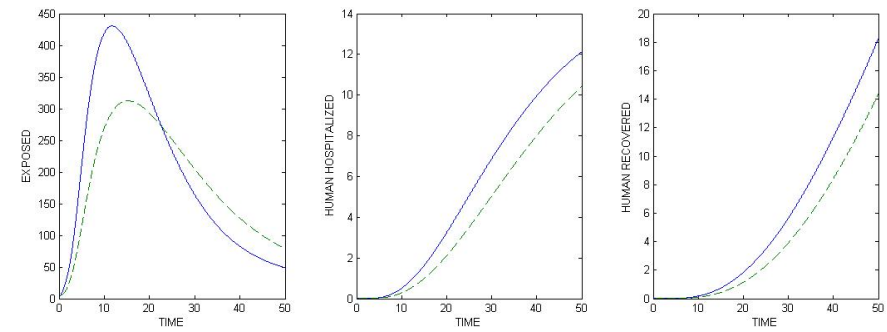
Now, $A_3 = 10^{-4}$ is held constant and A_1, A_2 is varied. The cost coefficients B_1 and B_2 remain 1 and 10^3 respectively. Note that varying A_1, A_2 refers to placing a different emphasis on minimizing the exposed and infected humans respectively. If minimizing the exposed is less important but more important than controlling the mosquito population, say $A_1 = 10^{-1}, A_2 = 1$, all classes see an increase in the number of infecteds and a decrease in the number of susceptibles. For this case the optimal strategy shows a noticeable increase



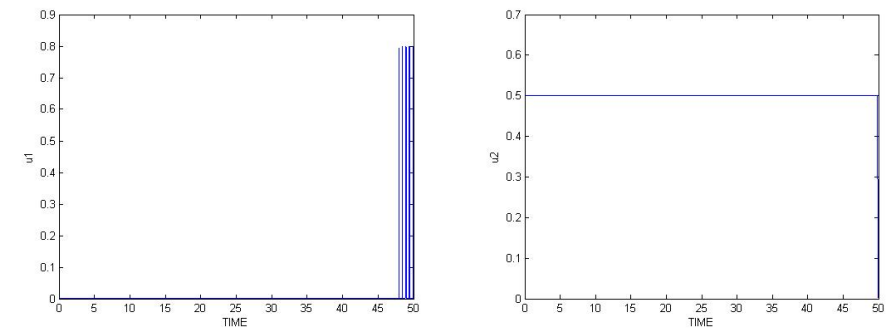
(a) Susceptible population



(b) Infected population

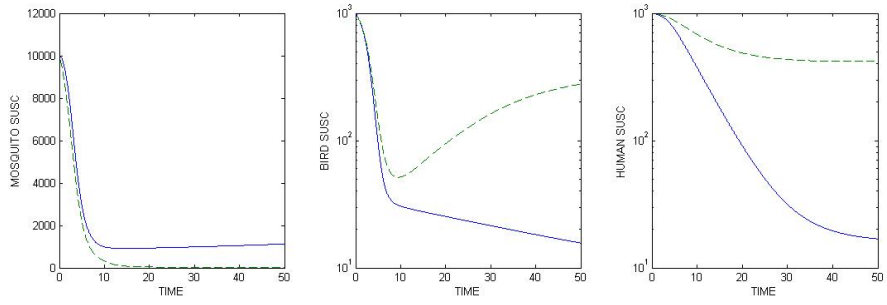


(c) Infected population

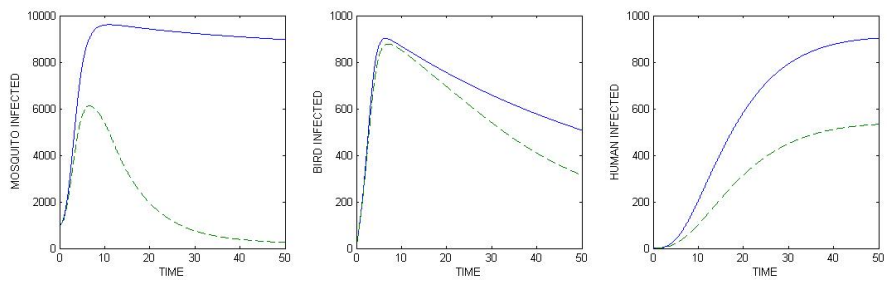


(d) Control

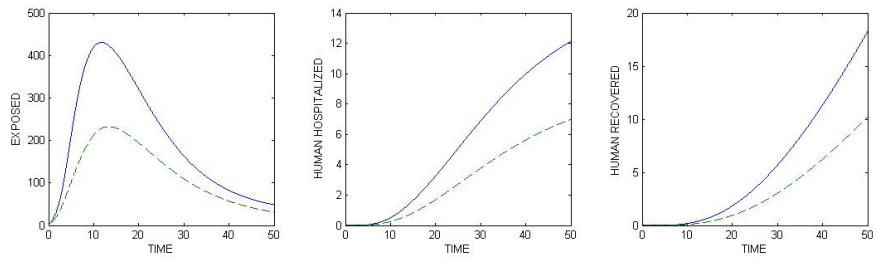
Figure 4.3: Effects of system 4.3-4.7 with 1000 infected mosquitoes when cost coefficients are unity.



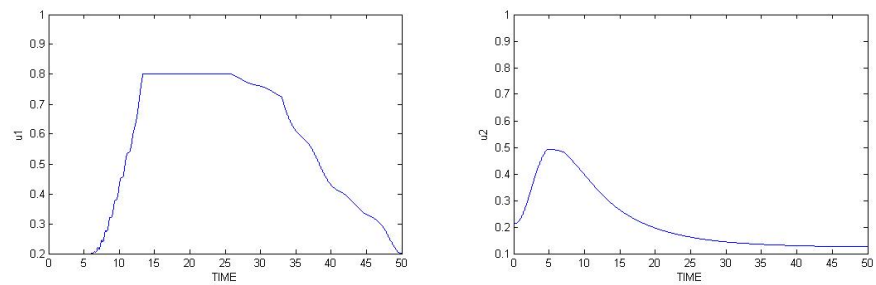
(a) Susceptibles



(b) Infecteds



(c) Exposed, hospitalized and immunes



(d) Control

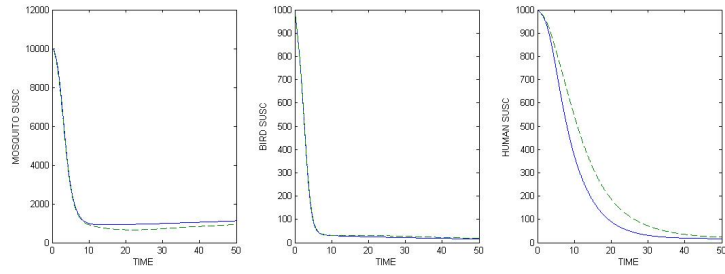
Figure 4.4: State and control system 4.3-4.7 with $A_3 = 10^{-4}$ and $A_3 = 10^{-4}$, $A_1 = A_2 = 1$, $B_1 = 1$, $B_2 = 10^3$.

occurring in the number infected mosquitos coupled with a small change in the infected birds as compared to figure 4.4. For this case, control u_1 begins before u_2 and remains for only a brief period of time followed by the application of u_2 . After u_2 is stopped, a second application of u_1 occurs. With $A_3 = 10^{-4}$ and $A_1 = 1$, $A_2 = 10^{-1}$, i.e., controlling the infected humans is less important than the exposed humans but more important than minimizing mosquitos, the state variables begin to merge the control/no control cases with a slight decrease in mosquito infecteds when applying control. Note that since this result is similar to the previous case, except that the maximum level is smaller for both control variables the state variables are not shown, however figure 4.5 shows the results when $A_1 = 10^{-1}$, $A_2 = 1$.

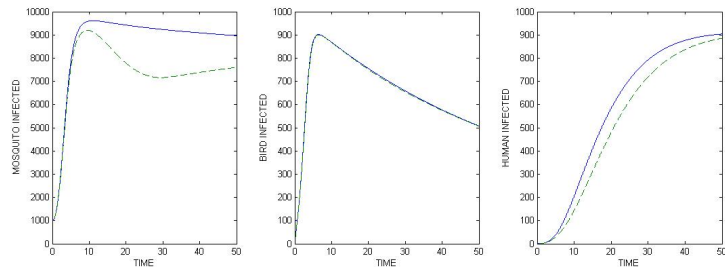
We now consider the case when $A_1 = A_2 = 10^{-1}$, $A_3 = 10^{-4}$ suggesting that minimizing the human infected and exposed classes are equally important. Again, $B_1 = 1$, $B_2 = 10^3$. Figure 4.6 shows the corresponding susceptible, infected and exposed dynamics. The associated controls for figures 4.5 and 4.6 are shown in figure 4.7. Note that in all three cases, u_1 is applied immediately for a short time followed by an application of u_2 and then a resumption of u_1 . Thus, these results suggest eliminating mosquitos first for a short period of time and then expend effort in preventing human/mosquito contact and resume mosquito elimination.

Consider the case of stressing the minimization of the human exposed class with expensive prevention efforts coupled with less importance given to killing mosquitos ($A_1 = 10$, $A_2 = 1$, $A_3 = 10^{-3}$, $B_1 = 1$, $B_2 = 10^3$, $0 \leq u_1 \leq 0.8$, $0 \leq u_2 \leq 0.9$). For this case the optimal control strategy suggests an early application of u_2 for approximately 25 days and an increase of u_1 peaking just before the decrease in u_2 . This strategy produces an increase in the human susceptible population and a slight decrease in the bird susceptibles as compared to figure 4.5. Mosquito and bird infecteds have a slight increase compared to figure 4.6 but a decrease in the human infected. Figure 4.8 shows the corresponding results for the state and control variables.

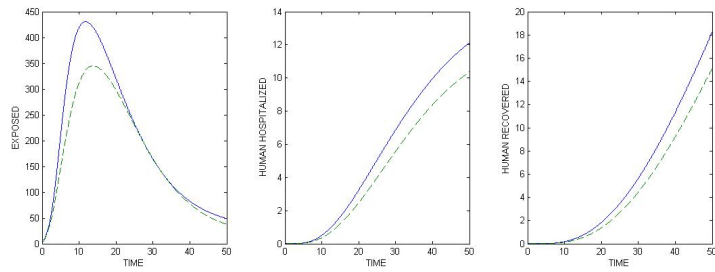
With a relatively large cost for prevention efforts, i.e., $B_2 = 10^3$, and giving less importance to minimizing the mosquito population, i.e., $A_3 = 10^{-4}$, produces figures 4.9.



(a) Susceptibles

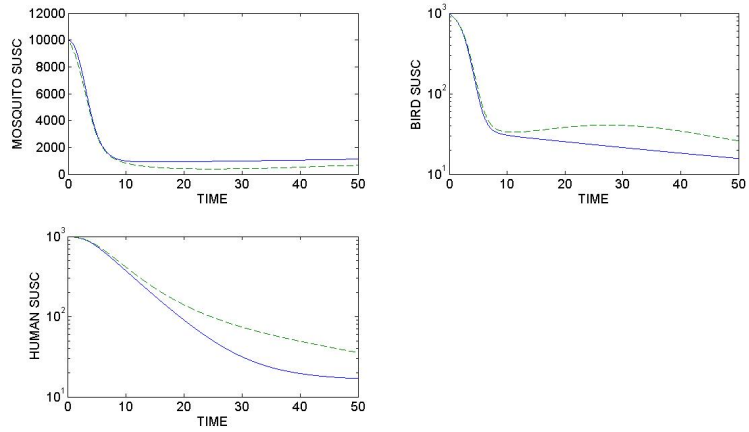


(b) Infecteds

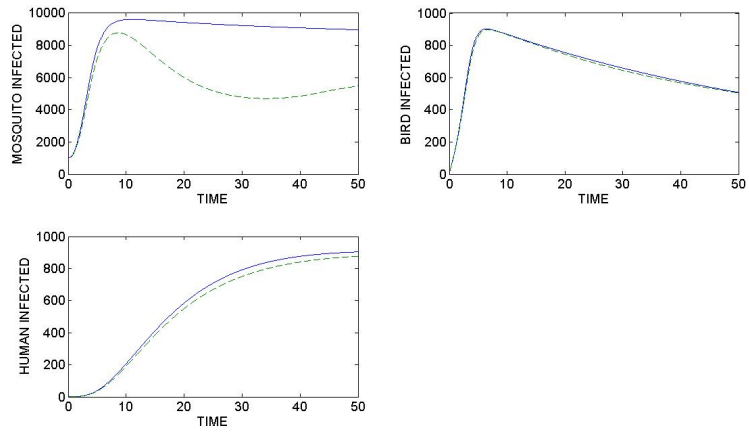


(c) Exposed, hospitalized, and immunes

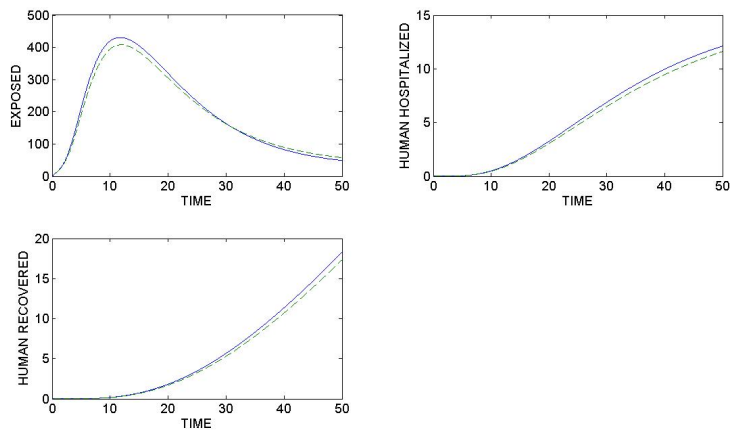
Figure 4.5: State system 4.3-4.7 with $A_1 = 10^{-1}$, $A_2 = 1$, $A_3 = 10^{-4}$, $B_1 = 1$, $B_2 = 10^3$



(a) Susceptibles

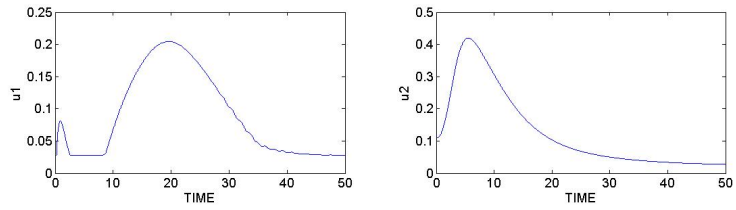


(b) Infecteds

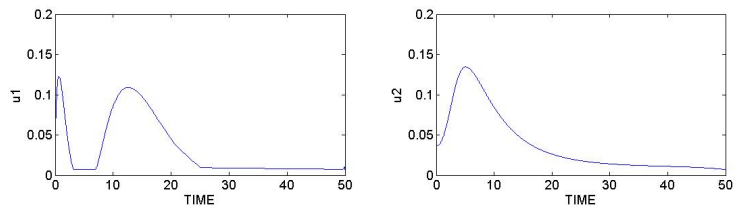


(c) Exposed, hospitalized, and immunes

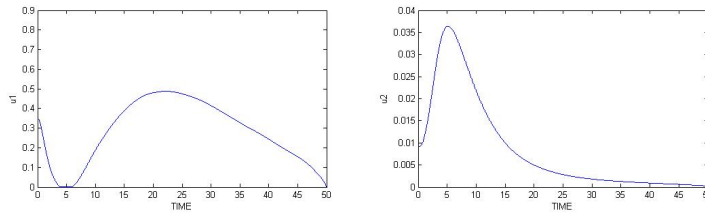
Figure 4.6: State system 4.3-4.7 with $A_1 = A_2 = 10^{-1}$, $A_3 = 10^{-4}$, $B_1 = 1$, $B_2 = 10^3$



(a) Controls when $A_1 = 10^{-1}$, $A_2 = 1$, $A_3 = 10^{-4}$.



(b) Controls when $A_2 = 10^{-1}$, $A_1 = 1$, $A_3 = 10^{-4}$.



(c) Controls when $A_1 = A_2 = 10^{-1}$, $A_3 = 10^{-4}$.

Figure 4.7: Controls of system 4.3-4.7 for varying cost coefficients with $B_1 = 1$, $B_2 = 10^3$.

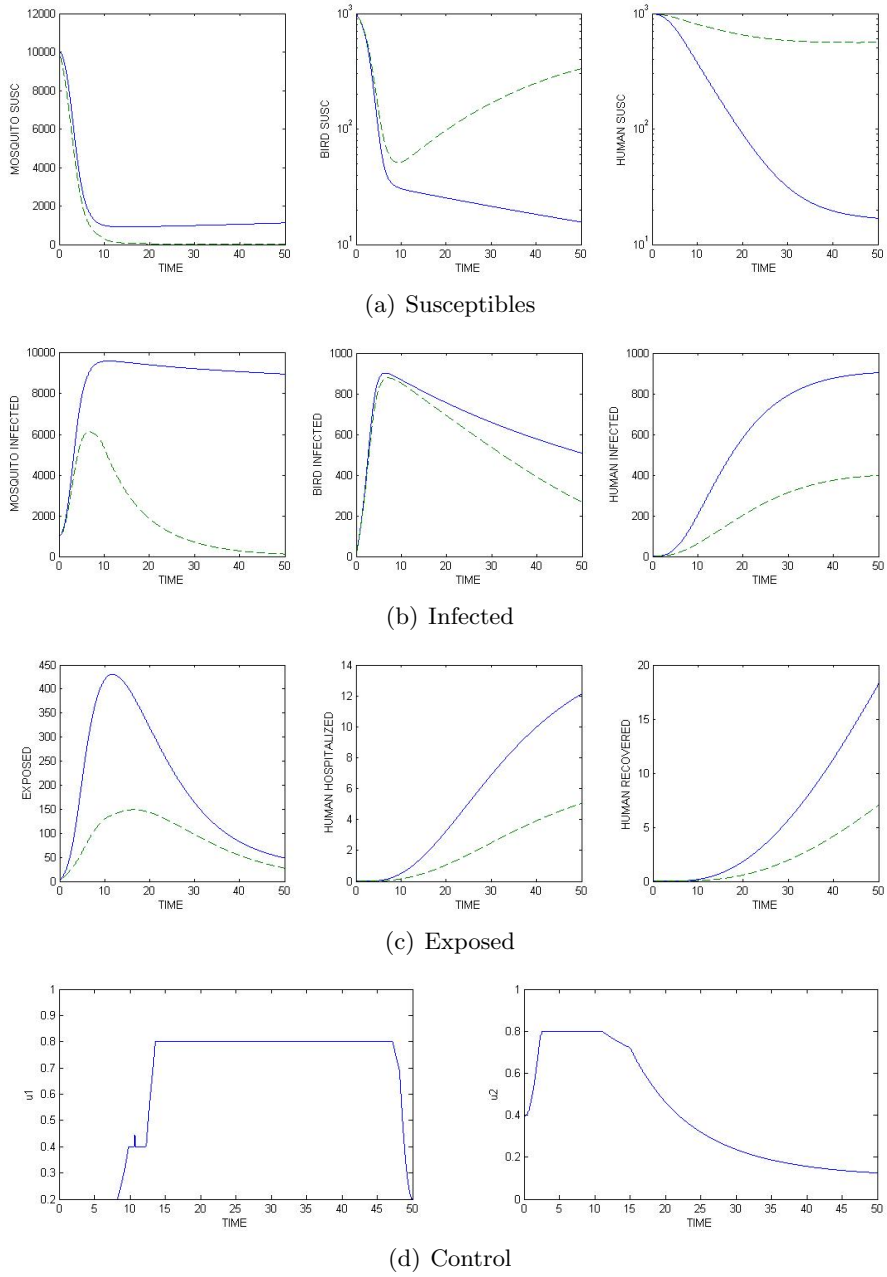


Figure 4.8: State system 4.3-4.7 with $A_1 = 10$, $A_3 = 10^{-3}$, $B_2 = 10^3$, $0 \leq u_1 \leq 0.8$, $0 \leq u_2 \leq 0.9$

Also, $0 \leq u_1 \leq 0.8$ and $0 \leq u_2 \leq 0.9$. Compared to figure 4.8, fewer bird and human susceptible occur as well a decrease in infected organisms from all three classes. A decrease in the exposed, hospitalized and recovered categories also occurs. Part d shows the application of control u_2 before u_1 as in the previous case, but the maximum is less for u_2 and the maximum for u_1 is maintained for a shorter period of time.

4.5 Conclusion

Given a fixed set of model parameters, we have obtained optimal controls results and corresponding populations for several scenarios of varying weight and cost coefficients in the objective functional. Certain cases lead to conclusions about the formats of the control strategies. These results suggest that when the exposed, infected and mosquito population all carry the same weight and when the cost coefficients are the same, the optimal solution requires an emphasis on preventing contact of the human and mosquito populations with little effort applied to limiting the mosquito population (see figure 4.3). Since it may be difficult to depend on humans to take preventive action, one may want to consider scenarios that require more effort at controlling the mosquito population. Thus a more realistic approach is to consider high costs for the the prevention efforts. We may also want to place more importance on lowering the exposed and infected human population than on the total number of mosquitos, by using a lower weight coefficient for the mosquitos. If the cost of prevention (control u_2) is relatively high and the weight of the total number of mosquitos is low, the optimal strategy suggests a brief period focused on killing mosquitos followed by prevention efforts and then an approximate equal time spent on a second round of distribution of insecticides (see figure 4.7). If the size of the mosquito population is assumed to be even less important, preventive strategies are applied first followed by a more sustained effort on the killing of mosquitos (see figure 4.4).

We note that there are limitations and possible extensions of this model and control problem. The model may be extended to include separate pesticides for the larvae and adult stages of mosquitos, suggesting the use of two controls of the insects. One could add a control for efforts to adjust the rate of hospitalization. A limitation is the difficulty

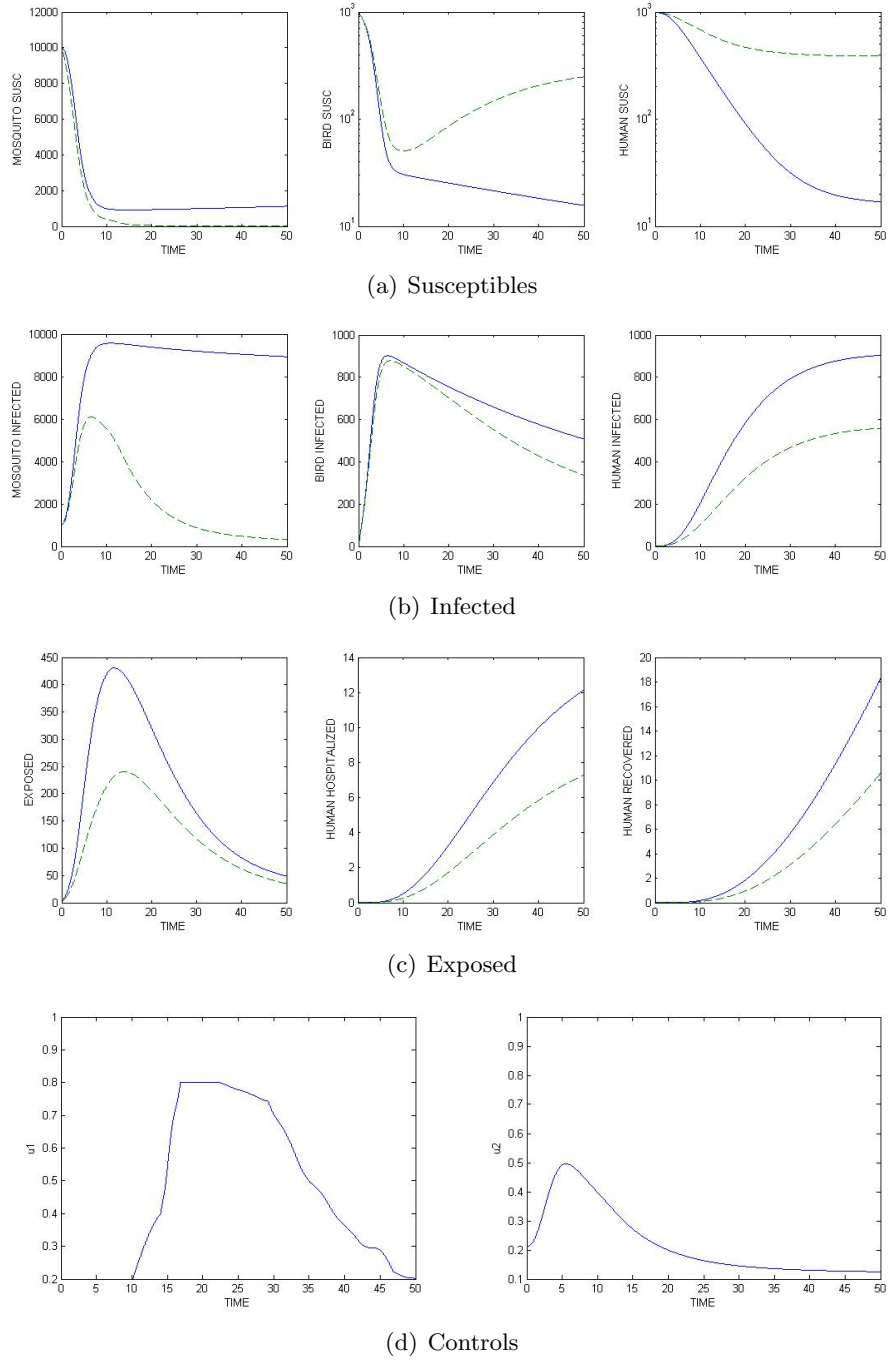


Figure 4.9: Control of system 4.3-4.7 with $A_1 = 1$, $A_3 = 10^{-3}$, $B_2 = 10^3$, $0 \leq u_1 \leq 0.8$, $0 \leq u_2 \leq 0.9$

in obtaining reasonable estimates for the parameters to apply this model to a specific location. The optimal controls and their resulting populations strongly depend on the choice of parameters.

These results show the utility of the optimal control tools in designing strategies for slowing the spread of this epidemic. Given a specific set of parameters (including cost coefficients), one can decide which of the two controls to give more emphasis.

Bibliography

- [1] *External Forcing of Ecological and Epidemiological Systems: A Resonance Approach.* Physica D, Vol. 190: 136-151, 2004.
- [2] S. Altezer, A. Dobson, P. Hosseini, P. Hudson, and M. Pascual P. Rohani. *Seasonality and the Dynamic of Infectious Diseases.* Ecology Letters, Vol. 9:, 467-484, 2006.
- [3] E. Asano, L. J. Gross, S. Lenhart, and L. Real. *Optimal Control of Vaccine distribution in a Rabies Metapopulation Model.* preprint, 2007.
- [4] N. D. Barlow. *The Ecology of Wildlife Disease Control: Simple Models Revisited.* Journal of Applied Ecology, Vol. 33: 303-314, 1996.
- [5] D. J. Bell and D. H. Jacobson. *Singular Optimal Control Problems.* Academic Press, New York, vol. 17 edition, 1975.
- [6] K. W. Blayneh, A. B. Gumel, S. Lenhart, and T. Clayton. *Backward Bifurcation and Optimal Control of West Nile Virus.* Preprint, 2008.
- [7] C. Bowman, A. B. Gumel, P. van den Driessche, J. Wu, and H. Zhu. *A Mathematical Model for Assessing Control Strategies Against West Nile Virus.* Bulletin of Mathematical Biology, Vol. 67: 1107-1133, 2005.
- [8] J. A. Chapman, K. W. Blayneh Feldhamer, A. B. Gumel, S. Lenhart, and T. Clayton. *Wild Mammals of North America: Biology, Management, and Economics.* The John Hopkins University Press, Baltimore, 1982.
- [9] M. J. Coyne, G. Smith, and F. E. McAllister. *Mathematic Model for the Population Biology of Rabies in Raccoons in the Mid-Atlantic States.* American Journal of Veterinary Research, Vol. 50: 2148-2154, 1989.

- [10] Gustavo Cruz-Pacheco, Lourdes Esteva, Juan Antonio Montano-Hirose, and Dristobal Vargas. *Modelling the Dynamics of West Nile Virus*. Bulletin of Mathematical Biology, Vol. 67: 1157-1172, 2005.
- [11] W. Ding, L. J. Gross, K. Langston, S. Lenhart, and L. Real. *Optimal Control of Vaccine Distribution in a Rabies Metapopulation Model*. preprint, 2006.
- [12] N. D. Evans and A. J. Pritchard. *A Control Theoretic Approach to Containing the Spread of Rabies*. IMA Journal of Mathematics Applied in Medicine and Biology, Vol. 18: 1-23, 2001.
- [13] S. Gao, L. Chen, and L. Sun. *Dynamic Complexities in a Seasonal Prevention Epidemic Model with Birth Pulses*. Chaos Solitons and Fractals, Vol. 26: 1171-1181, 2005.
- [14] B. S. Goh. *Necessary Conditions for Singular Extremals Involving Multiple Control Variables*. SIAM J. Control and Optimization, Vol. 4: 716-731, 1967.
- [15] S. A. Gourley, L., R. Liu, and Jianhong Wu. *Some Vector borne Diseases with Structured Host Populations: Extinction and Spatial Spread*. SIAM J. Appl. Math., Vol. 67: 408-433, 2007.
- [16] D. Greenhalgh. *An Epidemic Model with a Density-Dependent Death Rate*. IMA Journal of Mathematics Applied in Medicine and Biology, Vol. 7: 1-26, 1990.
- [17] A. C. Jackson. *Rabies*. Academic Press, New York, 2002.
- [18] H. J. Kelley, R. E. Kopp, and H. G. Moyer. *Singular Extremals, Topics in Optimization*. Academic Press, New York, 63-101 edition, 1967.
- [19] A. J. Krener. *The High Order Maximal Principle and its Application to Singular Extremals*. SIAM J. Control and Optimization, Vol. 15: 256-293, 1977.
- [20] S. Lenhart and J. T. Workman. *Optimal Control Applied to Biological Models*. Chapman I & Hall/CRC, Mathematical and Computational Biology Series, 2007.

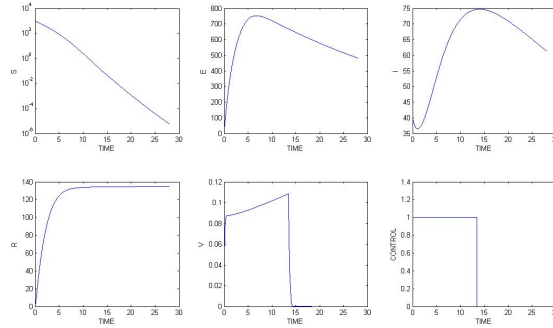
- [21] R. Lewis, B. Parker, D. Gaffin, and M. Hoefnagels. *Life*. McGraw-Hill Higher Education, New York, 6th ed edition, 2007.
- [22] D. L. Lukes. *Differential Equations: Classical to Controlled, Mathematics in Science and Engineering*. Academic Press, New York, 1982.
- [23] J. D. Murray and W. L. Seward. *On the Spatial Spread of Rabies Among Foxes with Immunity*. *J. Theo. Biol.*, Vol. 130: 327-348, 1991.
- [24] J. D. Murray, E. A. Stanley, and D. L. Brown. *On the Spatial Spread of Rabies Among Foxes*. *Proc. R. Soc. London B*, Vol. 229: 111-150, 1986.
- [25] L. S. Pontragin, R. V. Gamkrelize V. G. Boltyanskii, and E. F. Mishchenko. *The Mathematical Theory of Optimal Processes*. Wiley, 1962.
- [26] H. M. Robbins. *A Generalized Legendre-Clebsch condition for the Singular Cases of Optimal Control*. *IBM J. Res. Develop.*, Vol. 11: 361-372, 1967.
- [27] M. G. Roberts and J. Jowett. *An SEI Model with Density-Dependent Demographics and Epidemiology*. *IMA Journal of Mathematics Applied in Medicine and Biology*, Vol. 13: 245-257, 1996.
- [28] M. G. Roberts and R. R. Kao. *The Dynamics of an Infectious Disease in a Population with Birth Pulses*. *Mathematical Biosciences*, Vol. 149: 23-36, 1997.
- [29] C. A. Russell, L. A. Real, and D. L. Smith. *Spatial Control of Rabies on Heterogeneous Landscapes*. preprint, preprint.
- [30] C. A. Russell, D. L. Smith, J. E. Childs, and L. A. Real. *Predictive Spatial Dynamics and Strategic Planning for Raccoon Rabies Emergence in Ohio*. *PLoS Biology*, Vol. 3: 382-388, 2005.
- [31] D. L. Smith, B. Lucey, L. A. Waller, J. E. Childs, and L. A. Real. *Predicting the Spatial Dynamics of Rabies Epidemics on Heterogeneous Landscapes*. *PNAS*, 3668-3672, New Jersey, 2002.

- [32] D. L. Smith, L. A. Waller, C. A. Russell, J. E. Childs, and L. A. Real. *Assessing the Role of Long-Distance Translocation and Spatial Heterogeneity in the Raccoon Rabies Epidemic in Connecticut*. Preventative Veterinary Medicine, 2004.
- [33] J. Smith. *New Aspects of Rabies with Emphasis on Epidemiology, Diagnosis, and Prevention of the Disease in the United States*. Clinical Microbiology Reviews, Vol. 9: 166-176, 1996.
- [34] S. Tang and L. Chen. *Density-Dependent Birth Rate, Birth Pulses and their Population Dynamic Consequences*. J. Math. Biol., Vol. 44: 185-199, 2002.
- [35] P. van den Driessche and J. Watmough. *Reproduction Numbers and Sub-Threshold Endemic Equilibria for Compartmental Models of Disease Transmission*. Mathematical Biosciences, Vol. 180: 29-48, 2002.
- [36] Majorie J. Wonham, Thomas de Camino-Beck, and Mark A. Lewis. *An Epidemiological Model for West Nile Virus: Invasion Analysis and Control Applications*. Proc. R. Soc. Lond., Vol. 271: 501-507, 2004.

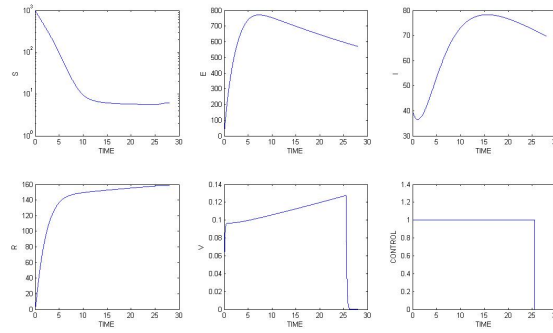
Appendices

Appendix A

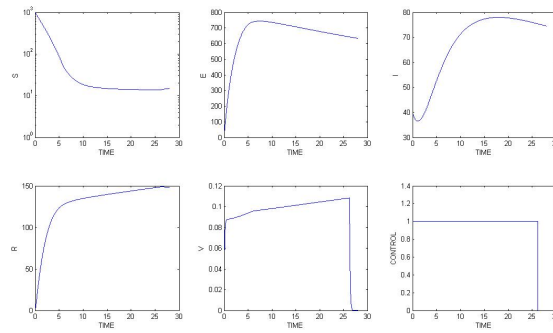
The First Appendix



(a) $u = 1$ for days 1-12. $B = 10^{-2}$

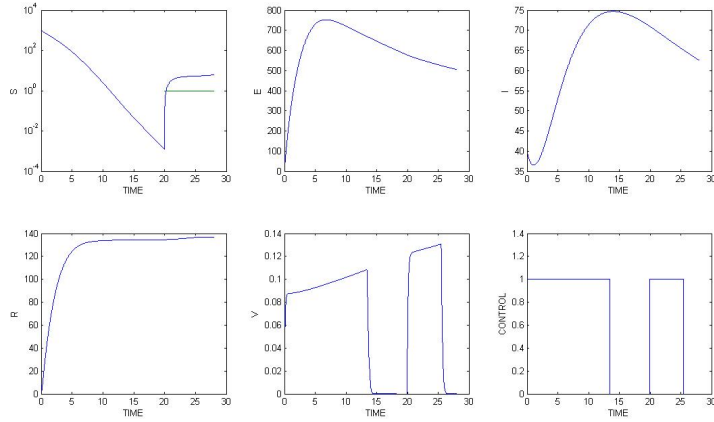


(b) $u = 1$ for days 1-25. $B = 10^{-2}$

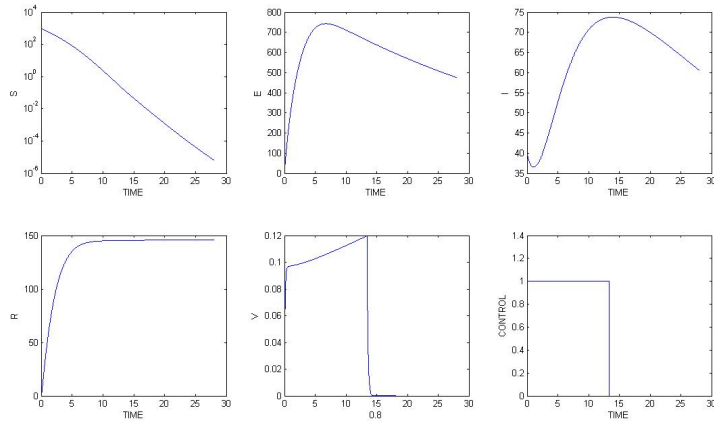


(c) $u = 1$ for days 1-25. $B = 10^{-2}$

Figure A.1: Controlled populations of system 2.2 during a 28 day interval (a) without a birth pulse. (b) during a birth pulse. (c) beginning on day 73 (about 1 week before the birth pulse).

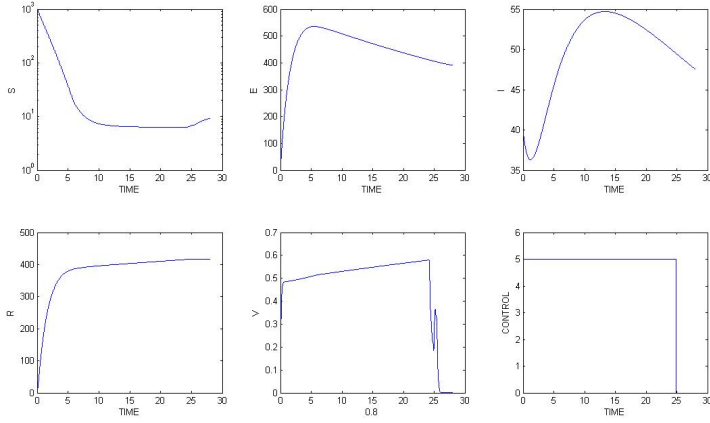


(a) $u = 1$ for days 1-12, 21-24. $B = 10^{-2}$

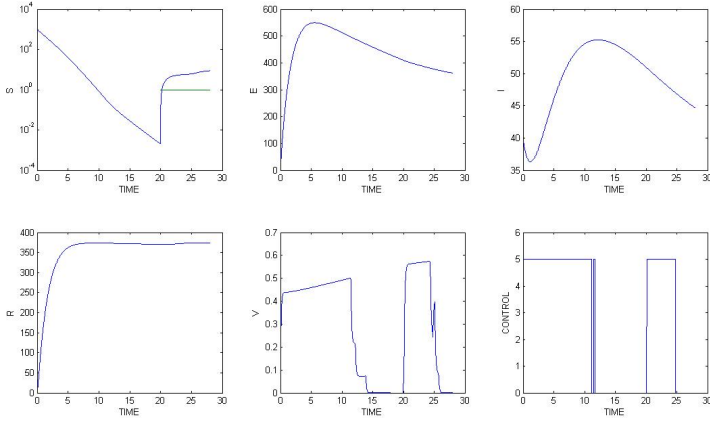


(b) $u = 1$ for days 1-12. $B = 10^{-2}$

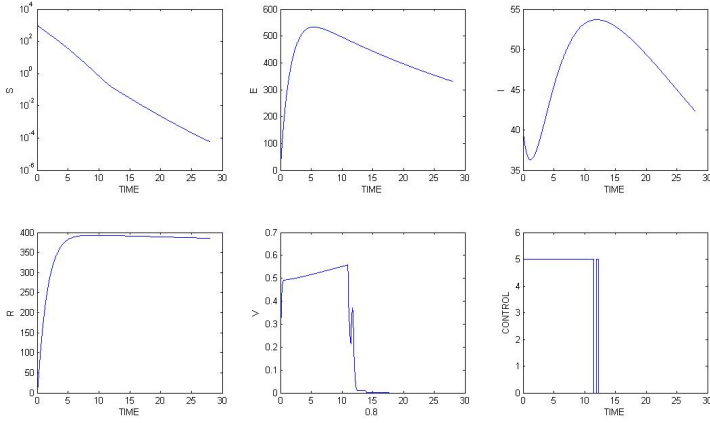
Figure A.2: Controlled populations of system 2.2 during a 28 day interval:(a) beginning March 1. (b) beginning February 20.



(a) $u = 5$ for days 1-24. $B = 10^{-2}$



(b) $u = 5$ for days 1-10, 21-23. $B = 10^{-2}$



(c) $u = 5$ for days 1-10, 12. $B = 10^{-2}$

Figure A.3: Results of system 2.2 with upper bound of 5 on the control for a 28 day interval:(a) beginning March 14. (b) beginning March 1. (c) beginning February 20.

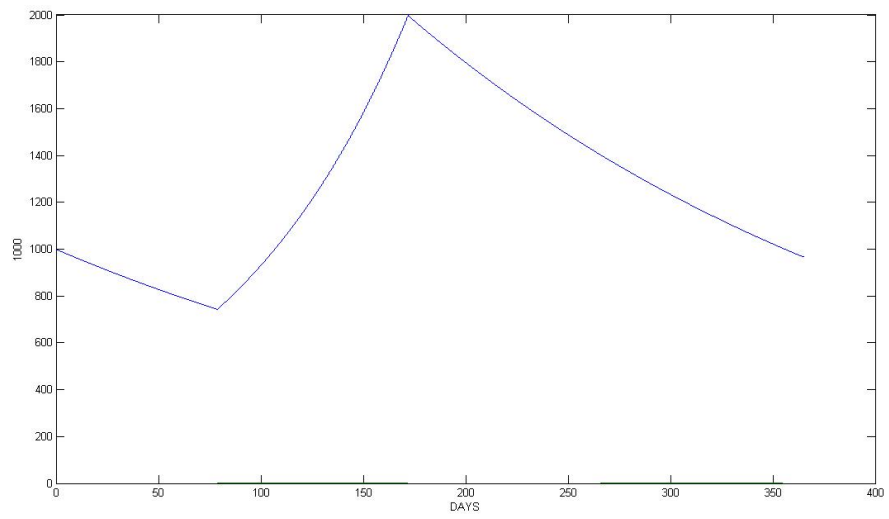
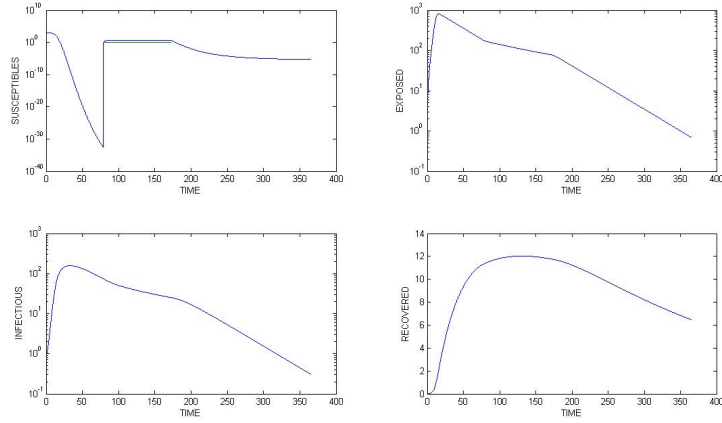
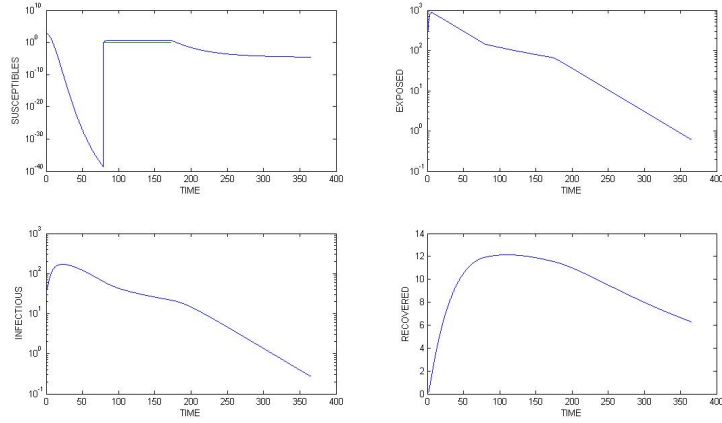


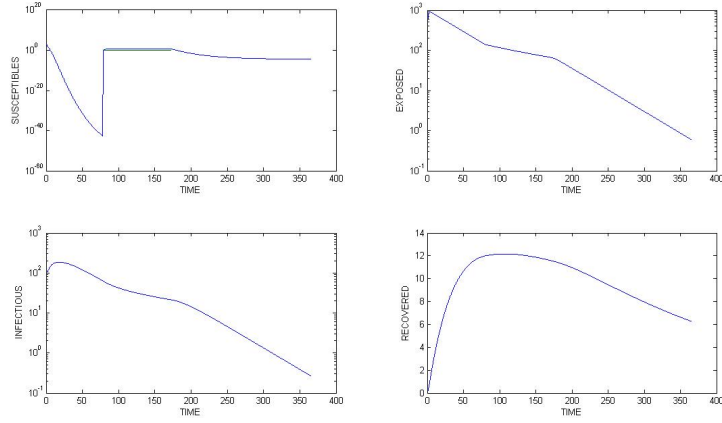
Figure A.4: Disease free population for 1 year



(a) 1 infectious raccoon



(b) 40 infectious raccoons



(c) 100 infectious raccoons

Figure A.5: Populations of system 2.1 with initial values of 1, 40 and 100 infected raccoons and no control

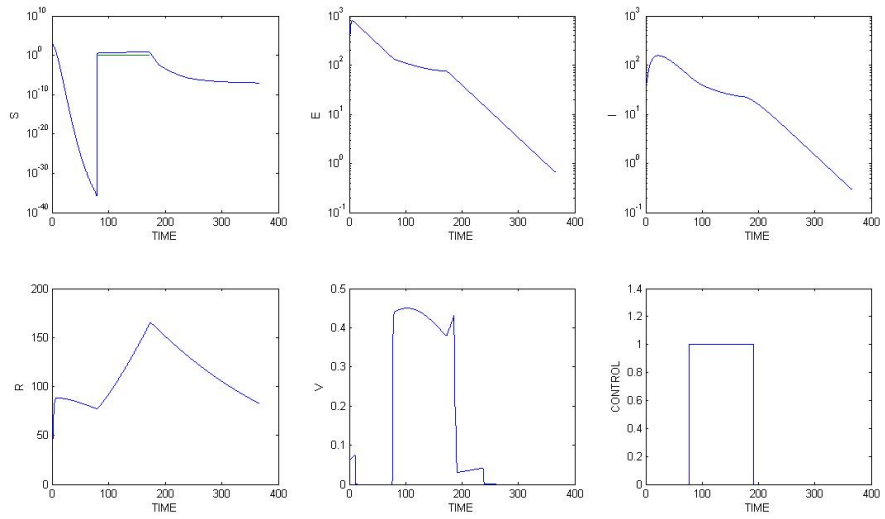


Figure A.6: Optimal control results of system 2.2 projected for 1 year with $I_o = 40$. $u = 1$ for days 75-191.

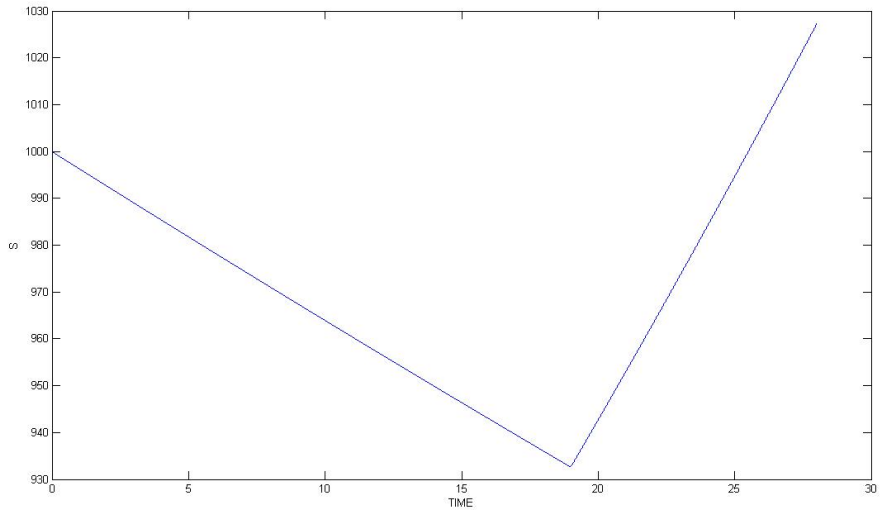


Figure A.7: Disease free raccoon population starting on March 1

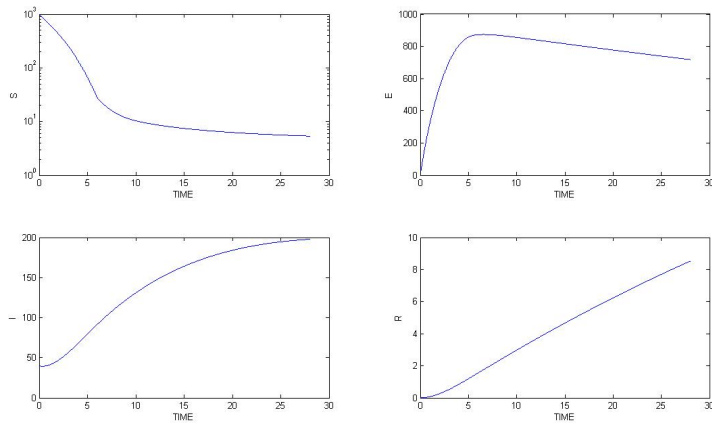
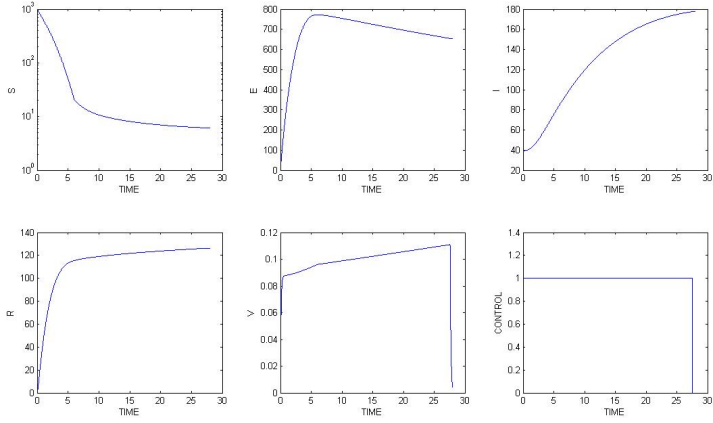
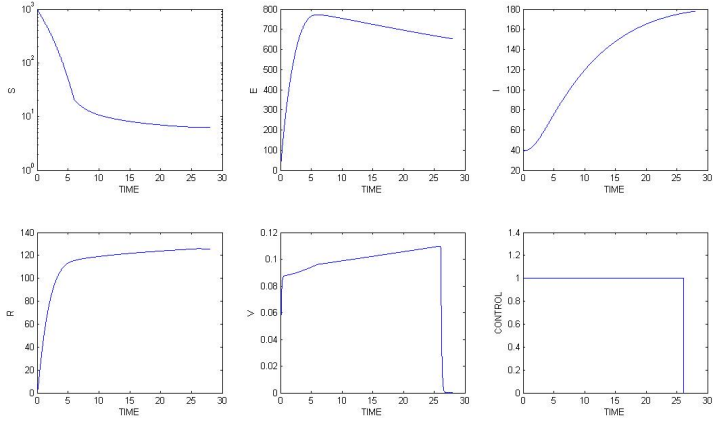


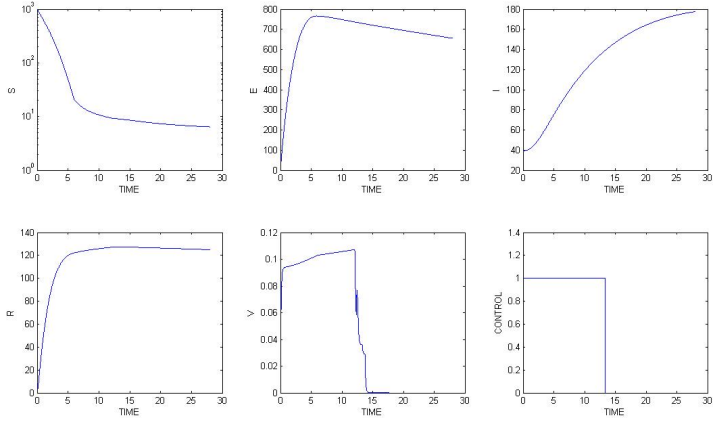
Figure A.8: State variables of system 2.2 with disease and no control: Simulation begins on March 14.



(a) $B = 10^{-4}$

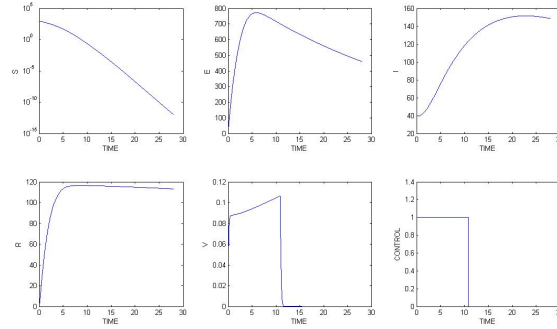


(b) $B = 10^{-2}$

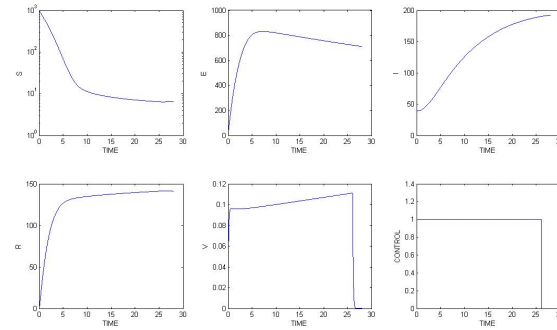


(c) $B = 10^0$

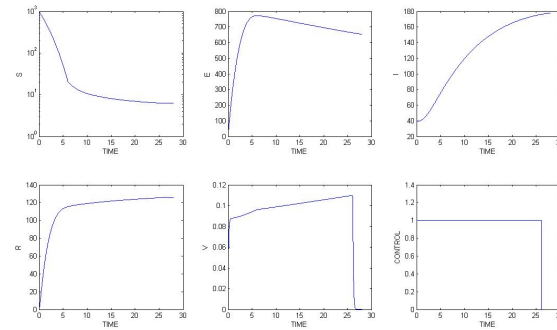
Figure A.9: Controlled results of system 2.2 from new parameters when (a) $B = 10^{-4}$, (b) $B = 10^{-2}$, (c) $B = 10^0$



(a) $u = 1$ for days 1-10. $B = 10^{-2}$

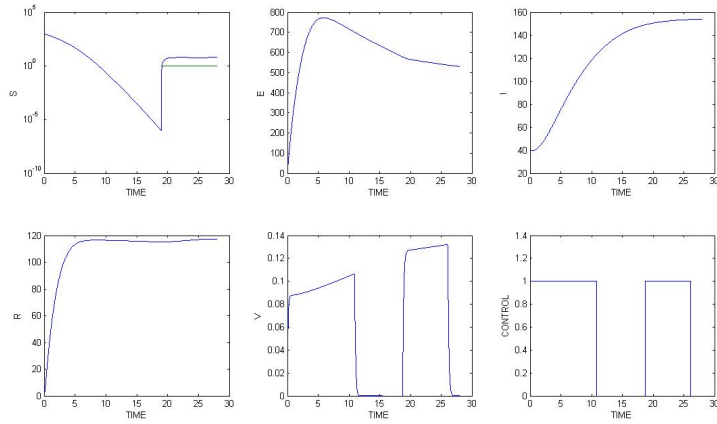


(b) $u = 1$ for days 1-25. $B = 10^{-2}$

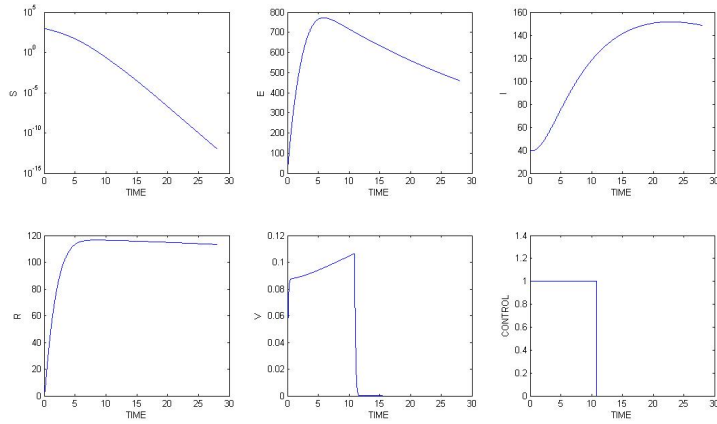


(c) $u = 1$ for days 1-25. $B = 10^{-2}$

Figure A.10: New parameter results of system 2.2 for a 28 day interval:(a) without a birth pulse. (b) during a birth pulse. (c) beginning on day 73 (shortly before the birth pulse).



(a) $u = 1$ for days 1-10, 19-25. $B = 10^{-2}$



(b) $u = 1$ for days 1-10. $B = 10^{-2}$

Figure A.11: Results of system 2.2 from new parameters for a 28 day interval:(a) beginning March 1. (b) beginning February 20.

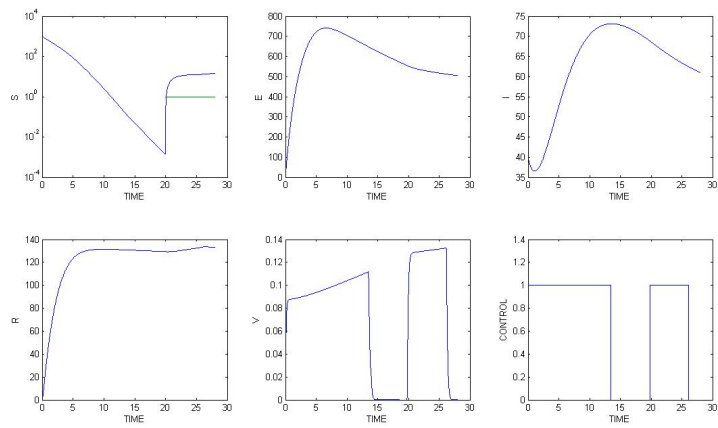
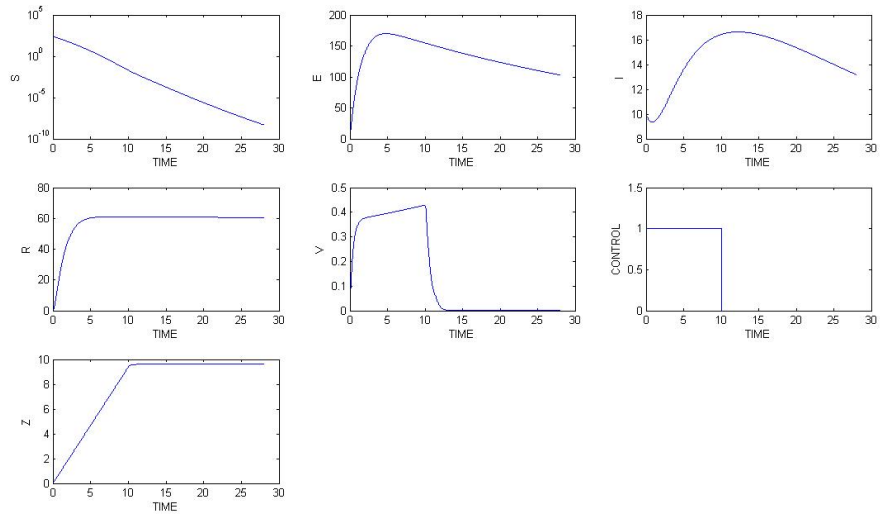
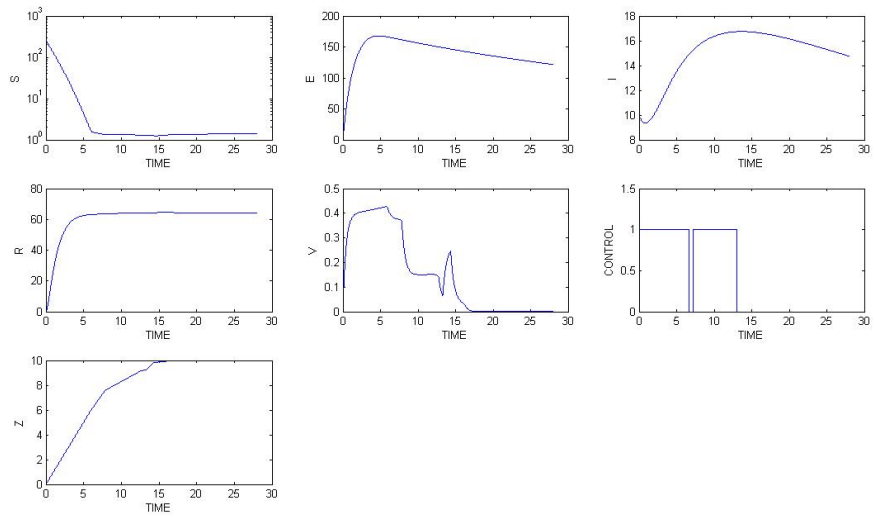


Figure A.12: Results of system 2.2 from new birth and death rate but the old infection period α beginning March 1.



(a) $\lambda_6 = 0.003, u = 1$ for days 1-10.



(b) $\lambda_6 = 0.30285, u = 1$ for days 1-7, 7-13.

Figure A.13: Results of system 2.2 from control constraint case (a) 28 day interval without a birth pulse. (b) 28 day interval beginning on March 14.

Table A.1: State Variables and Parameters

Notation	Description	Units
M_s	number of susceptible mosquitos	mosquitos
M_i	number of infected mosquitos	mosquitos
B_s	number of susceptible birds	birds
B_i	number of infected birds	birds
S	number of susceptible humans	humans
E	number of exposed humans	humans
I	number of infected humans	humans
H	number of hospitalized humans	humans
R	number of immune humans	humans
μ_1	mosquito natural death rate	day ⁻¹
μ_2	mosquito density dependent death rate	day ⁻¹ mosquito ⁻¹
μ_3	human natural death rate	day ⁻¹
μ_4	human density dependent death rate	day ⁻¹ human ⁻¹
γ_M	mosquito density dependent birth rate	day ⁻¹
γ_H	human density dependent birth rate	day ⁻¹
b	per capita biting rate of mosquitos	day ⁻¹
λ_B	bird immigration rate	(bird)day ⁻¹
λ_H	human immigration rate	(human)day ⁻¹
δ	bird emigration rate	day ⁻¹ bird
α	rate exposed humans become infectious	day ⁻¹
σ	hospitalization rate of humans	day ⁻¹
r	recovery rate of infectious humans	day ⁻¹
τ	recovery rate of hospitalized humans	day ⁻¹
β_1	probability mosquitos become infected	
β_2	probability birds become infected	(bird)mosquitos ⁻¹
β_3	probability humans become exposed	(human)mosquitos ⁻¹
r_0	mosquito mortality rate due to control	day ⁻¹
ρ	bird density dependent birth rate	day ⁻¹
$d_I,$	infected human death rate	day ⁻¹
d_H	hospitalized death rate	day ⁻¹
μ_B	natural death rate of birds	day ⁻¹
d_B	death rate of birds due to WNV	day ⁻¹
$u_1(t)$	effort of killing mosquitos	day ⁻¹
$u_2(t)$	effort of preventing human/mosquito	day ⁻¹

Table A.2: State Variables and Parameters

Parameter	Value
μ_1	10^{-3}
μ_2	$5 * 10^6$
μ_3	$9 * 10^{-4}$
μ_4	$2 * 10^{-6}$
γ_M	$51.1\mu_1$
γ_H	$2.85 * 10^{-3}$
b	3
λ_B	2.1
λ_H	$5 * 10^{-2}$
δ	$5.2 * 10^{-2}$
α	0.1
σ	$9 * 10^{-4}$
r	$2.0 * 10^{-4}$
τ	0.05
β_1	0.4
β_2	0.1
β_3	10^{-2}
r_0	$1.25 * 10^{-1}$
ρ	0.05
$d_I,$	$d_H + 10^{-5}$
d_H	$5 * 10^{-7}$

Vita

Timothy Joseph Clayton was born in Detroit, Michigan on April 21, 1965. He graduated from Carter High School, Strawberry Plains, Tennessee on June 1, 1983 and from Lee College, Cleveland, Tennessee on May 7, 1988 with a major in Mathematics. In 1988 he graduated from the University of Tennessee with a Master of Science degree in Mathematics.